DESIGNING A SOLAR PHOTOVOLTAIC POWER PLANT BY USING PV SYSTEM IN MOSUL

2023
MASTER THESIS
ELECTRICAL-ELECTRONICS ENGINEERING

Omer Rafea Tawfeeq ALDABBAGH

Thesis Advisor
Assoc. Prof. Dr. Muhammet Tahir GÜNEŞER

DESIGNING A SOLAR PHOTOVOLTAIC POWER PLANT BY USING PV SYSTEM IN MOSUL

Omer Rafea Tawfeeq ALDABBAGH

Thesis Advisor
Assoc. Prof. Dr. Muhammet Tahir GÜNEŞER

T.C.
Karabuk University
Institute of Graduate Programs
Department of Electrical and Electronic Engineering
Prepared as
Master Thesis

KARABUK
January 2023

I certify that in my opinion the thesis submitted by Omer Rafea Tawfeeq ALDABBAGH titled “DESIGNING A SOLAR PHOTOVOLTAIC POWER PLANT BY USING PV SYSTEM IN MOSUL” is fully adequate in scope and quality as a thesis for the degree of Master of Science.

Assoc. Prof. Dr. Muhammet Tahir GÜNEŞER ....
Thesis Advisor, Department of Electrical and Electronic Engineering

This thesis is accepted by the examining committee with a unanimous vote in the Department of Electrical and Electronic Engineering as a Master of Science thesis. 26/01/2023

Examining Committee Members (Institutions)		Signature
Chairman	: Assoc. Prof. Dr. Mustafa GÖKDAĞ (KBU)	....
Member	: Assoc. Prof. Dr. Muhammet Tahir GÜNEŞER (KBU)	....
Member	: Assoc. Prof. Dr. Abdülsamed TABAK (NEU)	....

The degree of Master of Science by the thesis submitted is approved by the Administrative Board of the Institute of Graduate Programs, Karabuk University.

Prof. Dr. Müsülüm KUZU ....
Director of the Institute of Graduate Programs

"I declare that all the information within this thesis has been gathered and presented in accordance with academic regulations and ethical principles and I have according to the requirements of these regulations and principles cited all those which do not originate in this work as well."

Omer Rafea Tawfeeq ALDABBAGH

ABSTRACT

M. Sc. Thesis

DESIGNING A SOLAR PHOTOVOLTAIC POWER PLANT BY USING PV SYSTEM IN MOSUL

Omer Rafea Tawfeeq ALDABBAGH

Karabük University
Institute of Graduate Programs
The Department of Electrical and Electronic Engineering

Thesis Advisor:
Assoc. Prof. Dr. Muhammet Tahir GÜNEŞER
January 2023, 137 pages

The demand for energy has increased as it is expected that the demand for energy in the world will grow by 41% during the next 20 years. environmental problems and energy crises are increasing day after day. Renewable energy is one of the best solutions for this problem, many countries around the world developed their ability in order to benefit from renewable sources to fill the shortage of energy. Photovoltaic energy is one of the Renewables emerging. The demand for solar PV energy is expanding significantly and may become the most competitive choice in many countries. As a result of the rising of conventional fuels utilized in the generation of energy, utilized of conventional fuels generation of energy leads to gas emissions like as (carbon dioxide, Nitrogen oxide, and Sulphur oxide), which cause damage to the atmosphere. One of the advantages of photovoltaic energy is that it is environmentally friendly, there are no outputs from the energy production process compared to gases from the energy production process by traditional fuels, energy production by photovoltaic energy is not accompanied by noise, the absence of mechanical movement led to a decrease in the cost of operating and maintaining Photovoltaic systems. The life span of Photovoltaic systems is between 25-30 years. The increase in R&D (research and Development) in the sector of Photovoltaic energy and the technological development taking place in this sector contributed significantly to the decrease in the prices of its components, which led to its widespread use in the domestic, industrial, and agricultural fields. Iraq suffers from a great shortage of electrical energy. During the past five years, the Iraqi Government started serious steps to produce electrical energy using renewable energies specifically electrical energy generation from solar photovoltaics.

In this thesis, a 100 MW –capacity Photovoltaic station was designed in the city of Mosul using PVSYST simulation software. The annual global horizontal irradiation rate for the site is 1825. The tilt angle of the solar panels was calculated for each of the year's months, and since the system to be installed is a fixed system. The simulation program determined the optimal Tilt angle. Several photovoltaic panels were calculated (total Panels needed), and the No. of panels in the series, and the No. of panels in the parallel string were calculated, the appropriate inverter was selected for the system, the collector box was also selected, the DC cables sections area are calculated also the AC cables sections area are calculated.

The annual Energy for PV array determined by the PVSYST it is equal to 181136 MWh also The Annual Energy exported to the grid is equal to 178352 MWh, also yield factor performance ratio, and capacity ratio are determined.

Key Words : On Grid Photovoltaic Plant, Tilt Angle PV Module, Central Inverter, Capacity Ratio, Performance Ratio, Yield Factor.

Science Code : 90544

ÖZET

Yüksek Lisans Tezi

MUSUL'DA FV SİSTEM KULLANARAK GÜNEŞ FOTOVOLTAİK SANTRALİ TASARLANMASI

Omer Rafea Tawfeeq ALDABBAGH

Karabük Üniversitesi
Lisansüstü Eğitim Enstitüsü
Elektrik ve Elektronik Mühendisliği Anabilim Dalı

Tez Danışmanı:
Doç. Dr. Muhammet Tahir GÜNEŞER

Ocak 2023, 137 sayfa

Önümüzdeki 20 yılda dünyadaki enerji talebinin % 41 oranında artması beklentisi ile birlikte çevre sorunları ve enerji temin krizleri de günden güne artmaktadır. Yenilenebilir enerji teknolojileri bu aşamada en iyi çözüm yöntemlerinden birisi olarak ülkelerin enerji açığını kapatmasına bir fırsat olarak görülmektedir. Fotovoltaik enerji, yenilenebilir enerji yöntemlerinden kendisine talebin önemli ölçüde genişlediği ve birçok ülkeye rekabetçi olma fırsatı sunan teknoloji olarak öne çıkmaktadır. Enerji üretiminde kullanılan konvansiyonel fosil yakıtların atmosfere zarar veren (karbon dioksit, Azot oksit ve kükürt oksit) gaz emisyonlarına yol açtığı bilinmektedir. Bu sebeple, fotovoltaik enerjinin çevre dostu olması, geleneksel yakıtlarla enerji üretim sürecinden çıkan gazlara kıyasla enerji üretim sürecinde hiçbir zararlı çıktı olmaması, enerji üretimine gürültü eşlik etmiyor olması, mekanik enerji hareketinin olmaması, işletme ve bakım maliyetinde düşüşe neden olması önemli avantajlar olarak görülmektedir. Fotovoltaik sistemlerin ömrü 25-30 yıl

arasında olduğu hesaplanmaktadır. Fotovoltaik enerji sektöründe Ar-Ge (araştırma ve geliştirme) artışı ve bu sektörde meydana gelen teknolojik gelişme, bileşenlerinin fiyatlarının düşmesine önemli ölçüde katkıda bulunmuş, bu da evsel, endüstriyel ve tarımsal alanlarda yaygın olarak kullanılmasına yol açmıştır.

Günümüzde Irak, büyük bir enerji arzı darboğazı sıkıntısı çekmektedir. Geçtiğimiz beş yıl boyunca Irak Hükümeti, yenilenebilir enerjileri, özellikle Fotovoltaik Güneş enerjisi yöntemi ile elektrik üretimi için ciddi adımlar atmaktadır.

Bu tezde, Musul şehrinde PVSYST simülasyon yazılımı kullanılarak 100 MW kapasiteli bir Fotovoltaik Güneş Enerji Santrali tasarlanmıştır. Musul şehrinin yıllık global yatay güneşlenme oranı 1825'tir. Kurulacak sistem sabit montaj bir sistem olduğundan güneş panellerinin eğim açısı yılın her ayı gözetilerek optimize edilmiştir. Simülasyon programı yardımıyla optimum eğim açısı belirlenmiştir. İhtiyaç duyulan fotovoltaik panel sayısı hesaplanırken, seri bağlanan panel sayısı ve aynı eviriciye bağlanan panel dizisi sayısı da belirlenmiştir. Tasarlanan sistem için en uygun evirici ve toplayıcı kutusu belirlenmiştir. Ayrıca kullanılacak DC kablo ve AC kablo için optimum kesit alanı hesaplanmıştır PVSYST tarafından belirlenen fotovoltaik dizi sistemi ile tasarlanan Güneş Enerjisi Santralinin yıllık enerji üretimi 181136 MWh olarak hesaplanmıştır. Bu miktarın 178352 MWh’I şebekeye verilebileceği belirlendiğinden systemin verim faktörü performans oranı ve kapasite oranı da belirlenmiştir.

Anahtar Kelimeler : Şebeke üzerinde Fotovoltaik tesis, Eğim açısı, PV modülü, Merkezi İnverter, Kapasite oranı, Performans oranı, Verim faktörü.

Bilim Kodu : 90544

ACKNOWLEDGMENT

I would like to give thanks to my advisor, Assoc. Prof. Dr. Muhammet Tahir GÜNEŞER, for his great interest and assistance in preparation of this thesis.

CONTENTS

Page

Page

Page

LIST OF FIGURES

Page

Page

Page

Page

LIST OF TABLES

Page

SYMBOLS AND ABBREVIATIONS

SYMBOLS

λ	:	The wavelength
β	:	Latitude angle
ψ	:	Longitude angle
δ	:	Solar declination angle
ω	:	The hour angles
ϕ_S	:	Azimuth angle
α	:	Tilt angle
∂	:	ecliptic angle

ABBREVIATIONS

MPP	:	Maximum power point
NOCT	:	Normal operating cell temperature
STC	:	Standard test conditions
AM	:	Air mass ratio
DC	:	Direct current
AC	:	Alternative current.
PWM	:	Pules width modulation.
MPPT	:	Maximum Power Point Tracking
LSPPPs	:	Large Scale Photovoltaic Power Plants
LSPPP	:	Large Scale Photovoltaic Power Plant
HV	:	high voltage
MOSFET	:	Metal Oxide field effect transistor semiconductor
IGBT	:	Insulated Gate Bipolar Transistor semiconductor
CCC	:	current carrying capacity

CSA	:	Cross section area of cable
LCD	:	Liquid Crystal Display
VSAT	:	Vertical single axis tracker
HSAT	:	Horizontal single axis tracker
PSAT	:	Polar aligned single axis tracker
TSAT	:	Tilted single axis tracker
TTDAT	:	Tip-tilt dual axis trackers
AADAT	:	Azimuth-altitude dual axis trackers
E	:	The Energy.
m	:	Mass.
c	:	Speed of the light.
h	:	Plank's constant.
q	:	Boltzmann's constant
T_{abs}	:	The absolute temperature
GSC	:	Solar constant
d_S	:	The diameter of the sun
L_{ES}	:	The main distance between the earth and sun
M_S	:	The radiation flux density of the sun
Gg	:	Global radiation
τ_G	:	Transmission factor
n_{day}	:	the day number
L	:	The latitude of the site
G_b	:	Direct beam solar radiation
G_d	:	Diffuse solar radiation
PV	:	Photovoltaic
N-type	:	Negative type material
P- type	:	Positive type material
I_{ph}	:	Photon current
R_s	:	Series resistance of the PV cell.
R_p	:	Shunt resistance of the PV cell
I_{SC}	:	Short circuit current
V_{OC}	:	Open circuit Voltage
I_D	:	Diode current.

I_p	:	Shunt current
I_o	:	Saturation current
q_e	:	Electron charge
T_{mod}	:	Module temperature
A	:	Ideality factor
I_{mpp}	:	Maximum power point current
V_{mpp}	:	Maximum power point voltage.
P_{mpp}	:	Power at the maximum power point.
A_{mod}	:	The area of the PV module or cell
G_a	:	The ambient irradiation.
T_{amb}	:	Ambient temperature
G	:	Solar radiation
T_{cell}	:	Cell Temperature
η_{con}	:	Conversation Efficiency
η_{ref}	:	Module efficiency at STC.
β_{pv}	:	Temperature coefficient of module (%/CO).
T_{ref}	:	Reference temperature
$\eta_{inverter}$	:	Inverter efficiency
GlobHor:	:	Horizontal global irradiation
Glob Inc	:	Global incident in plane
DiffHor	:	Horizontal diffuse irradiation.
GlobEff	:	Effective Global
Wind Vel	:	Wind velocity
d	:	Inter row distance
L_{mod}	:	Length of PV modules
$V_{mod(max)}$	:	Maximum module voltage expected at the site high temperature
$V_{mod(min)}$	:	Minimum module voltage expected at the site high temperature
$T_{amb(min)}$	:	Ambient low temperature of site
$T_{amb(max)}$	:	Ambient high temperature of site
T_{nom}	:	Nominal operation cell temperature
T_{STC}	:	Temperature at standard test conditions

T_{PC} : Temperature coefficient of maximum power (Pmax)

$V_{inv,inp,max}$: Maximum inverter input voltage

$V_{inv,inp,min}$: Minimum inverter input voltage

$N_{s,string, max}$: The Maximum No. of the PV Modules in the series string.

$N_{s,string,min}$: Minimum No. of the PV Modules in the series string

$N_{parallel\ strings}$: No. of PV Modules in Parallel strings

$I_{inv,max,DC}$: Maximum inverter input current

$P_{inverter\ DC\ rated}$: inverter maximum DC input power rated

$P_{(PV\ Peak)}$: Maximum power PV generator array

$V_{INV,\ DC\ TURN-OFF}$: Inverter DC turn-off voltage

$I_{Mod,\ Sc,\ STC}$: PV Module short circuit current at Standard Test Condition.

$I_{nominal\ fuse}$: Nominal fuse current

$I_{nominal\ string}$: Nominal string current.

$N_{s\ string}$: No. of PV modules in series string

ΔV : Voltage drops value of DC cables for (string /array

As : Cross section area of the cable

$L_{DC\ Cable}$: length of DC Cable (string/array)

$N_{Parallel\ string}$: Number of parallel strings in the PV system

$I_{string,\ Mpp,\ Stc}$: Maximum power point current of string at STC

$N_{series,\ MOD}$: Number of PV modules in series

$V_{Mpp,\ MOD,\ stc}$: Maximum power point voltage of PV module at STC

σ cu : conductivity of copper which equal to 56 mΩ-1.mm- 2

$L_{AC\ Cable}$: length of AC Cable

$I_{Inverter\ AC}$: Inverter AC current

Cosφ : Inverter power factor.

A_S : Cross section area for AC Cable

$V_{Inverter\ AC}$: AC voltage inverter

CBs : Circuit Breakers

PR : The performance ratio

Y_f : Yield factor

PART 1

INTRODUCTION

At the beginning of this century, the demand for energy has increased as it is expected that the demand for energy in the world will grow by 41% during the next 20 years, environmental problems and energy crises are increased day after day, Renewable energy is one of the best solutions for this problem many countries around the world developed their ability in order to benefits from the renewable sources to fill the shortage of energy, reduce greenhouses gas emissions, increase the employment, ensure the energy security and improve the energy efficiency. The sun is one of the largest abundant sources of renewable energy currently known, it is free and inexhaustible. Fossil fuel sources are being used to produce the majority of electrical energy. As a result of the development in the various field of life, this was accompanied by a large consumption of energy. Because of the increase in the price of traditional fuels used in energy production. With the rise in global temperatures and global warming accompanying energy production .it has become necessary to search for renewable energy sources that do not affect the climate and one of these sources is solar photovoltaic energy PV [1, 2]. When compared to the 24 terawatt of power that humans typically consume annually, the 233 pet watts of sunlight that reaches the earth's surface are abundant amount [3].

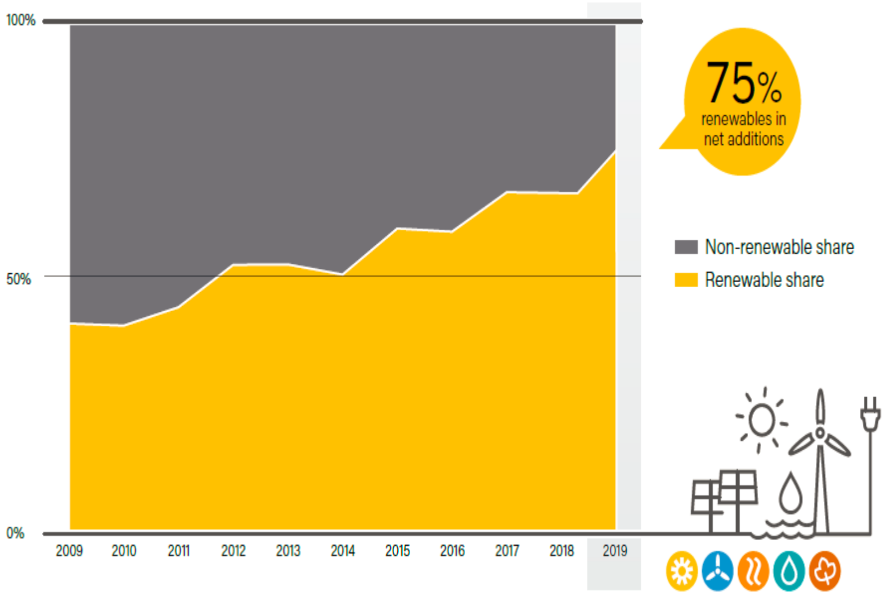

Figure 1.1. Renewable and non-renewable resources during 10 years with power generation capacity [4].

The photovoltaic energy sector witnessed a significant expansion during the previous years due to the increase in demand for energy in various sectors including residential, commercial, and industrial sectors. On the other hand, the rise in carbon dioxide emissions and climate changes taking place in the world prompted a rise in demand for renewable energies to compensate for the shortage in global energy supplies. as shown in Figure 1.2. The production of electrical energy expanding by photovoltaic energy for ten years 2010-2020.

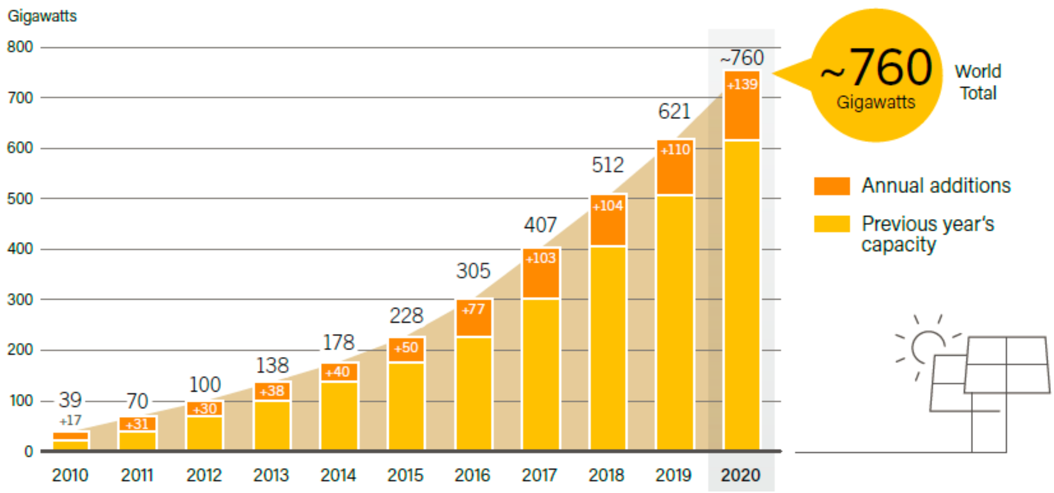

Figure 1.2. Electrical energy expanding by photovoltaic(2010-2020) [4].

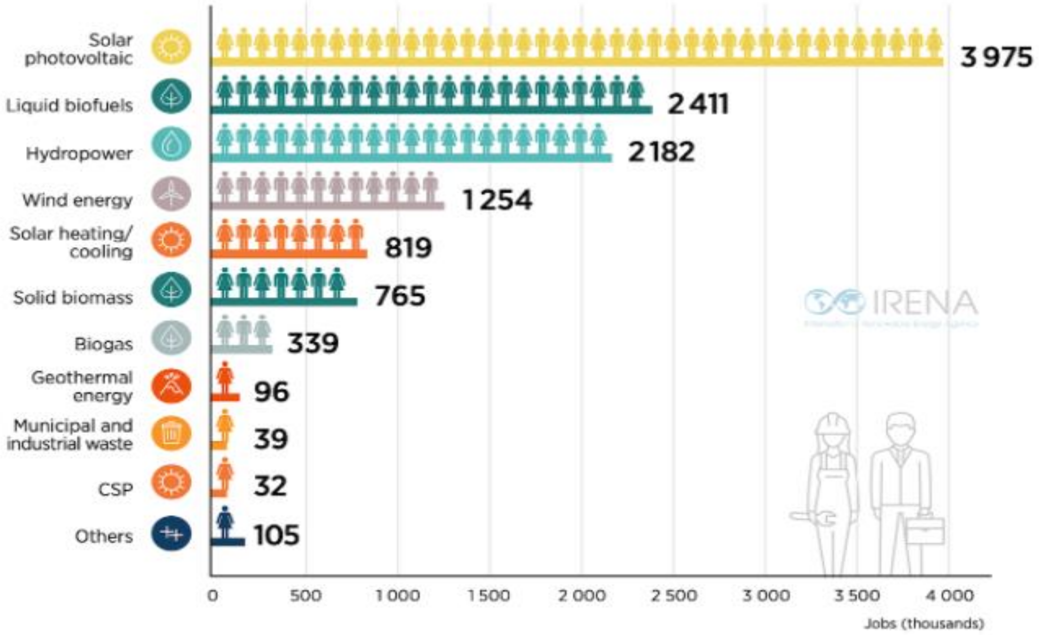

Figure 1.3. Employment of each renewable sector [4] .

As it shows the amount of the annual solar photovoltaic energy for each year and the amount of energy added for every year, in comparison with Figure 1.4 which shows the amount of solar energy produced globally by photovoltaic panels until 2019. the production reached 627 GW worldwide for the year 2019, while the amount of global energy generated by Photovoltaic panels for the year 2020 is approximately 760 GW worldwide where the increase in the added energy globally amounted to approximately 133 GW. And here we should be noted that the added capacities of photovoltaic energy were during the period of the corona pandemic (COVID-19).

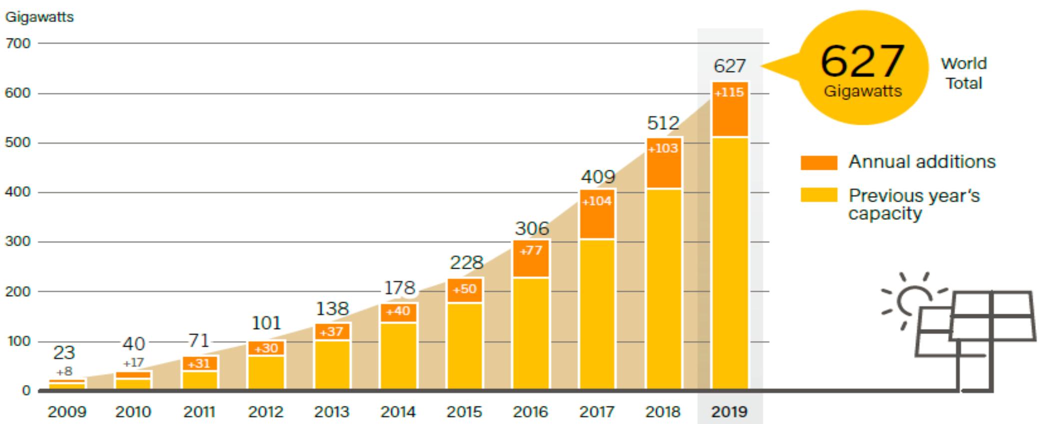

Figure 1.4. Electrical energy expanding by photovoltaic(2009-2019) [4].

Despite the restrictions imposed during the corona pandemic and requests to stay at home. This caused an increase in the demand for energy. the epidemic also caused delays in shipments and delivery of equipment's used in the solar energy industry such as panels, inverters, and other auxiliary devices. Despite these obstacles, there are many countries that have achieved great success by adding capacities in photovoltaic energy and achieving growth in PV power markets. And among these countries, United States of America witnessed significant expansions in the field of photovoltaic energy during 2019-2020 as shown in Figure 1.5.

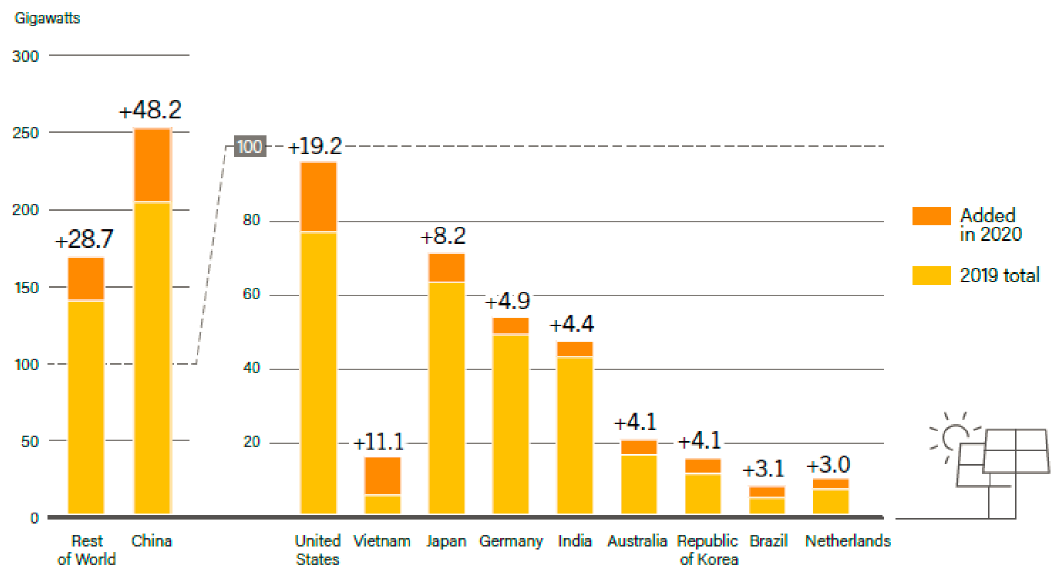

Figure 1.5. Top 10 countries for capacity added during 2020 [4].

The demand for solar PV energy is expanding significantly and may become the most competitive choice in many countries whether for domestic use or commercial, industrial and even in agriculture applications. large scale utility projects have begun to be widely applies. many countries have contributed to this energy by increasing their capacities of solar photovoltaic energy which has led to an increase in global growth.

There are many countries that have sufficient operation capacities to cover approximately 5% of their electricity needs by solar photovoltaic energy and among these countries are, Japan at 8.5%, Italy 9.4%, Chile 9.8%, Australia 9.9% and Germany 10.5%. There are many countries that have achieved good growth in the field of solar photovoltaic energy including Spain, the United Kingdom, India, and UAE (United Arab Emirates) [4] as illustrated in Figure 1.6.

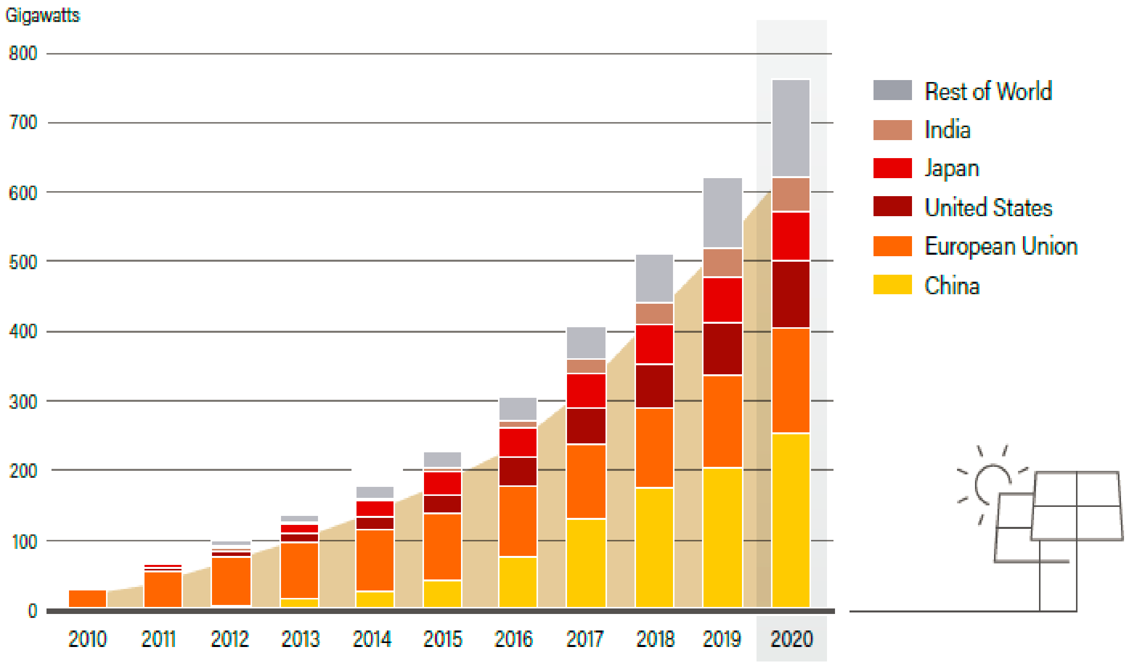

Figure 1.6. The Capacity of Global Photovoltaic generation according the country and regions, 2010-2020 [4].

Iraq suffers from a great shortage of electrical energy. Citizen is supplied with electrical energy at a rate of 15 hours/day this supply rate is not fixed. this quantity decreases in summer and winter season .as this quantity decrease to reach approximately to 10 hours/day. while the average supply hour increases during the full and spring season to reach approximately 20 hour/day or more.

The electricity generated in Iraq depending on Gas power stations we can consider it as a base load It is using Petroleum gas fuel which contributes 50 % of generated power. the steam power stations contribute 28% of generated power using heavy oil fuel, diesel power stations contribute 15% of generated power using gas oil fuel, and the hydro-electrical power stations involved 7% of Generated power. Figure 1.7 show the quantity of electrical energy from different types of electrical stations, while Figure 1.8. Show the distribution of electrical energy produced by different electrical stations and the shear of each governorate from generation [5].

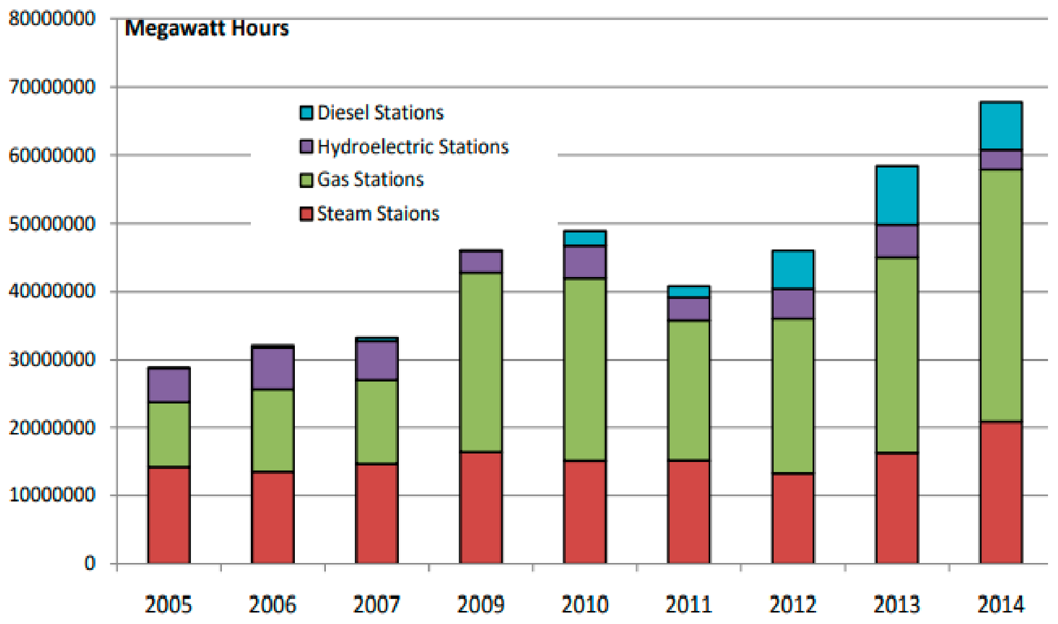

Figure 1.7. The quantity of the electrical energy from different types electrical stations [5].

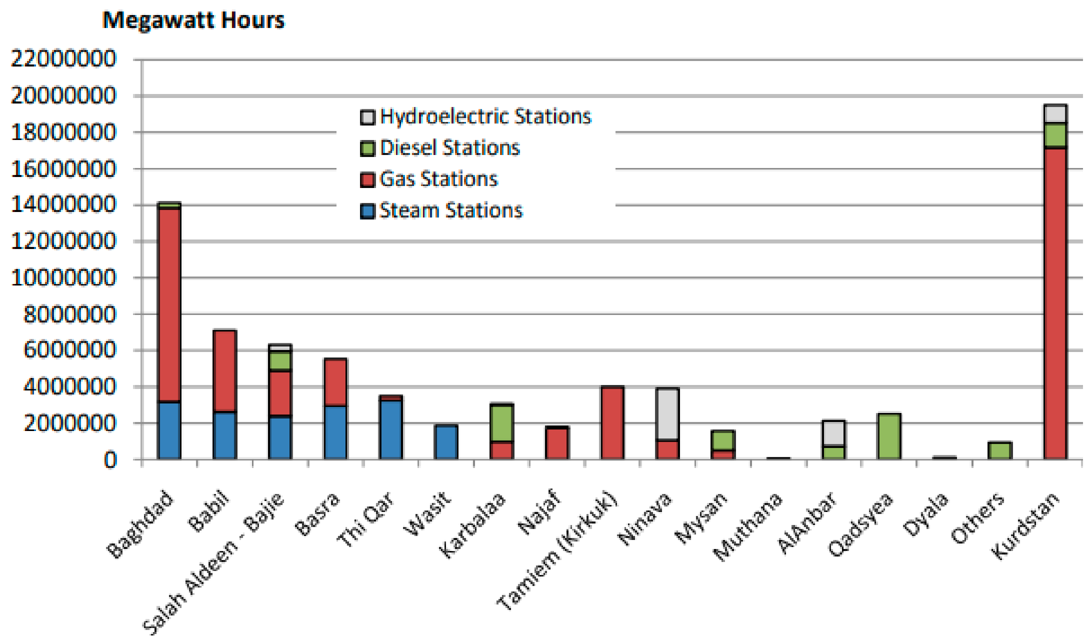

Figure 1.8. Different electrical stations and shear of each governorate from generation [5].

Most of the oil producing countries, including Iraq have not adopted the use of solar energy to generate electrical energy to meet their requirements for electrical energy. the main reason for this is the availability of oil in these countries as well as the low values of extracting the oil from the earth, and lack of encouraging incentives for solar energy and renewable energies, and these countries don’t take into consideration the damages caused using fossil fuel to produce their electrical energy needs on the environment.

During the past five years, the Iraqi Government started serious steps to produce electrical energy using renewable energies specifically the production of electrical energy from solar photovoltaic. the ministry of electrical and renewable energies announced a project for the establishment of solar photovoltaic plants in all Iraqi cities and the capacities of these plants ranged from 80-100 MW.

One of the most important factors that increased steps toward solar energy in Iraq is the rise in global oil prices and the high cost of extracting it from the earth as well as the sources of fossil fuels is heading towards extinction after the period of time and the other main reason is the climate change which comes as a result of the use of fossil fuel, which lead to global warming and increase in carbon dioxide emissions.

PART 2

LITERATURE REVIEW

In the recent years. The demand of energy is increased, without energy the humanity can not continue. Photovoltaic energy is one of the renewable energy sources, which witnessed a large growth during the previous years. Photovoltaic energy and other renewable energies (wind energy, hydraulic energy, etc.) can fill the gap in energy demand, Photovoltaic energy an environmentally friendly and not caused any pollution or Co_2 emissions. This expansion in the use of photovoltaic energy led to an increase in the studies related to photovoltaic power generation and the identification of factors and parameters that effected directly or indirectly on PV system's performance. The previous helps us to enhance the PV system's energy output during it is lifetime.

Some of the studies introduced the performance evaluation of a 10MW photovoltaic power plant, the annual rate of the temperature of the site is 27.3C^o and with an excellent solar radiance rate of 4.94 kWh/m2/day. The study calculated the various kinds of power losses (temperature, grid connecting, etc.) [6]. While the other study analysed the performance of a 100kW grid-connected PV system by using Polycrystalline silicon PV modules. They find that the system's yearly performance percentage is about 80%. The system generates 165.38 MWh/year and the magnitude of net energy exported to the grid is 161 MWh /year [7]. Other researchers going to design a PV system to meet the request of electricity in the department of engineering to reduce the electrical energy bill .they find that the engineering faculty consumed about 96 MWh annually .they designed a photovoltaic system with a capacity of 65.7 kW the system production will be 97.02 MWh/year and this amount will cover the energy demand for engineering faculty and the capital cost of this system is 177.000 USD and the period to pay back the money will be during 5.5

years, this system will reduce about 85 ton of greenhouse gas emissions every year [8].

Other researchers used the pvsyst software to design a grid-connected PV system for Modon Mohan Malaviya University of technology in India. the system losses and system output determined .and from pvsyst. The software they determined the optimal size of PV modules and the optimal number grid inverters. It is the optimal solution to provide the university by electrical energy. the PV system produces about 901 MWh/year [9]. The researcher designed and simulated a solar photovoltaic system with the capacity of 30 kW by using pvsyst software their site was artificial lack at Indonesia according to the weather conditions and Indonesia's climate. The researcher used in simulation different amounts of PV orientations Tilt angles (0^o,5^o,10^o,20^o,30^o) and used a previous types of PV modules Si-mono and Si-poly with different energy capacities and based on analyses they chose Si-mono PV panels with energy capacity 310 W_p with orientation tilt angle 5^o [10]. Another study refers to the important factors affecting the designing of the solar PV systems according to the amount of energy coming from the sun per square meter, the energy that falls on a unit area in unit time, and the ambient temperature, all these factors presented an important point in PV system designing [11]. The researchers indicate that the choice of the site of the solar power plant is very important, noticed that there is no wildlife in the area of the power plant site, there is no health risks the solar power plant will not cause a health hazard and it is environment friendly and finally, there are no historical and archaeological places in the solar power plant site or area [12].

The other researcher refers to the use of the string inverter as better for large systems instead of microgrid inverters which are suitable for residential applications to reduce the risk of underperformance [13].

Some studies refer to one of the factors effecting on the PV system’s performance it is potential induced degradation (PID), which can be define as a Potential difference of a few hundred volts between the solar cell of a module and module structure can occur [14] . This voltage difference leads to leakage current strolling between the solar cell and module structure [15]. When PID occurs the PV system will loss 20% from it is efficiency and lead to reduce PV module's performance and dependability [16]. Some studies refer to the temperature and humidity that can be affected negatively of photovoltaic system performance that runs in high DC voltages [17]. Other study shows the methods can be detected the PID also refer to the tried to treatment the PV panels by a layer of Phosphorus Silicate glass (PSG) to reduce the effect of PID process by coating the glass to prohibit the entering the Sodium ions in the solar encapsulation of the panel [18].

While other studies refer to the non-repeatedly programmed maintenance incorrect installation and aging effect all these factors can be accelerated the damage of the photovoltaic elements system and lead to Arc faults. Arc faults lead to fire hazards to the PV system and for multi-systems utility-scale, commercial and residential .to avoid the fire hazard the arc faults should be discovered in early time [19]. In the combiner box and re-combiner box, the possibility of arc faults is pointed out because it is common for measurements to be taken at this equipment while operators check the performance of the array or PV system [20]. The other studies refer to the main three types of electrical arc faults that happen in photovoltaic systems. series arc, parallel arc, and grounding arc and these faults because of insulation breakdown or connector misconduct [21]. Other study shows the necessary conditions for PID occurrence which include cell level, module level, system level and environmental factors (humidity, temperature) [22].

Another study shows Hot spots are high temperature areas affecting a part of the solar module and lead to a reduction in the energy generated and acceleration spoiling in the material a rounding damaged area. It is seldom stable most of the time it is intensity increases until leads to complete failure in the PV performance. The hot spots detected by the infrared thermography technique, hot spot led to irreversible damage to the photovoltaic modules and lead to a decrease in the energy of the PV system and the performance [23].

While there is another study that proposed a new method to detect the hot spots method utilized Artificial Intelligent (AI), this method can be detected the hot spot, with an accuracy of about 82.25% and using two parameters, string voltage and string current [24]. The hot spots lead to reduce PV module lifetime. The short circuit current of the impacted cell lowers below the operational current of the entire system, wasting the power produced by other cells as heat. The formation of hotspots causes voltage losses during operation at the affected PV module [25]. Another study proposes a detection method. This technique depends on equivalent DC impedance (EDCI), which has valuable characteristics for hot spot identification, in the panel's strings. Several straightforward current sensors and resistive voltage dividers are used to measure the equivalent DC impedance of the strings of the PV panel. there are two-state relay is used to open circuit the hot spotted line after detection [26].

Other recent works include the effect of Partial shading (PS) which is a recurrent phenomenon that takes place when some cells in the PV module or PV array are shaded by trees, bird litter, buildings, and passing clouds or any external object [27]. The performance of the PV cells is affected if all it is cells are not received equally illuminated [28]. We can classify the partial shading into two types: dynamic shading and static shading, the first one is a result of the moving clouds above the PV array. The static shading is a result of the impact of the PV string each other during the sunshine. The effect of the dynamic shading signification to the large-scale PV system. While the sun light will have reduced because of shading. The performance and the efficiency will reduce too. The problem in the shading states, that the PV cell will have based reversed and the losses will have appeared as a temperature [29]. A 30% the reduction in the performance of the cell can be observed because of the total shadow of just a single PV cell [30]. To treat the increase of the temperature which caused a hot spot because of shading the common solution is using by-pass diodes. The by-bass diode will behave as an open circuit, when shading is occurring the current will be mismatched and the by-pass diode will behave as a close circuit and the current pass through it. Usually, the PV module which contains 72 or 60 cells having 3 by-pass diodes [31]. The shading phenomenon effects the I-V curve and P-V curve of the PV cell. The researchers explain that there is possible to detect the effects of shading on the PV cell. The detection method depends on a comparison between I-V curves produced under shading circumstances with those produced in the regular operating circumstances [32]. In the large-scale grid connected PV power plants and even in the small PV systems. The effect of shading is very important and plays a vital role many researchers did not indicate the shadow that occurred by the PV string panels each other and did not refer to the distance between inter-rows [33-37].

The previous studies include another factor that impacted the performance of the PV system, the accumulation of soiling, and natural dust on the upper roof of PV modules leading to a significant retro gradation of the PV efficiency. The studies show that dust has an impact on the modules' performance in a desert climate. The outdoor experiments reveal that when the dust increased the soiling losses increased [38].

While another study shows that the output power of PV modules that are kept dirty(unclean) for more than six months, especially in arid areas, decreases by up to 50% [39]. Another study was carried out to determine the soiling losses in hot-day desert climate conditions. The study companies between four power plants in two locations rural and urban and used three various installation types (roof top-fixed tilt, ground mount-fixed tilt, and 1-axis tracking). The soiling losses in rural surroundings are more than the soiling losses in urban surroundings for the same PV system and the rooftop-mounted have soiling losses less than ground mounted, and they found that the light rainfall cleaning is about 61% effective compared to the manual cleaning. it is economical option for plants owners [40]. Development and research in PV systems focused on their studies on the efficient operation strategies, sizing, and design of these systems. A significant portion of the loss in glass normal transmittance. strongly based on synchronism of the dust accumulation density with the orientation of the PV modules face in terms of the predominant wind direction and PV module tilt angle [41]. Another study indicated that the electrical energy produced through the PV unit decreased due to the accumulation of dust on the unit. To know the decrease in the energy produced, a long-term economic analysis was conducted to assess the amount of energy decrease due to the accumulation of dust and to predict system efficiency and maintenance costs [42]. Another study determined the pollution rate of PV units for the purpose of developing a protocol to measure pollution in PV units that operate with a two-axis tracking system for countries located on the surface of the Mediterranean [43]. Another study refers to characterizing and the negative affecting of the dust on the performance mode of the PV module's surface. The research investigates the effect of accumulation of 13 different samples (clay, cement, coarse sand, salt, wood dust, stone dust, loam soil, charcoal, bird droppings, laterite, carpet dust, ash, and sandy soil) The study shows that the deposition(on PV module surface) of coal powder causes a significant deterioration in the performance of the photovoltaic unit by 98% due to its effect on light transmittance, while the effect of salt powder deposition on the performance of the photovoltaic unit was 7% [44].

Another study concluded that varying the tilt angle (during winter and summer) would enhance the photovoltaic system's performance and increase the amount of energy generated [45]. Another study indicates that using the manual system to change the tilt angle for each month leads to an increase in energy production compared to fixed systems, but it is expensive. The use of tracking systems leads to an increase in the productivity of the PV unit, but it is expensive in terms of operation and maintenance [46]. Another study compared a photovoltaic system that uses a two-axis tracking system that moves at a tilt angle between 13^o - 61^o throughout the year, and a fixed system with a tilt angle of 14^o. The results of the study showed that the rating daily gain of solar radiation was 29.5 %, for the tracking system which led to an increase in the amount of energy produced by 34.5 % compared to a fixed system for the same site [47].

Another study refers to the amount of yield gain increases in the case of using tracking systems by 15-35% or more compared to fixed systems, as well as saves space in the lands used [48]. According to another study classified sun trackers in accordance with their operating principles in to three kinds: the first is passive, these systems are characterized by devoid of electrical motors and controllers circuits, simple and, their accuracy is constrained. The second kind is microprocessor relies on software to determine the sun's location at every moment in time and to operate motors. These systems are usually utilized in large projects where one controller tracks several arrays because of their high cost. The third types are electro-optically trackers. The basic theory of working relies on the properly oriented illumination differences of two photo resistors. The motor is controlled by an electrical circuit until the resistance of the two photo resistors is equal. this sort of tracker is amazingly accurate so that installation should be very exact [49]. Another study that compared two systems, one fixed and the other tracking the sun, and both systems with the same capacity found that the energy produced from PV units that use a tracking system increases by 33% more than the energy produced from units that use a fixed system [50]. According to another study, the average amount of energy obtained by a solar panel in a single-track system is 1.35 times larger than the average amount of energy obtained by the same panel in a stationary system, while the average amount of energy obtained in a two-axis tracking system is 1.04 times larger than the average amount of energy obtained by the same panel in a one axial tracking system [51]. The energy payback time was determined by another investigation. It took two to five years to complete the investigation. The study's findings demonstrated that grid-connected photovoltaic systems can achieve an energy payback of 6 to 15 times over the duration of a 30-year lifespan [52]. Another study compared the energy produced from three systems: a two-axis tracking system, a single axis tracking system, and a fixed system for the same location. The energy produced from the systems was (38334, 37567, 33082) respectively Mwh per annum [53].

Another study, the researchers chose a mono crystalline photovoltaic panel, the panel was simulated by a pvsyst software, and the output power was measured. Then the temperature was changed (increasing the temperature) and the output power was measured. The researchers concluded that by increasing the temperature, the output power of the panel decreases, and this decrease negatively affects the efficiency of the panel [54]. Another study indicated to when the air temperature rises and the solar radiation increases, that leads to the temperature of the PV module will increase. The temperature of the PV module decreases with the increase in air speed. The PV module temperature may reach 50-65 Co (In the summer, at 12:00 noon). When the irradiation is very strong. the voltage and the output power decreased when cell temperature increased, While the cell current increased when cell temperature increased [55].

The inverter is an electrical device it converts DC/AC energy it is a higher performance device, But the inverter efficiency never reaches 100%, inverters operate at their best efficiency between 85 to 96 percent for rated power near to nominal rating. The overall number of losses for a single-phase inverter might range from 8 to 20 percent of the energy produced [56].

Another previous study included the effect of losses and capacity of the inverter on the performance of large photovoltaic stations. The study compared three types of central, string, and micro inverters. The results of the study showed that the central inverters produce (generate) the highest amount of energy and have the least number of losses. While string inverters produce modest amounts of energy and incurring moderate losses. micro inverters produce(generate) less quantity of energy and have caused more losses. The unit cost (one-watt generation cost) of central inverters is 0.31USD/W, string inverters are 0.406 USD/W, and micro inverters are 0.829 USD/W. The increase in inverter capacity led to a lower the unit production cost. The use of high-capacity inverters has a positive impact on improving the performance of large-scale stations [57].

Another study indicated that there are several options (methods) for connecting the PV array to the inverter. It compared these options (methods). The first method is to connect (link) all the PV arrays to the inverter, while the other two methods include connecting the portion (link) of the PV array to each DC level of the inverter and whether the connection is using a DC / DC converter or without it. The study concluded that in the case of the first connection, the voltages in all photovoltaic units(modules) are forced to be similar, as photovoltaic units that suffer from a lack of similarity and inaccuracy in orientation (for units that use tracking systems), as well as those that suffer from shading problem, will affect units that do not suffer from these problems. In the other two cases, the voltage control will be independent for each part of the matrix connected to a level of the inverter, and as a result, there will be higher accuracy in the event of a mismatch in the system (reaching the optimum operating point) that the use of DC / DC Between the inverter and the photovoltaic array enables the inverter to work at a constant and equal voltage for each input of the inverter inputs. Although it reduces efficiency and raises the cost [58].

Another study shows that the choice of equipment for a PV power plant is important in deciding how much the return rate of investment costs and maintenance, and operation costs should be calculated too. And it is shown in PV power plants there are two types of inverters that should be installed central and string inverters. The study compared the two types of inverters. The string inverter has many MPPT trackers, the system which includes the string inverter has much flexibility. Due to the string inverter's small capacity, when one (string inverter) fails, it has little impact on the overall performance of the entire solar power plant. In contrast to the central inverter, whose failure leads to a significant impact on the PV power station. The study shows that the cost of AC cable and equipment is greater when using string inverters to model and that the cost of DC cable and equipment is higher when used in central inverters [59]. Another study refers to galvanic Isolation which is one of the essential PV system specifications. It is safety reasons for some national codes in which the PV unit is linked to the low voltage distribution grid. The PV topology must be properly designed to meet this need because galvanic isolation prevents it from being standardized, a low- or high-frequency transformer is used to accomplish this. Additionally, the study refers to the codes and standards that appeared as a result of PV applications expanding. To provide a secure, high-quality, and consistent functioning The standard codes are continuously by international and national committees and governments to a safe high quality and normalized operation. The (IEC)(CENELEC), (IEEE)often define these international standards, Governments base their local rules on international norms while also taking into consideration regional characteristics like environment, grid layout, and the proportion of renewable energy to installed electricity. If the national codes are accepted by the international commissions, they can become an international standard such as German standards codes [60].

Another research refers to the lighting protection for the PV power plants. Lighting protection is a very important protection in the PV system, especially in the regions which classified as having the highest occurrence of lighting activities. Lighting protection is essential for PV systems from power generation losses and damage. the researcher shows according to the IEC 61173 standard which recommended to use surge protection devices (SPD) for PV system installation which is classified under IEC 62305 and IEC 61727 standards. The performance of the PV power plants will have decreased because of the Shadow which is a result of the installation of an external lighting protection system. when increasing the number of the lighting pole will increase the shadow on the top surface of the PV array. The study compared two lighting systems of lighting PV protection, the first one is, the air terminal lighting pole, and the second is the early streamer emitter lighting pole. The study results were that the air termination lighting pole is unsuitable for PV plants especially a crystalline and thin film [61]. another Previous study shows that the PV systems are installed under three divisions. The solar farm, residential, and commercial buildings. the residential and commercial sectors are installing PV systems on their roofs. There are many parameters, and factors that should be considered when a lighting protection system is designed. they classified the protection as internal and external lighting protection systems [62].

Another study refers to that PV systems are almost often situated outside or on rooftops, which raises the chances of lightning strikes. As a result, this would have an impact on both the economical side and the amount of power generated. system designers alike need to keep this in mind. Lightning protection in PV systems is highly significant and practically necessary to prevent flaws and equipment damage that result in severe impacts. The researchers' findings show that the position of the PV mounting system's grounding leg significantly affects how current is distributed under a non-isolated LPS (lighting protection system) [63]. Another study refers to, because of solar panels are installed in open and large areas they are usually exposed to the lighting strike. the strong electromagnetic field which is a result of the lighting strike which generates an induced extremely high voltage for underline cables. inverters and DC lines and the other requirement. In this study, the researcher modeled a lighting protection system by using a virtual surge test lab (VSTL) simulation and investigating the lighting effect on a large-scale solar power plant. They found that a properly designed lighting protection system can significantly reduce the induced voltage to an acceptable range and this can save the DC lines, the frames, and PV panels from both indirect and direct lighting effects. And they found the relation between the induced voltage which is a result of the lighting effect is increased with an increase in soil resistivity. hence, the solar power's location should be chosen at swampy or wetland because of low earth-resistance [64].

Another study indicated that studying the impact of losses in photovoltaic systems contributes to finding the appropriate size of cables that contribute to reducing the total cost of these systems. The study concluded that the cables used in the system must be within the voltage drop values and thermal limits [65]. Another study refers to PV system designers knowing that the voltage drop leads to system losses and this loss can be avoided by increasing the cable sizing and this will lead to an increase in the system cost. they tried to keep the voltage drop below 1.5% due to standers [66]. Another study focused on studying the impact of temperature on the DC cable and finding a solution to it to improve performance and predict generation. The study was conducted by installing DC cables in an arid region and semi-arid regions (the temperature ranges between 35-40 or more degrees Celsius). The study found a voltage drop reduce by 12 % to 18%. The study concluded that when choosing the appropriate DC cable size, it can save 2400 kWh - 5700 kWh annually, as well as reduce CO2 emissions by 1200 Kg - 3000 Kg annually. By using the suitable size of DC cable, cable losses may be reduced to around 1%, which results in a 1.8 to 2.4 times increase in energy generated. All these elements contribute to system balance and lower levelized cost of energy (LCOE) costs [67].

Another study refers to the several simulation programs. This simulation software is utilized in a feasibility study, sizing, of PV systems. and optimization of economical and technical analysis to avoid poor reliability, over size, and high installation cost [68]. Another study makes a comparison between SAM and PV syst software simulation, SAM program is designed to evaluate the performance and economics of PV systems. This software's advantages include ease of use, and the ability to manually add specific inverters and modules. The disadvantages of this software. Three-dimensional shadow creation is not offered by this program; no weather information is provided for any other global locations (just locations in the program). The pvsyst software simulation analysis the performance and financial estimation of

PV systems. the characteristics of this program it is having large databases of PV system components and weather information are two of this system's features. has the capacity to spot flaws in system design using a loss diagram; findings contain many simulation variables. The limitations of this software include the inability to perform shadow analysis and the inability to enlarge the program screen to see all parameters. According to the study's findings, pvsyst is more accurate and durable than ASM [69]. Another study refers to another software, HOMER. It is utilized for sensitivity analysis, technical analysis, and financial analysis. calculates the quantity and potential combinations of a list of several technologies [70].

Another research involved floating Photovoltaic systems. This kind of system float on the surface of irrigation canals, dam reservoirs, toiling ponds, and quarry lakes. floating PV systems witnessed a high expansion worldwide. Because of the low temperature of the water which cools the PV panels the electrically generated power is high than the system installed on land. Because of the floating system installed on the water surface. The land can be used for other purposes this type of PV systems is less obtrusive since they are generally hidden from public view a floating PV system helps to create fish-spawning environments and control algae [71]. Because of the numerous advantages of floating systems, it has attracted a wide attention, as a new power generation system. This kind of system can reduce water evaporation [72]. Another study refers to the types of floating PV installation is including two types: The canal top and offshore floating PV power plants. the research concluded Although the support structure for floating PV plants might cost up to 25% of the total project expenses, this sum is frequently less than what it would cost to obtain and prepare a similar piece of land [73].

Another study refers to the efficiency of PV installations effecting by the accumulation of dust specially in the desert areas and industrial areas, Regular cleaning of the PV panels is necessary to reduce this affection. Traditional cleaning can create cracks on the surface of PV panels because of harsh brushing, and manual cleaning consumes time and energy. The researchers developed a variety of techniques for the PV panels to self-clean coating, mechanical, and electrostatic techniques These techniques can clean PV panels with little energy and costs [74]. Another study shows that after 45 days of cleaning with non-pressurized water, a PV panel's efficiency will reduce to 50%. To solve this defect by using a minimum amount of energy and water. they found the efficiency of PV stayed the same when cleaning with a combination of cationic and anionic surfactants utilized [75]. Researchers have designed a model capable of cleaning the surfaces of the panels in the photovoltaic system. This device consists of a sensor unit, a cloud interface, and a robot equipped with a brush, and the cloud interface is used to control and monitor the robot that moves along the photovoltaic panels (array) back and forth. The researchers programmed the device to automatically clean, the sensor unit senses the level of dirt. The researchers concluded that the device is able to clean the system from the accumulated dust in a timely manner before the efficiency of the system is affected by the accumulation of dust on it. The system is applicable to big solar installations [76].

In another study, photovoltaic energy technologies (the three generations) were compared. The study concluded that the first generation, which is known for its high efficiency and low production costs, dominates the market, while the second generation (thin film), which is known for its lower costs of materials and manufacturing but is less developed than the first generation and has recently seen a decline in Market share, is also known for its lower costs of materials and manufacturing. Despite the third generation's great efficiency, light weight, and low price, it has not received extensive commercial marketing. [77]. While another study the researcher compared between types of PV system modules, the study found: That monocrystalline possesses a high level of efficiency, it is ideal for commercial applications has a high-power output, is less affected by extreme heat, is space-efficient, and has a long lifespan. It has a 20–25 percent efficiency, but the costs are high, the production process is cumbersome, and it requires a lot of labor. The second type of solar cell, known as polycrystalline, is less costly, less effective, sensitive to high temperatures, has a short life, and is not a space-saving solution. Its efficiency ranges from 15 to 20 percent. the thin film is adaptable easy to manufacture, much less expensive, and less affected by extreme heat, it is efficiency between 7 to 10 percent, a much shorter lifespan, within a few months of installation, the effectiveness of these cells declines by roughly 20%, they take up a lot of space and much less efficient [78]. Another study shows that greenhouse gases are produced during the production of electricity (traditional methods), but no gases are emitted during the generation of electricity using renewable sources of energy. The studies showed that photovoltaic systems require primary energy to manufacture the system's components before they can produce electricity. These gases are emitted by this energy. Moreover, by analyzing the various stages of these systems' component life cycles. The study concluded: Thin-film modules(panels) use less energy during manufacturing stages have a quicker energy payback time and emit less greenhouse gases, but their efficiency level is low. that while crystalline modules have good conversion efficiency, they also have very high substantial greenhouse gas emissions and energy requirements for energy payback [79].

PART 3

THE SOLAR ENERGY

3.1. SOLAR ENERGY INTRODUCTION

In the last decade generation of electricity by using sunlight has been resurgent exponentially all over the world. Either by concentrating solar power (indirectly) or photovoltaic (directly). Humans can benefit from 2500 terawatts of energy that comes from the sun to the earth's surface this amount of free and clean energy can be technically accessible by using solar technologies. Solar technologies these days are no longer expensive [80].

Figure 3.1. Photovoltaic (PV) solar power generation. Sudair /Saudi Arabia [81].

Figure 3.2. Concentrated solar power project. Nur Energie/Tunisia [82].

3.1.1. The Sun

The sun is the central star from our solar system. The separation distance between the sun and the planet earth is 1.496 $\times 10^{11}$ m (the astronomic unit, AU). The volume is approximately 13$\times 10^{5}$ that of Earth. The diameter of the sun is 1392$\times 10^{3}$ km. The mass of the sun is 1.993 $\times 10^{27}$ kg. It contributes to 99.68% of the solar system's overall mass. The pressure at the center is over one million atmospheres, 15$\times 10^{6}$ K temperature at the center, and 6000 K at the surface. The radiation of energy is equal to 38$\times 10^{26}$ W and the energy that the Earth receives is 1.7$\times 10^{18}$ W [83].

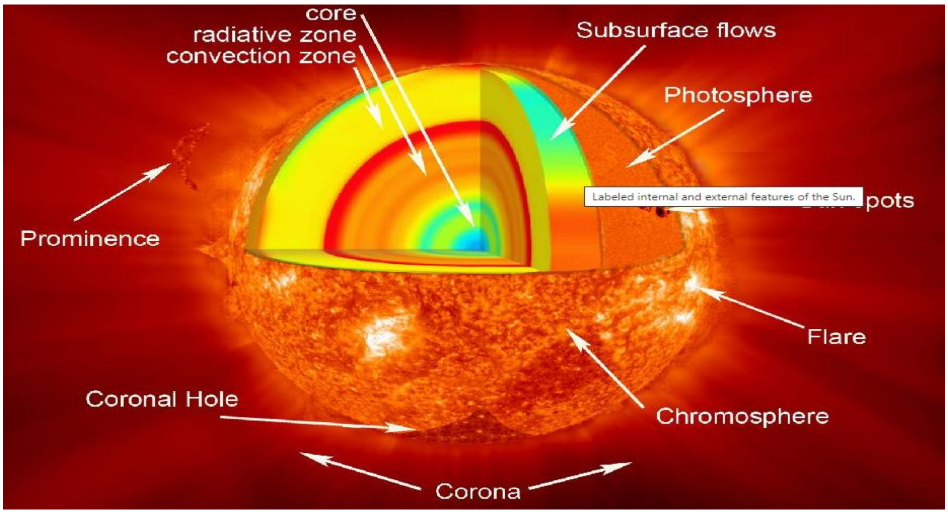

Figure 3.3. The sun schematic structure [84].

The sun star is completely made of gases. Sun has constants of an admixture of gases, hydrogen(H_2) is a larger portion (75%), Helium (He) 23%, and 2% other [85]. In the center of the sun, the pressure-temperature conditions are suitable, so nuclear fusion can happen. In the fusion reaction, which occurs in the sun and melts hydrogen into helium under a high temperature (15 $x10^6$ K), the results of this process the mass loss convert into energy which can be represented by Einstein's formula as shown in the following equation [83].

$$E = mc^2 \qquad (3.1)$$

Where:

E= The energy.
m= The mass.
c= The speed of the light.

From equation (3.1). every second 650 $x10^6$ t, of hydrogen, is transformed into 646 x 10^6t of helium each second. The difference between the two values is turned into energy. The sun radiates energy (4 million tons per second) away from it uniformly across all directions [86]. This is in good accordance with the Blackbody radiation equation for Plank as shown:

$$\omega_\lambda = \frac{2\pi hc^2 \, \lambda^{-5}}{e^{\frac{hc}{\lambda Tabs\, q}} - 1} \;\; (w/m^2 \,/unit\ wave\ length\,) \qquad (3.2)$$

Where:

h=6.63 $x10^{-34}$ (constant of Planck).
q =1.38 $x10^{23}$ joules per kelvin (Boltzmann's constant).
λ= The wavelength.
T_{abs}= Absolute temperature.

From the previous relation can be determine the sun's surface energy density yields. the separation distance between the sun and the planet earth is 1.469×10^{11} m (approximately 1.5×10^{11} m), The intensity of radiation that leaves the sun is comparatively constant intensity. The solar constant G_{SC}, it is the solar intensity of radiation that travelled through the distance 1.5×10^{11} m to the earth, it is equal to 1367 W/m^2.

The energy emitted from the sun can be divided into radiation for a material consisting of electrons and protons, which emanate from the sun and travels at a speed of 500 meters per second. It must be considered that the percentage of these electrically charged particles that reach the Earth is a few percentages. The second type of energy emitted is Electromagnetic radiation, which is emitted mainly by the photosphere. These radiations include both long and short-wave frequencies. If losses are ignored, the solar radiation flux density M_S, which is obtained from Stefan-Boltzmann's constant temperature with photons and degree of emission, decreases with the square of traveling distance. The M_S can be determined at the E_{SC} of the earth's atmosphere by:

$$E_{sc} = \frac{M_s \pi D_s^2}{\pi (2L_{Es})^2} \tag{3.3}$$

Where:

D_S= sun's diameter.
M_S= sun's radiation flux density.
L_{ES} = The separation between earth planet and sun

As a result of the movement of the earth around the sun (during a whole year) in its elliptical orbit, this movement leads to the occurrence of seasonal changes, resulting in the fluctuation of radiation occurring (during seasonal changes) at the earth's atmosphere rim [86].

3.1.2. Solar Radiation

The sun light is a form of electromagnetic radiation, And the light we see is a simple form of the total energy emitted by the sun. The visible light that we see is a little subset of the electromagnetic spectrum. the solar spectrum's wavelength, which ranges from 0.25 to 4.5 µm. The wavelength range between 0.25 to 0.30 µm is near to ultraviolet, and the part between 0.7-4.5 µm is near infrared. the visible light between (0.3 -0.7) µm [87].

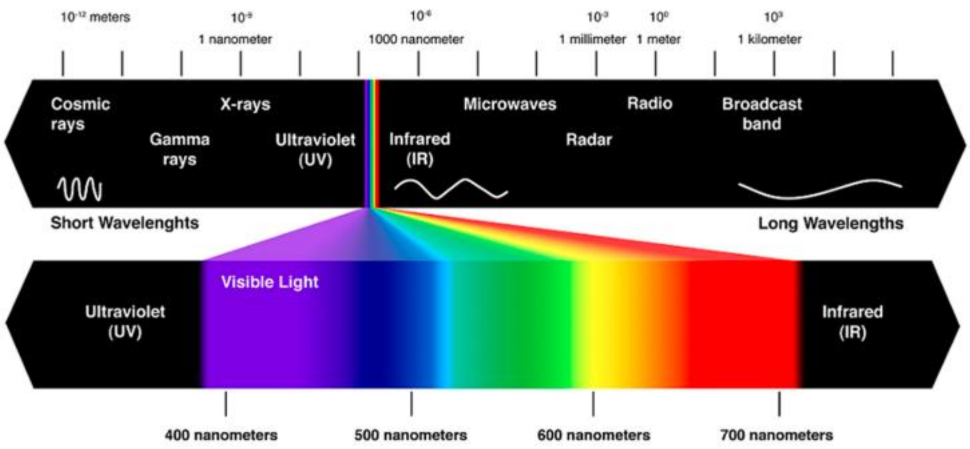

Figure 3.4. The Electromagnetic spectrum [88].

3.1.3. The Interaction of Solar Radiation with Atmosphere

A large proportion of sun light (solar irradiation) that inters the planet suffers from a series of absorption and diffusion in the atmosphere. Clouds reflect Solar radiation 20%, atmosphere components reflect 6%, and the earth reflects 4%. The quantity of solar radiation reflected outside the earth is estimated at about 30%, and the earth's surface absorbs 50% of the solar radiation either directly or diffused [8]. Diffusion process happens when the solar radiation changes his direction through the sky without energy transfer and energy losses, while the Absorption process is happening solar radiation converts it to other energy forms, in many instances, it is converting to heat. throughout that operation the global radiation G_g as a result of the operation of multiplying the transmission factor τ_G and the solar constant G_{SC} as shown in the equation [89].

$$G_g = G_{SC}\,\tau_G \tag{3.4}$$

Where:

G_g =Global radiation

τ_G =Transmission factor

G_{SC} =solar constant

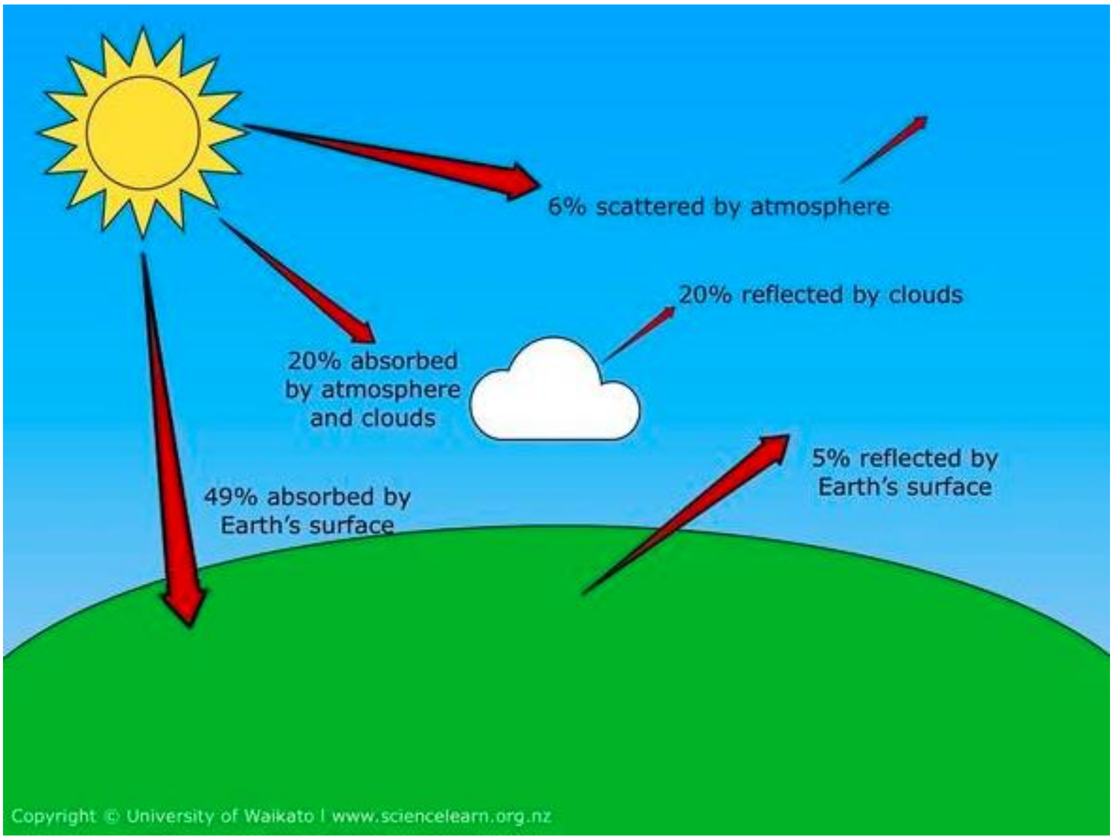

Figure 3.5. The sun light from the sun to earth through earth atmosphere [11].

3.1.4. Definition of Solar Radiation Parameters

Determining the real solar radiation for any specific site is very important subject for PV systems. There are some parameters by which we can describe the specific site of sun and time for any given point in the world. Some of these parameters are explained below:

- Any site on the earth's surface can be described from two angles, latitude (Φ) and longitude (ψ).
- Latitude Φ: It can be characterized as the angular site, south or north of the equator, it falls within the range; -90° ≤ 0 ≤ 90°. altitude is zero at the equator, it is positive at the locations between the northern pole and equator, and it is negative at the locations between southern pols and the equator. (90°< Φ <-90°).
- Prime Meridian is the meridian passing through Greenwich and it is the one chosen longitude, longitudes are measured from zero to 180° east of the prime meridian and 180° west (or -180°).

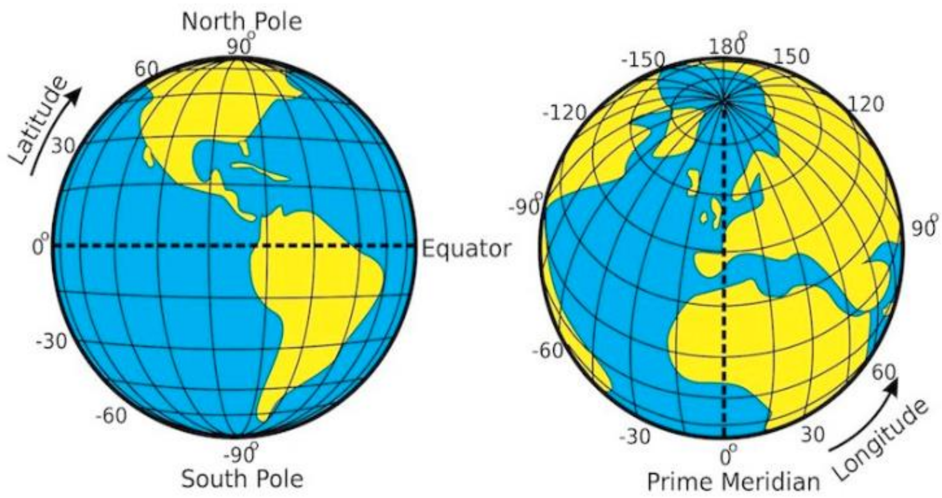

Figure 3.6. Geographical coordinates on earth [91].

- Solar Declination angle δ: it is the angle which formed between the equator's plane and a line drawn from the sun's center to the center of the earth. The days of the year determines the amount of it. at the northern of the equator and the sun is directly overhead the angle's amount positive, At the southern of equator and the sun position overhead the value of this angle is negative, it is a value between the range more or equal (-23.45°) and less or equal (23.45°). The relation below using to calculate the solar declination angle [92].

$$\delta = 23.45 \sin\left[\frac{360}{365}\left(n_{day} - 81\right)\right] \tag{3.5}$$

Where :

δ = angle of solar declination.

n_{day} = The day number (during the year) , where day 1 is January 1st and day 365 is December 31st.

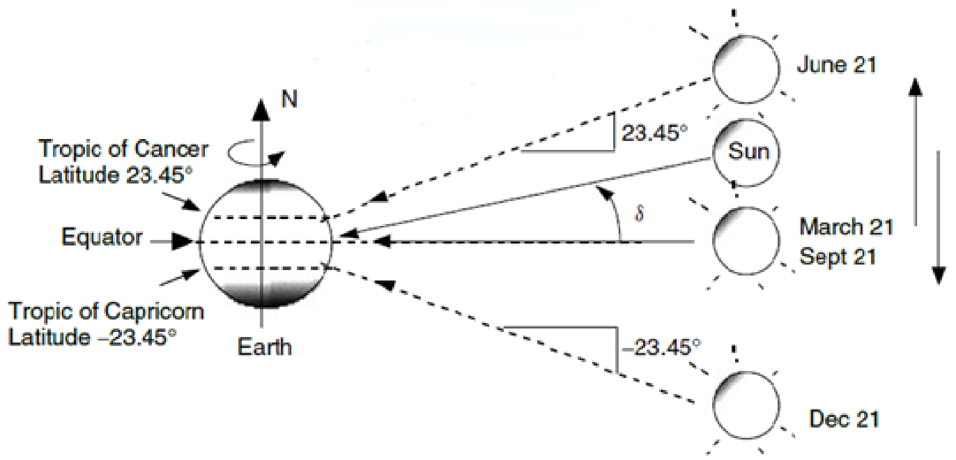

Figure 3.7. Solar Declination angle [92].

Table 3.1. Each month's first day [92].

Month	Each month's first Day(n_{day})
January	1
Fibruary	32
March	60
April	91
May	121
June	152
Julay	182
Augest	213
Septemper	244
Octoper	274
November	305
Decemper	335

- Azimuth angle ϕ_S: It is the compass direction from which the sun light is coming. When the sun sets in the west of the south, it has a positive value; when it rises in the east of the south, it has a negative value (sunrise). It depends on the day number,the latitude, and the most essential factor is the time of day. Azmuth angle uses true south as it is reference. in the southern Hemisphere Azmuth angle is measured relative to north (because of the sun is directly on the north). The following relation can find the azimuth angle [92] :

$$\sin \phi_S = \frac{cos\delta \sin \omega}{\cos \beta} \qquad (3.6)$$

Where:

ϕ_S = Azimuth angle
δ = angle of solar declination..
ω = Angle of the hour.
β = angle of altitude.

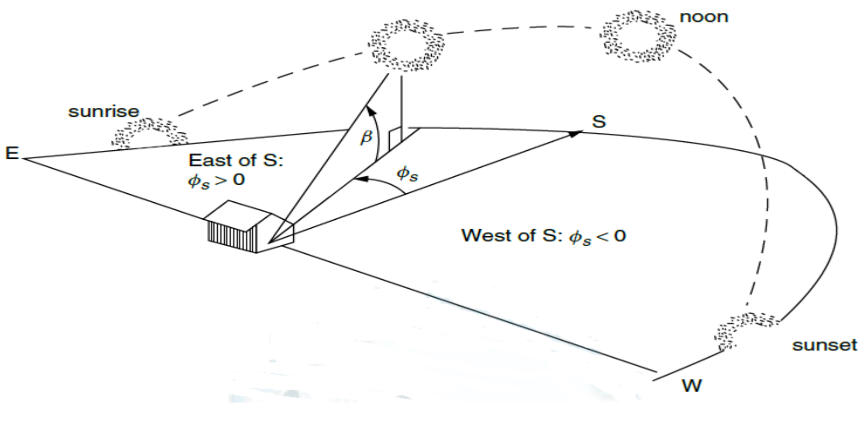

Figure 3.8. The altitude angle and it is azimuth angle [92].

- Altitude angle (β): It is the angle formed by the local horizon and the sun. when the sun just setting or rising it is at zero degrees, it is value at 90° degrees When the sun site overhead directly. It is depending on the day number, the latitude, and the most essential factor is the time of the day. The following relations can be used to determine the solar altitude angle for any given location and time [92].

$$\sin\beta = \sin L \sin\delta + \; cosL\; cos\delta\; cos\omega \tag{3.7}$$

And:

$$\beta = 90^o - L + \delta \tag{3.8}$$

Where:

L= The site's latitude.

- Tilt Angle: It's the angle in which the sun's ray will be perpendicular to the PV panel (Module) at the noon, it can have presented by the following relation [92]:

$$Tilt\ angle\ \alpha = 90^o - \beta \tag{3.9}$$

- Solar Hour angle (ω) is the number of rotational degrees (number of degrees) required by the earth until the sun will be directly overhead at the local meridian. The sun is directly above the sun's meridian, a particular line of longitude. The angle hour is the variation (difference) of the local meridian and the meridian of the sun, When the sun is directly overhead, it is zero, but before and after local solar noon, it has a negative value and positive value respectively. The earth rotates 15^o/h or 360^o in 24 h. The hour angle can be calculated by using the formula below [92]:

$$Hour\ angle\ (\omega) = \left(\frac{15^o}{hour}\right).(hours\ before\ solar\ noon) \tag{3.10}$$

Table 3.2. The relationship between the hour angle and time.

Hour angle in degrees(ω)	Solar time
90^o	Six hours following solar noon
75^o	Five hours following solar noon
60^o	Four hours following solar noon
45^o	Three hours following solar noon
30^o	Two hours following solar noon
15^o	One hours following solar noon
0^o	Sun overhead (solar noon)
-15^o	One hour before to solar noon
-30^o	Two hours before solar noon
-45^o	Three hours before solar noon
-60^o	Four hours before solar noon
-75^o	Five hours before solar noon
-90^o	Six hours before solar noon

3.1.5. Solar Radiation Types

There are three different forms of solar radiation:

1. Diffuse solar radiation (G_d): it can be defended as the ray directly reaching a specific location on the earth it can represent by light scatted by the dust particles and clouds in the atmosphere. this kind of radiation includes the albedo which is the reflected light from the ground or things like buildings and trees.
2. Direct (beam)solar radiation (G_b): it can be defined as the ray incident on a specific location on the surface of the earth after reaches from the sun in a straight path
3. Global solar radiation (G_g): It can be represented by the sum of diffusion and direct(beam) radiation in the horizontal plane .it can be represented by the following relation [86].

$$G_g = G_b + G_d \tag{3.11}$$

When calculating the total solar radiation, it must be taken into consideration that the direct radiation and diffuse radiation, have varying mean angles when they hit the receiving surface, and whose proportion is susceptible to seasonal and daily changes. when sky is pure the direct radiation is greatest, but when the clouds block the sun light the diffuse radiation is dominate, and the albedo is usually low; but it is extremely valuable in the sites which witnessed fallen snow, because of strong reflections [86, 87].

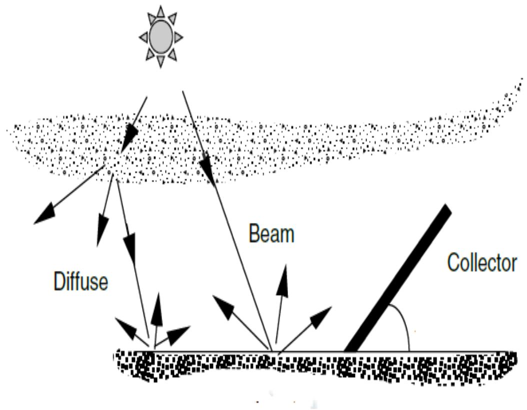

Figure 3.9. Light from the sun through the earth atmosphere [92].

3.2. PHOTOVOLTAIC SYSTEM

3.2.1. Photovoltaic Cell

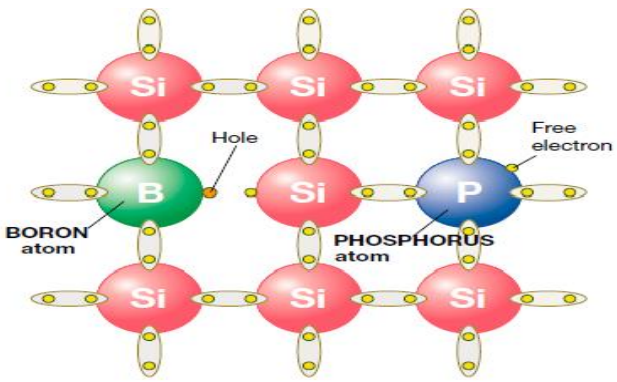

Figure 3.10. Doped silicon [93].

A photovoltaic (PV) cell is essentially a type of P-N junction that has been designed to convert sunlight into electricity. It is converting sunlight to energy but does not store it. It is a thin wafer of silicon surmounted by a tiny grid of metallic fingers that form one of it is contacts. the pure silicon change it is electrical properties when it is exposed to lighting or heating and it can be gradually converting it from an isolator state to a conductor state, to do that the silicon is doped with a very small amount of impurity atoms. boron or phosphorus is used in this process to get a P-N junction. Silicon has four valence electrons able to establish bonds with near atoms, boron has three valence electrons and phosphorus has five valance electrons. When the silicon is doped with phosphorus this process supplies an abundance of free electrons which are known as majority carriers and leaves behind here a few amounts of holes which is a result of the thermal generation of the electron-hole pairs, which are known as minority carriers. At the end of this operation, the N-type or negative-type material is created it is a reasonably good conductor. The same scenario is occurring when silicon doped with boron in this process supplies an abundance of the hole which is called majority carriers, and a few electrons known as minority carriers. at the end of this operation, P-type or positive type of material is created also, it is a reasonably good conductor. In this state there are two types of materials are created, n-type which has a large number of surplus electrons (N layer), and p-type material which has a large number of surplus holes (P layer). A p-n junction forms by joining p-type and n-type materials together. in the connection region between n-type and p-type materials. The free electrons in the n-type begin to diffuse and move towards (p-layer), because of this moving a negative charge layer or region is established behind the free electrons on the n-side. On the other side (p-type). The holds began diffusing and moving towards the n-side, as a result of this moving a negative charge layer is established behind holes which leave n-side .as a result of this an electrical field is created through the P-N junction, this field is known as depletion layer or region, which resist further diffusion of charges. The junction permits current to flow in one direction by applying a voltage from an external source (behave as a diode [87, 93].

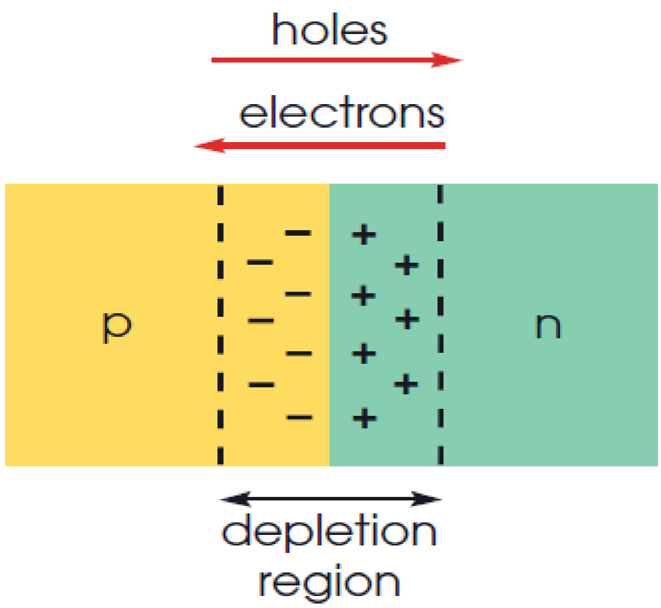

Figure 3.11. The P-N junction [87].

Interaction of photons falls from the light of the sun with the atoms in the PV cell produces an electron-hole, ‘in both the n-region and p-region. The interior electric field separates the extra electrons from the holes (resulting from photon absorption by portion of the material) and pushes them in opposing directions in regard to one another. In a semiconductor material, the energy gap between the conduction band and valance band is minimum electrons can facilely travel to the conduction when they gain enough energy from an external source (sunlight, luminous radiation, or heating), and this process is known as the photovoltaic effect [93].

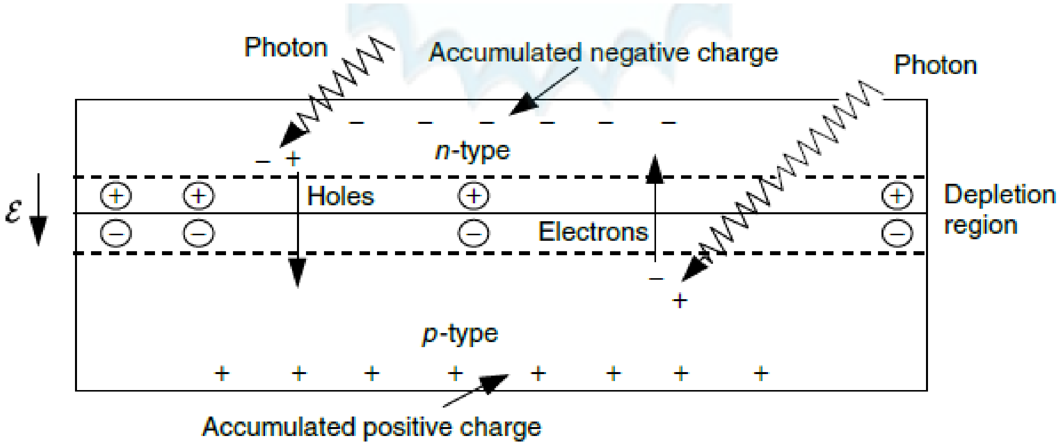

Figure 3.12. Creating the electron-hole pair by effect of photons [92].

The strong electric field prevents the electrons from turning around after they have left the depletion region (work as diode) and prevent it's return in the reverse direction. When the junction relates to the external conductor, a closed loop (circuit) is formed .in this circuit the current flow from the layer having high potential (N-layer) to the layer having lower potential (P-layer) the amount of generated current depending on the amount of the light(sunlight)that the cell exposed, this current known as photon current (I_{ph}) [93].

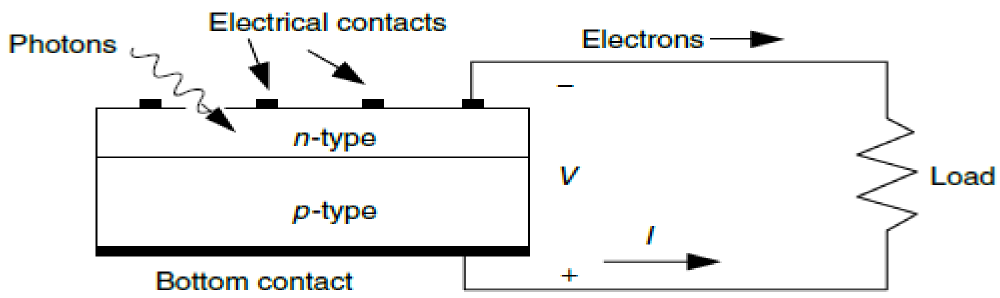

Figure 3.13. The photovoltaic cell working principle [92].

3.2.2 The Equivalent Circuit of Photovoltaic Cell (Solar Cell)

Understanding how a solar cell's electrical system operates requires to making an equivalent electrical module based on readily study able and analyzed known electrical components. The ideal solar cell module can represent by an electrical current source and diode; However, in practical terms, there is no ideal solar cell. Therefore, resistors are placed in the parallel and series as a simulation of reality as illustrated in Figure 3.14 [92].

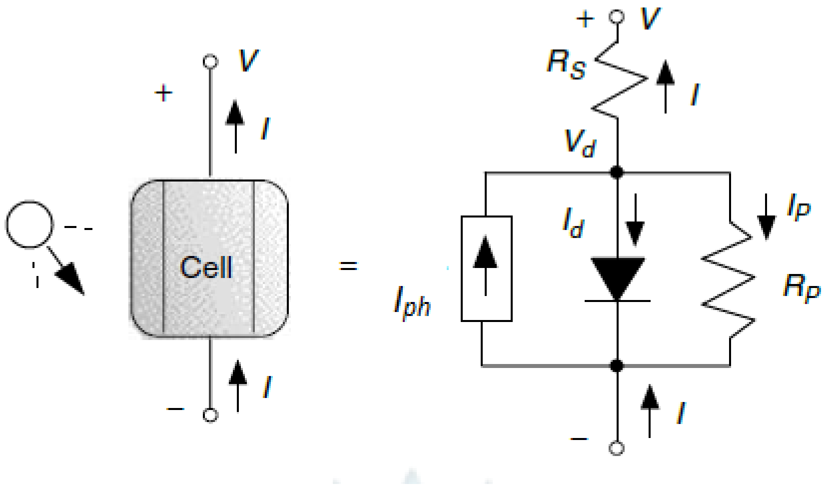

Figure 3.14. Equivalent circuit for photovoltaic [92].

It is simple to understand how series resistance works physically since it displays the current flow in the circuit that is provided by the contacts, fingers, bus bars, and the cell's bulk semiconductor material. The designer of the PV cell keeps the series resistance value as small as possible the amount of R_s can be represented by the relation below [87].

$$R_s < \frac{0.01\ V_{oc}}{I_{sc}} \tag{3.12}$$

The shunt resistance is more enigmatic, due to the non-ideal nature of the p-n junction, the amount of R_p can be represented by the relation below [87].

$$R_p > \frac{100\ V_{oc}}{I_{sc}} \tag{3.13}$$

The solar cell is handled as a normal diode in case of the absence of sunlight. a diode current (I_d) is produced and flows through an external circuit when a PV cell is connected to it. Without the sunlight, the solar produces no voltage or current. When charge carriers traveled gradually from the semiconductor to the electrical conductor, leakage current and voltage drop began to occur. The output current on the terminal of the circuit shown in Figure 3.14 can be determined by subtracting I_p and I_d from I_{ph}.

The parallel resistance R_p describes the leakage current, and the voltage drop has described by the series resistance R_s and The flattening of the solar cell's I-V characteristic curve is illustrated by the combination of parallel resistance and series resistance. [94].

PV equivalent equation circuit in the standard form can be represented mathematically in the following relation. by using the diode Shockley equation and Kirchhoff current low (KCL) [92].

$$I = I_{ph} - I_d - I_p = I_{ph} - I_o\left\{e^{\left(\frac{q_e\,(V+I\,R_S)}{q\,T_{mod}\,A}\right)} - 1\right\} - \left(\frac{V + IR_s}{R_p}\right) \tag{3.14}$$

Where:

I_{ph}= photon current.

I_o=saturation current.

I_d= diode current.

q =Boltzmann constant.

I_p =shunt current.

q_e =electron charge.

R_s= The PV cell's series resistance.

T_{mod}= Module temperature.

R_p= The PV cell's parallel resistance.

A=ideality factor.

3.2.3. The Solar Cell's Current and Voltage Characteristics (I-V) and Parameters

The curve of the I-V characteristics is shown in Figure (3.16). when sunlight falls on the solar cell or module surface, the terminals of the cell or module will produce an open-circuit voltage (VOC) when they are not connected to a load, but there is no current flowing(I=0). When the two terminals (positive, negative) of the cell or module are connecting (the PV module is not harmed by that) in this case, I_{SC} short circuit current will flow (I_{SC}=I_{ph}); but there is no output voltage, and it value equal to zero. In the two instances, no power was generated (no power at the ends of the I-V curve) [92].

The open circuit voltage can be calculated by using the below formula [83].

$$V_{OC} = \frac{qT_{mod}}{q_e} \; ln\left(\frac{I_{ph}}{I_o} + 1\right) \tag{3.15}$$

Where:

q =Boltzmann constant.
T_{mod} = module temperature.
q_e = electron charge.
I_{ph} =Photon current.
I_o = saturation current.

By using the below relation can be find the photon current in the cell [83].

$$I_{ph} = q_e G \; (L_N + W + L_P) \tag{3.16}$$

Where:

I_{ph}= photon current.
q_e = electron charge.
$L_N L_P$= the minority-carrier diffusion length for electronics and holds.
G= uniform generation rate.
W=The depletion region's width.

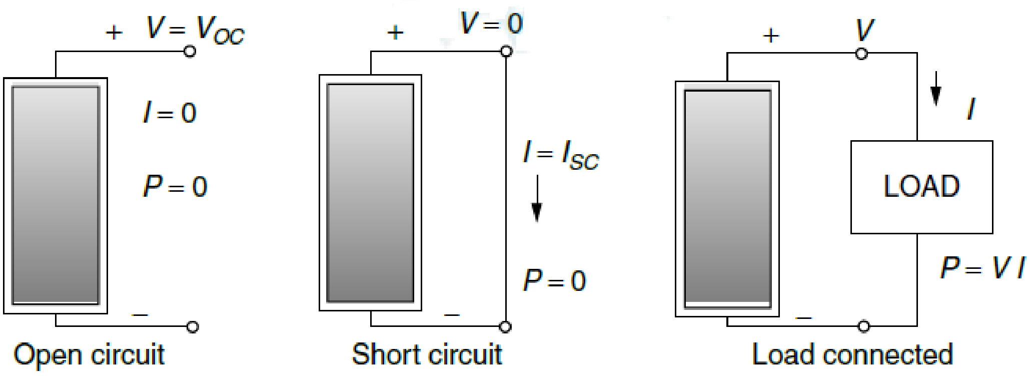

Figure 3.15. PV module in (open circuit ,short circuit ,and when connected to a load) states [92].

The I-V curve also shows the amount of power generated when the voltage is produced and the current flow in the case of the actual load is connected as shown in Figure (3.16). when the current (I_{mpp}) and voltage(V_{mpp}) are multiplied, when they reach their maximum value, it produces the point (MPP) on the I-V curve near the knee. Fill Factor is another parameter often used to describe cell or module performance it is a ratio that measures how much power there is at the maximum power point divided by the product of the short circuit current(I_{SC}) and the open circuit voltage (V_{OC}). The fill factor can be represented mathematically by the flowing relation [92].

$$Fill\ factor\ (f.f) = \frac{Power\ at\ the\ maximum\ power\ point}{V_{OC}\ I_{SC}} \quad (3.17)$$

Where power (MPP) represented in relation.

$$Power\ at\ the\ maximum\ power\ point\ (P_{mpp}) = I_{mpp}V_{mpp} \quad (3.18)$$

So the

$$Fill\ factor\ (f.f) = \frac{I_{mpp}V_{mpp}}{V_{OC}\ I_{SC}} \quad (3.19)$$

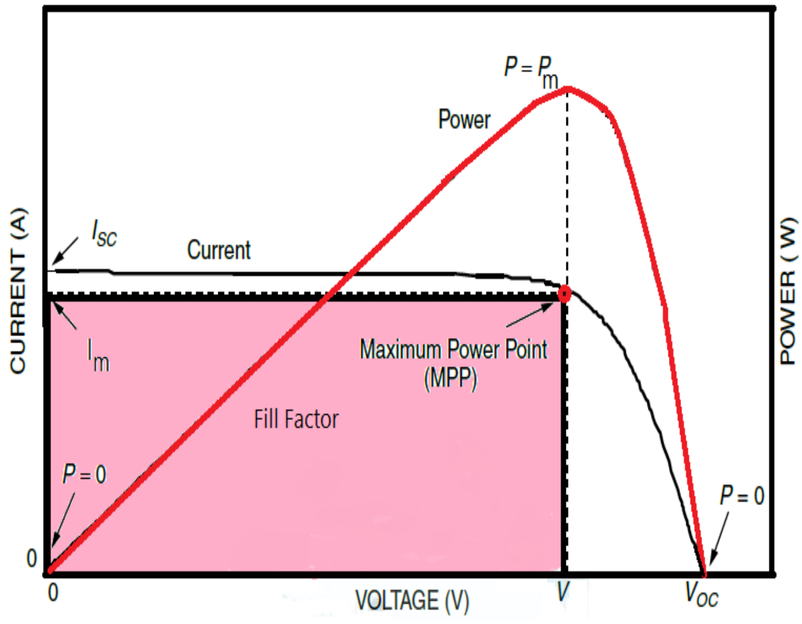

Figure 3.16. I-V characteristics curve[92].

Conversion efficiency is known as the proportion of power that is measured at the maximum power point divided by the incident light power (input power) it is represented by the below relation.

$$\eta_{con} = \frac{P_{mpp}}{P_{incident(input\ power)}} = \frac{I_{mpp}V_{mpp}}{A_{mod}G_a} = \frac{I_{sc}V_{OC}f.f}{A_{mod}G_a} \quad (3.20)$$

Where:

A_{mod}=The area of the PV module or cell(m^2).
G_a= The ambient irradiation (W/m^2).

Because of the changing in the value of insolation and the temperature of the PV cell is not stable around the day hour. The V-I curve is changing and it is affected by these changes. with a view to allowing fair comparison of one solar cell or module to another. There are now recognized (STC)standard test conditions. Performance parameters (I_{SC}, V_{OC}, V_{mpp}, I_{mpp}, and conversion efficiency)of the PV module are consistently mentioned by their manufacturers in their datasheets under (STC) and

(NOCT) Normal operating cell temperature. cell temperature, not ambient temperature, it can represent mathematically by using the below formula [92].

$$T_{cell} = T_{amb} + \left(\frac{NOCT - 20^{O}}{0.8}\right).G \quad (3.21)$$

Where:

T_{amb}= Ambient temperature.

G=Solar radiation.

Table 3.3. Test conditions reference [92].

Test condition	Solar radiation	Temperature C^{o}	Air mass
STC	1000 W/m^2	25^{o}	1.5
NOTC	800 W/m^2, wind speed 1 m/s	20^{o}	1.5

3.2.4. Insolation and Temperature Impact on the I-V Curve

The performance of a solar cell or module is significantly influenced by temperature and insolation. Whereas the I-V curve is a function of the performance of the cells or modules, Figure 3.17. Shows the impact of irradiation on the I-V curve, when irradiation decreases, the short circuit current will decrease proportionally, while the open circuit voltage (V_{OC})also decreased (small effect); But it does so in a logarithmic method, resulting in little variations in V_{OC} [93].

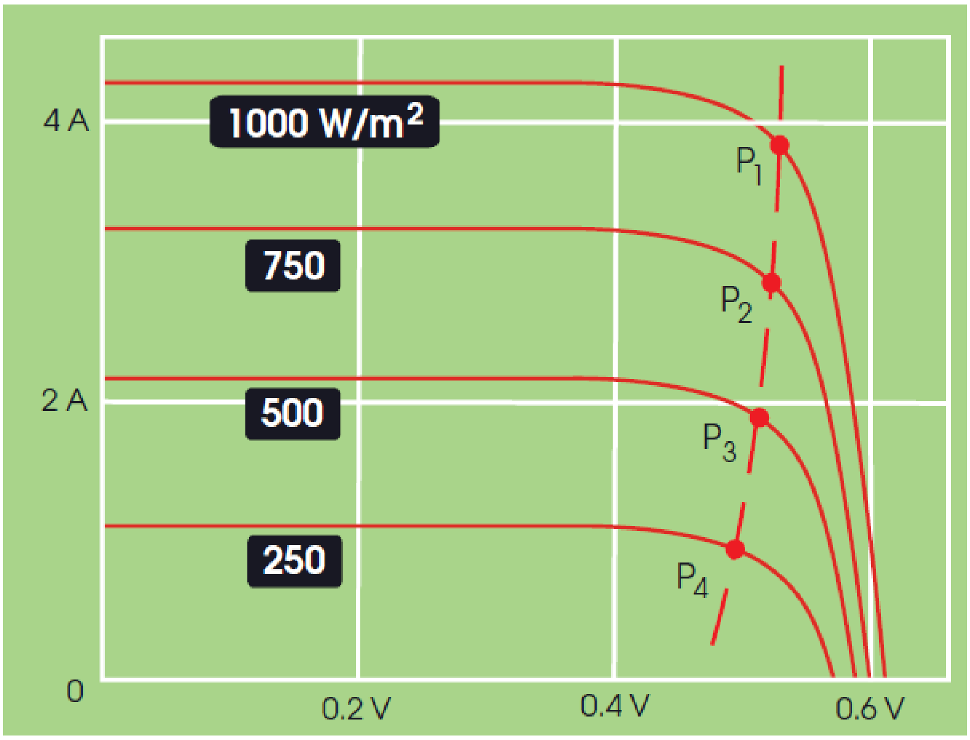

Figure 3.17. The I-V characteristics curve's relation to radiation [87].

When solar cell /module temperature rises. The short circuit current (I_{SC}) increases only slightly, while the open circuit voltage (V_{OC}) is significantly reduced. The performance of the module is better on clear, cold days than on hot days [92]. Figure 3.17. shows how the maximum power point (MPP) changes on the I-V curve as the maximum power P_{mpp} value decreases, shifting it downward and to the left., when solar cells suffering to lower radiation or high temperature.

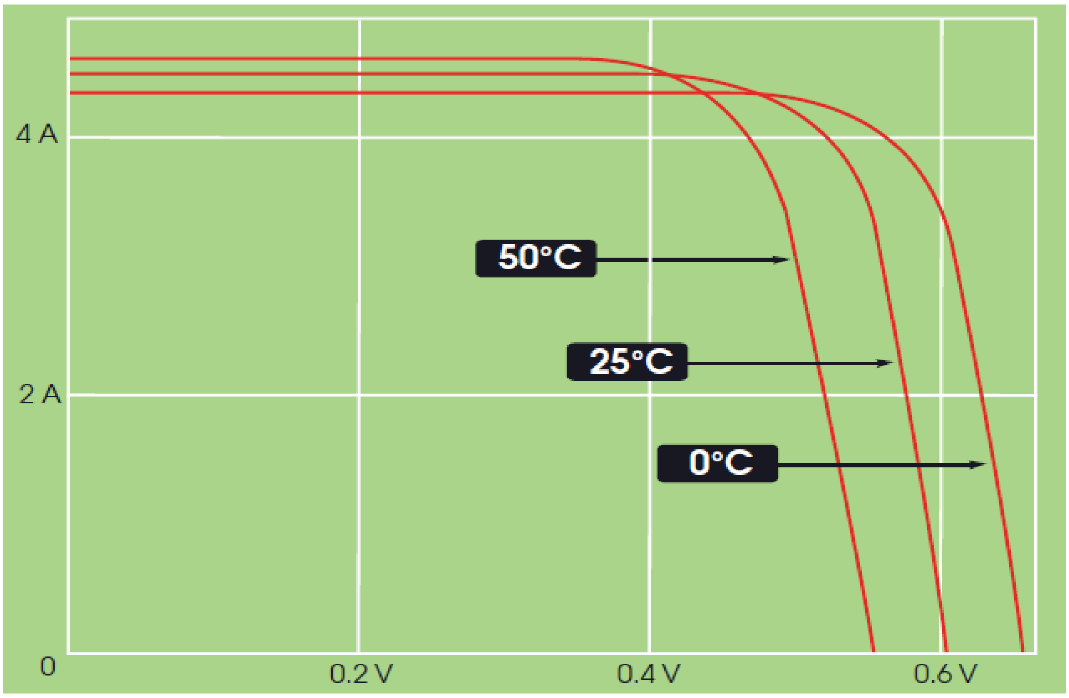

Figure 3.18. The I-V characteristics curve's relation to temperature [87].

Conversion efficiency is not affected by the decreasing of irradiation or increasing of temperature directly, which mean that the conversion efficiency is the same both on clear, cold as well as cloudy or hot day. Therefore, the smaller power generated with a cloudy sky or cold day can be referred no drop in efficiency but reduced protection of current and voltage because of lower solar irradiation or high temperature. The efficiency of the PV module is a vital point in choosing the PV module to be used, it is affected by temperature. The formula below shows the relation between the efficiency and temperature of the PV module [95].

$$\eta_{pv} = \eta_{ref} * \left[\frac{1 - \beta_{pv(T_{amb} - T_{ref})}}{100}\right] \tag{3.22}$$

Where:

η_{ref}= Module efficiency at STC.

β_{pv} = Temperature coefficient of module (%/C^O).

T_{ref} =Reference temperature.

T_{amb} =Ambient temperature.

Table 3.4. The characteristics of PV modules for various standard technologies [95].

PV module type	NOCT (C^{O})	β_{pv}(%/C^{O})	η_{ref} (%)
Poly silicon	45	0.4	13
Mono silicon	45	0.4	11
CdTe	46	0.24	7
CIS	47	0.26	7.5
Amorphous silicon	50	0.11	5

3.2.5. Photovoltaic Terminologies Definition

1. Solar cell: It is the smaller unit in the PV system. It is a p-n junction device made from thin wafer silicon, has a high sensitivity to light, and is capable to convert sunlight to electric current directly. This device is surrounded by a front and back electrically conductive cover, only one solar cell produces roughly 0.5 volts and could provide power between 1-1.5 watts.
2. PV module several solar cell units are connected in series and arranged parallel in rows (parallel link).to obtain suitable power. The multiple modules are connecting solar cells (in series and parallel) to the increased output voltage and current.
3. PV panel: The most fundamental part of a solar power system is the PV panel. It describes a collection of modules that have been packaged or pre-wired off-site. The panel size is Identified According to the designer's desire.
4. PV array: It describes a collection of panels interconnected with each other for a particular function. the photovoltaic generator has more than one set of PV array which is called sub-array [92].

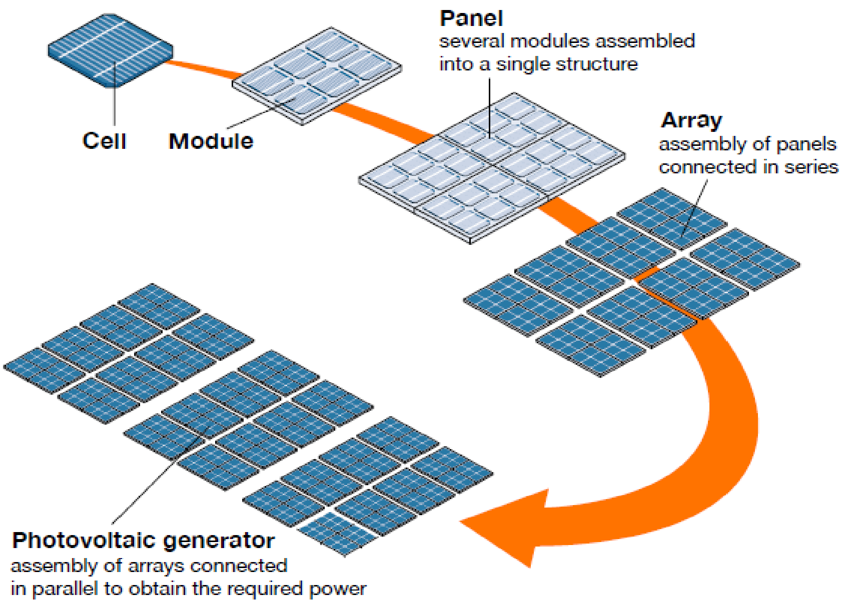

Figure 3.19. The PV cell can be combined to be PV module, panel and PV array [93].

3.2.6. Types of Photovoltaic Cell and Modules

Photovoltaic modules /cell are one of the components of the PV system modules that comes in different configures of material, efficiency, cost, and size. PV modules' task is to convert solar energy into electrical energy (in the form of direct current DC). There are various kinds of module materials and technologies used like:

3.2.6.1. Technology Based on Crystalline Silicon

The solar cell is composed of (single junction) one layer of high absorbing material or multi-junction (utilizes various physical configurations). crystalline silicon subdivided into monocrystalline cell and multi (poly)crystalline silicon cell [77].

- Monocrystalline solar cells/modules are manufactured of high purity, a single, uniform, thin silicon crystal. It is distinguished by it is hexagonal form and dark crystal appearance. It has an efficiency of 20 to 25 percent (rate of efficiency is high), high output, less effect by high temperature, space-efficient, long-life span, highly suitable for commercial application, the expensive manufacturing process is slow [78].

Figure 3.20. Mono crystalline module [93].

- Polycrystalline solar cells/ modules are manufactured of multi-grains of silicon crystals. Its appearance is a brilliant blue and has distinct squares. Polycrystalline modules are the most prevalent ones on the market. They account for 70 percent of all the world's PV modules used. It has an efficiency of 15-20% less efficiency, less expensive, shorter life duration, sensitivity to high temperatures, and is not space efficient [78].

Figure 3.21. Poly crystalline module [93].

3.2.6.2. Thin Film Technology

In this technology thin layers of PV material are layered on a foundation like plastic, metal, or glass to produce modules. Less than 1% of the silicon used in the production of crystalline modules is contained in the finished product, thin film efficiency of 7-10%. It is flexible, because of the economies of scale the price is much lower, easy to produce, high temperature has less of an impact on the modules, is much less efficient, they occupy a lot of space, during the first few months after installation the efficiency of these cell drops by roughly 20%, much shorter life, less than 1% of the silicon used to make crystalline modules is contained in the finished product. [78]. This technology is divided into Amorphous silicon PV cell(a-si) and non-silicon-based PV cell (polycrystalline technology) which are subdivided according to the material used as [77]:

- Solar cells are made of cadmium telluride (cdTe).
- Gallium Arsenide (GaAs).
- Solar cells are made of copper indium gallium diselenide (CIGS).

Multi-junction technology and Silicon cells in the form of strings or ribbons are two other promising PV cell technologies. [92].

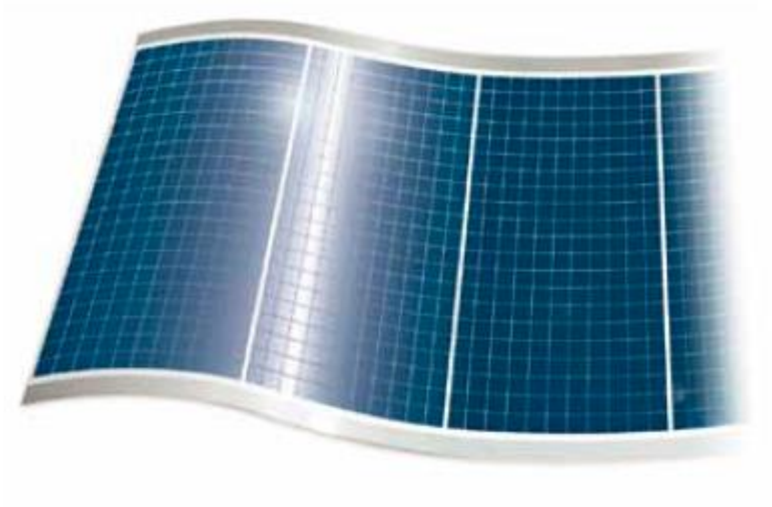

Figure 3.22. Thin film technology [93].

3.2.7. Series and Parallel Module Configuration

To increase the voltage, it is possible to connect modules in series, to increase the current It is possible to connect modules in parallel. From the Figure 3.23. Module in case of series connection can be presenting by adding I-V curves along the voltage axis. Adding together each individual module yields the total voltage at any given current (which flows through each of the modules) [92].

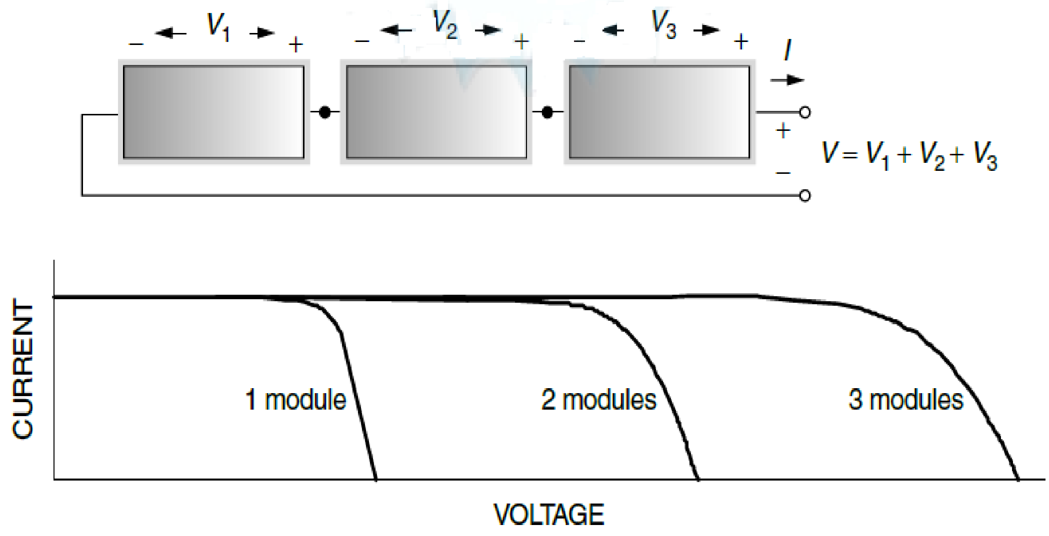

Figure 3.23. Series Module Configuration [13].

In a parallel connection, each module has the same voltage and the overall current equals the sum of currents. The I-V curve of a parallel combination at any voltage given is Adding together each individual module yields the total current as shown in Figure 3.24 [92].

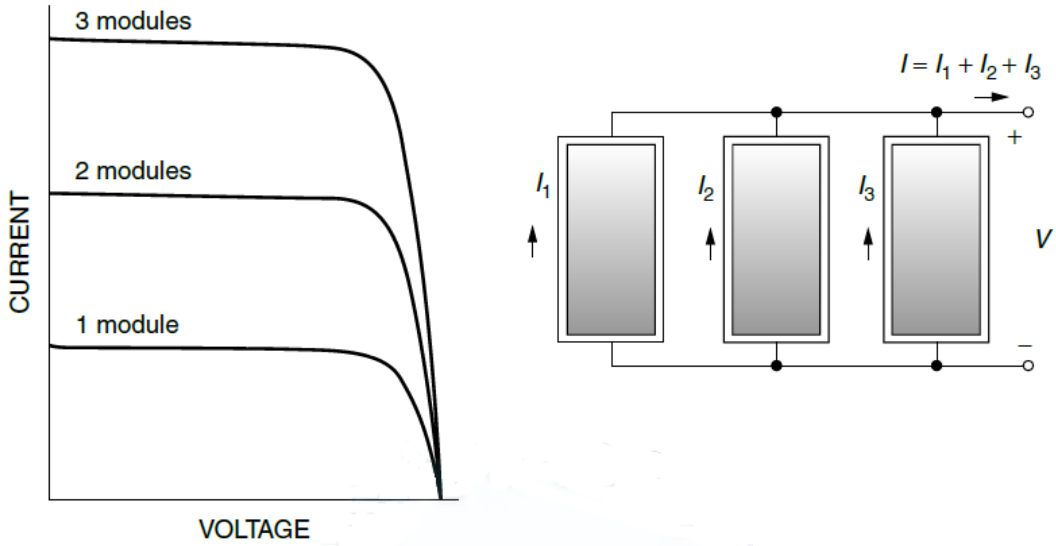

Figure 3.24. Parallel Module Configuration [92].

When a lot of power is required, the array will normally be made up of several series and parallel modules. in this case, the adding together every one of modules I-V curves yield the total I-V curves. combining modules in series and parallel can be wired in two ways [92]:

- The modules in a series could be arranged as strings and connected the strings in parallel (modules in series that are linked in parallel) as shown in Figure 3.25.

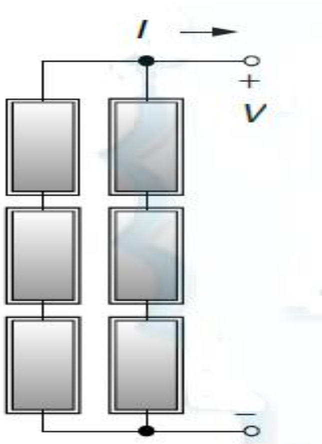

Figure 3.25. The strings wired in parallel [92].

- The parallel modules may be connected first (one unit), then could be connected in series as Figure 3.26.

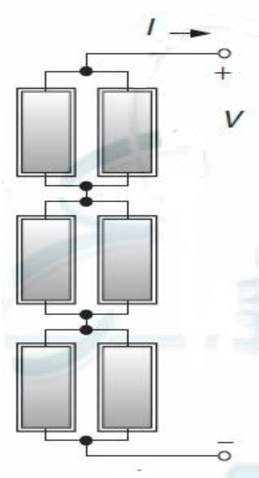

Figure 3.26. Modules in parallel that are linked in series [92].

Adding together each individual module's I-V curves yields the total I-V curves, which, in both cases, it is similar when everything is operating properly. When a whole string is off (unavailable)for any circumstance. The array may continue to provide the required voltage to the load; but the current will be reduced, which differs when a parallel set of modules is withdrawn from the service (that is the reason to choose the connecting of strings in parallel form) [92].

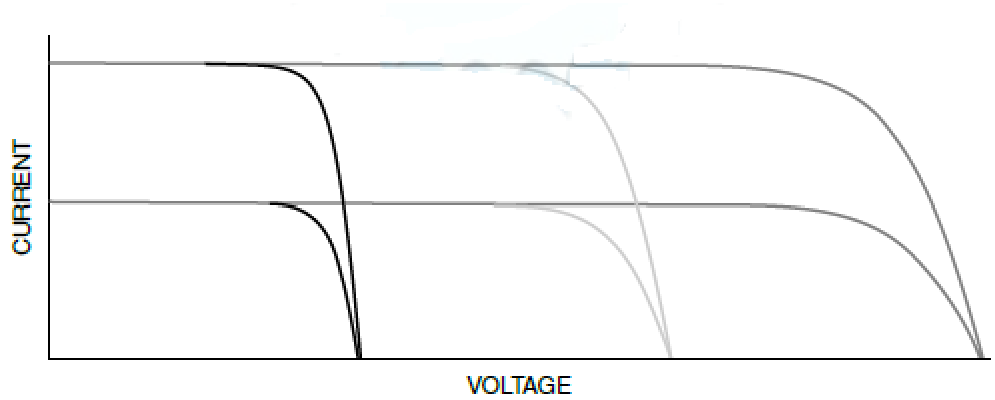

Figure 3.27. Typical I-V curves of a series/parallel module combination [92].

3.3. INVERTERS OF PV SYSTEMS

The inverter is the most important device for converting DC electricity (direct current) supplied by a photovoltaic array into AC power delivered to the grid. Inverters are used Advanced electronics to generate alternating current power (AC) at the suitable frequency and voltage which correspond with the grid supply [87]. Figure 3.28. Shows the inverter has three phases. The optimum switches for the circuit can be chosen based on the required power and voltage. to create a square wave voltage by turning on and off (S1 S4, S3 S6, S5 S2) at the required AC frequency (inverter output). It is a simple control strategy, but it contains high harmonic voltages and currents. To adjust load voltage control and lessen harmonic distortion, pulse width modulation PWM (high frequency) techniques can be used. When magnetic fields are irregular, harmonic content can cause overheating and affecting on the overall operation [97].

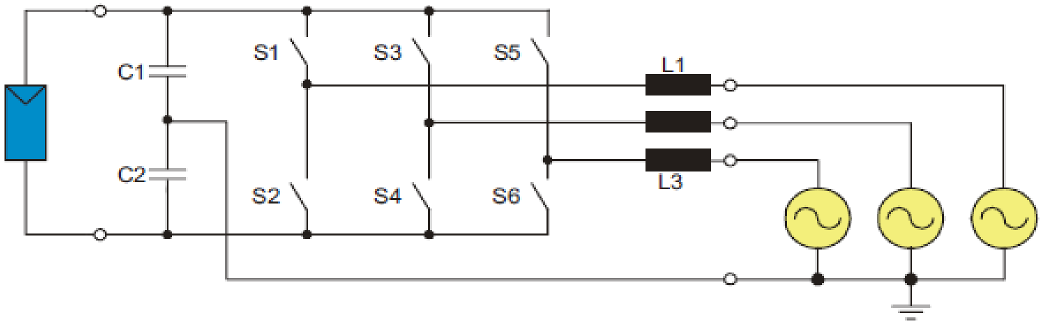

Figure 3.28. Three Phase Full Bridge Inverter [96].

Inverter devices should be having the ability to control with PV array's power output under a variety of sunlight circumstances. To enhance the generation of energy, most often utilized the Maximum Power Point Tracking (MPPT). The inverter can convert DC to AC with an efficiency of up to 98 percent, while efficiency drops significantly when it is run at a power level that is less than roughly 25 percent of its maximum rating [87].

The efficiency refers to the proportion of available solar energy that is converted and supplied to the electric grid. inverters typically have an overall efficiency of 92 to 98 percent. Inverters usually spend about 4 to 8 percent of the energy they convert during the conversion process [97]. inverter efficiency can be represented in the following formula [98].

$$\eta_{ivcerter} = \frac{P_{ACoutput}}{P_{DC\,input}} \tag{2.23}$$

The conversion efficiency is not constant and is affected by the Dc power input, operating voltage, and environmental factors such as temperature and irradiance. Inverters can be classified according to the size and topologies as:

- **Central inverters:** This type of inverter is used for large-scale PV plants whose sizing rate is between 100kW-1MW or more. as shown in Figure 3.29. the central topology connects thousands of photovoltaic panels (PV panels) to one inverter. PV panels are connected to form PV arrays. Each array has hundreds of parallel strings connecting to it (by combiner box) and each string is consisting of hundreds of PV panels connecting in series, so as to provide a high string voltage (H.V) string. Central inverters are known for reliability and ease of installation, but a drawback is that each string's maximum power point tracking (MPPT) is absent. And the second drawback is increased mismatch losses (losses occur when several modules with different characteristics are utilized in the same array). This might lead to troubles with arrays which that have different tilts, different orientation angles, suffer shading or have various module kinds [99].

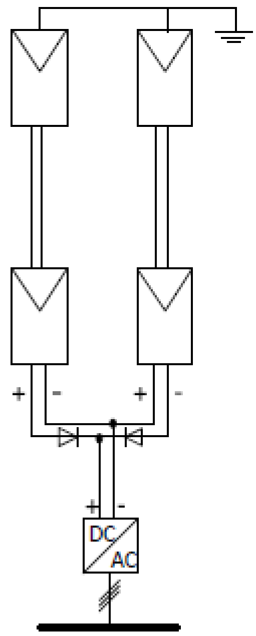

Figure 3.29. Central Inverter [2].

These types of inverters are typically 3-Phase and could contain a grid transformer (grid frequency transformer). It is including galvanic isolation from the grid. Sometimes need a national electrical grid is connected [99]. master-slave configuration of central inverters is sometimes utilized when irradiance is low, some inverters shut down enabling the remaining inverters to function close to ideal loading. when the irradiance is high all inverters share to load. Acting one time only the needed number of inverters are operational. the design life can be increased since the running time is divided equally across the inverters [99].

- String inverters: One string of modules is connected by these inverters as shown in Figure 3.30. The power range of string inverters is between 1-3 kW [87]. MPPT is offered at the string level, with each string independently of the others it is important When modules can't be arranged in the same orientation, modules with a variety of characteristics are utilized, or if there a shading problems occurs.

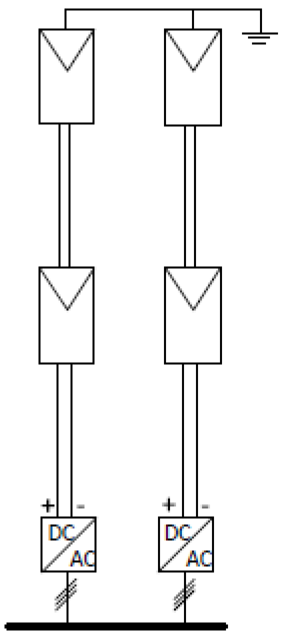

Figure 3.30. String Inverter [2].

This type of inverter is usually a single phase. the advantage of string inverters, firstly non-specialist workers can service and replace the unit. Secondly, having a spare string inverter on hand is practical. This makes it simple to deal with unanticipated scenarios, such as inverter failure. In contrast, a large central inverters failure along the repair period might lead to considerable yield losses before it can be replaced [99].

The converter efficiency in string inverters is high (up to 97.8%) because the string inverter is placed near the string module which leads to reducing the DC cabling used to connect. The string inverter has a high component's cost [60].

inverters can either be transformerless or use a transformer to set up the voltage as shown in Figure 3.31. the PV-generated voltage must be more than the AC side (grid) voltage in the case of transformerless string inverters, or DC to DC setup converters must be utilized. the advantages of the transformerless inverters are High efficiency, lower weight, smaller size, and low cost; but on the other hand, additional safety equipment such as DC sensitive earth leakage circuit breaker must be utilized and the live part should always be protected. The installation as a whole should be protected with IEC protection (class II), as inverters without transformers can produce more electromagnetic interference [99].

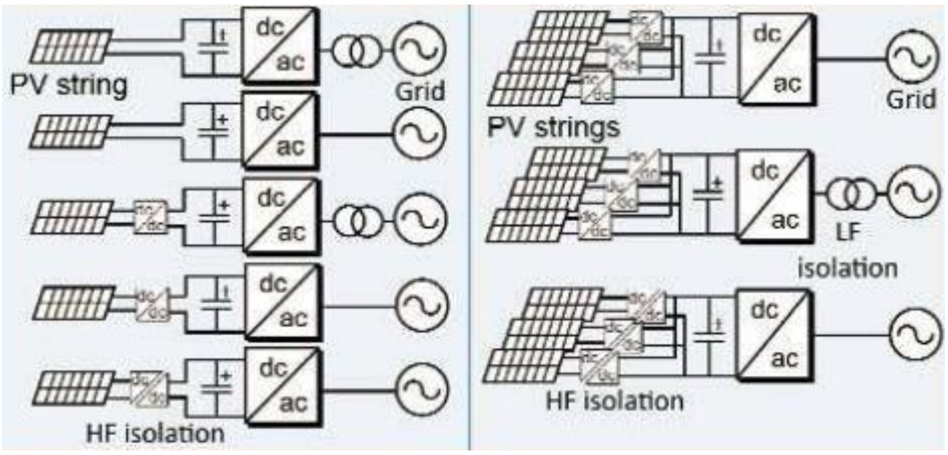

Figure 3.31. Srting inverters and multi-string inverters with/without transformer [60].

- **Multi-String Inverters:** This inverter can take in power from several module strings having varied peak power, orientations, and perhaps shading, making every string operate at its own maximum power point (MPP) [8]. The power range of multi-string inverters is between 10-450 kW [60]. As shown in Figure 3.32. Each string has a DC-to-DC converter installed for MPP tracking and power combination to a DC bus. For a single string of Photovoltaic systems, multi-string inverters have the optimal MPP tracking. When PV strings of different orientations and different rates of power are combined, in this case, the multi-string inverter comes in useful [97].

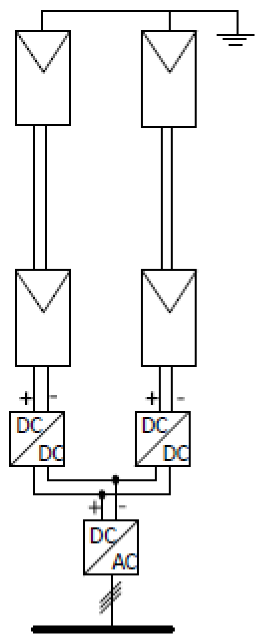

Figure 3.32. Multiple-String Inverter [2].

- **Micro-Inverters (Module integrated inverters):** Micro inverters as shown in Figure 3.33. Are complete PV system units made up of PV panels, inverters, and other elements. Micro-inverters are fully functional, environmentally friendly units. resulting in an inverter device that can independently provide AC power that is compatible with the grid. Micro inverters make system design easier by enabling any number or group of units to connect to the grid directly [97].

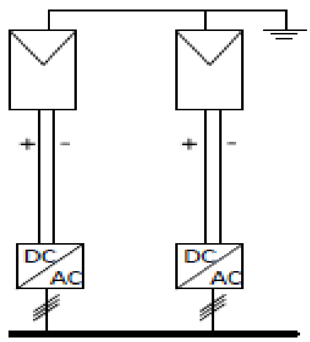

Figure 3.33. Micro-Inverters [2].

There are four topologies used in connection PV systems. Central, string, multi-string, module integrated. inverters that are used on this topology are given the name of the topology that is being used. Table 3.5. Shown the comparison between the inverter types [2].

Table 3.5. Comparison between the inverters types [2].

		Central	**String**	**Multi-string**	**Module integrated**
General Characte ris-tics	Robustness	H	L	M	V.L
	Reliability	L	H	M	V.H
	MPPT tracking	L	H	M	V.H
	Flexibility	L	H	M	V.H
Power Losses	Switching	H	L	M	V.L
	Mismatching	H	L	L	V.L
	DC power losses	H	L	M	V.L
	AC power looses	L	M	M	H
Power Quality	Voltage balance	L	M	L	L
	DC voltage variation	V.H	M	H	V.L
	AC voltage variation	L	H	H	V.H
cost	Dc cables	H	L	M	V.L
	Installation cost	M	H	M	V.H
	Maintenance	L	M	H	V.H
	AC cables	H	M	M	H

- AC collection grid topologies.

The grid for collecting AC ($LSPPP_S$) can be divided into three systems.

1. **Radial collection**

The radial collecting system is shown in Figure 3.34. includes many Photovoltaic generators coupled to a single feeder, resulting in a single string. The majority of (LSPPP$_S$) use this topology. The advantages of this topology are simplest and cheapest. The drawback of this topology is low reliability and that means it is less attractive in the case of (LSPPP$_S$).

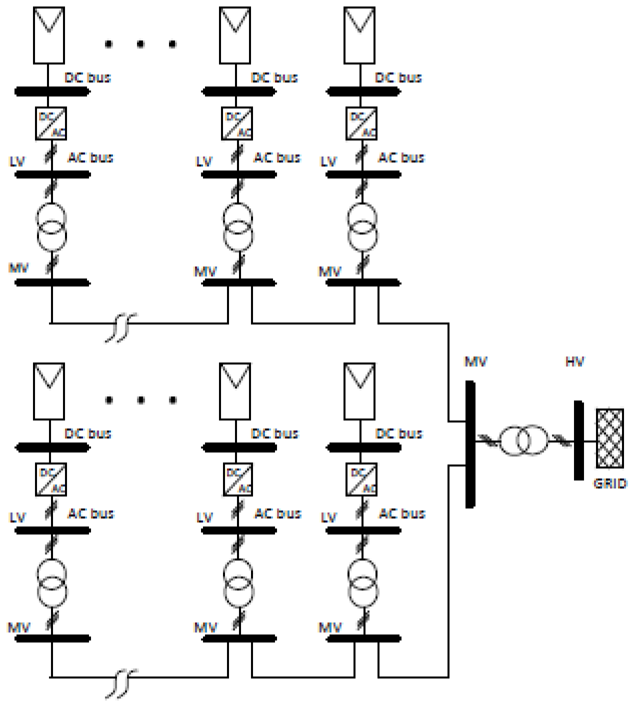

Figure 3.34. Radial collection [2].

2. **Ring Collection**

The ring collecting topology is utilized to increase the large-scale Photovoltaic power plant's reliability This connection is the same as radial in design, but it contains an additional feeder on the other side of the string. as shown in Figure 3.35. If one of the PV generators fails, The PV generators on the other side of the feeder will continue to supply power to the large-scale Photovoltaic power plants. The disadvantages are the difficulty of installation and cost. In the case of several inverters are interconnected to the transformers' L.V side. In this arrangement, if one of the inverters fails only a small part of power in the large – scale Photovoltaic power plants Is lost (less than 1 percent of the power generated) .5% is the reduction in power generation, in the case of any transformer station is lost [2].

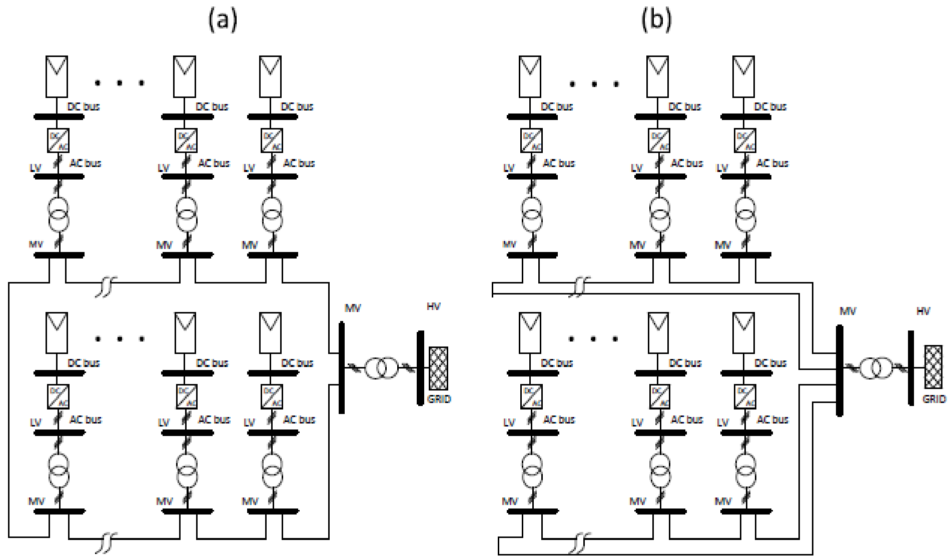

Figure 3.35. Ring collection.(a) first case. (b) second case [2].

3. Star Collection

In this configuration, one Photovoltaic generator is coupled to the main collector. As shown in Figure 3.36. The main collector is often located in the center (Middle)of an (LSPPP) to decrease cable distance and to have the same losses between Photovoltaic generators. The advantage of this configuration is the higher reliability than other previous configurations. The disadvantages are represented by each Photovoltaic generator has it is own feeder, which raised the overall cost. the main collector can be divided into two busbar and each group of Photovoltaic generators coupled to this sub-bus bar as illustrated in Figure 3.36 b [2].

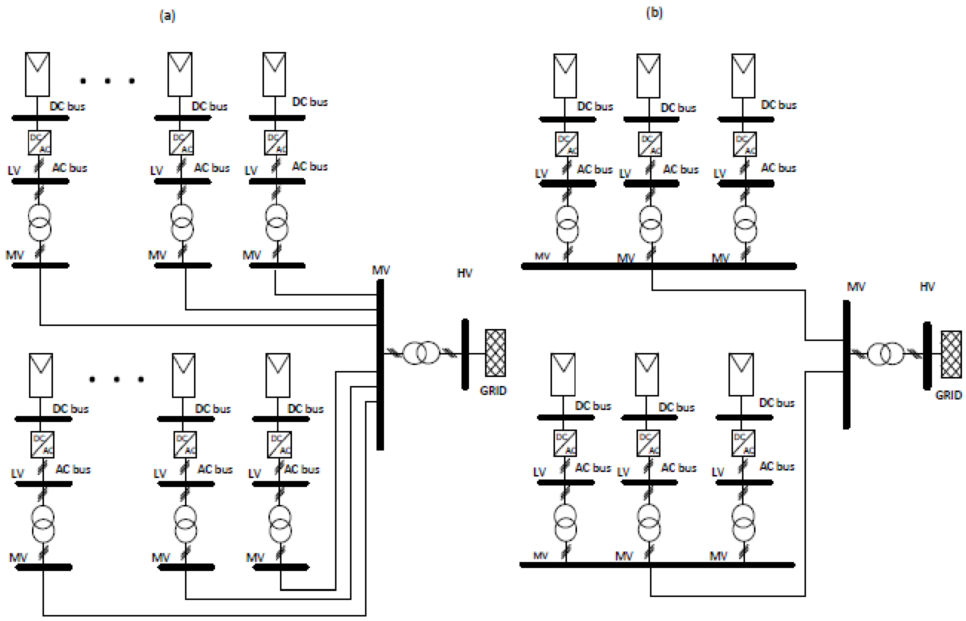

Figure 3.36. Star collection [2].

3.4. COMBINER BOX (COMBINER JUNCTION)

The combiner box is one of the Photovoltaic system components as shown in Figure 3.37. The individual strings (series connected) constituting an array are parallel arranged through the combiner box [99]. The combiner box is a device between the Photovoltaic array and the inverter. It may contain protective and isolation equipment such as the main DC isolator switch (This makes it possible to easily accessible isolate the PV array from the inverter) and it may be containing surge protection (against lighting). The combiner box also includes the fuses [8]. In the case of the combiner box not containing the protective and isolation equipment (DC) the protection unit should be added for the PV system [87].

Figure 3.37. Combiner box [93].

3.5. DC AND AC CABLING

PV systems that are grid-connected required both DC-AC wiring to interconnect the different components. DC and AC cabling are not interchangeable since they are designed for the electrical properties of their respective forms of electricity [100].

3.5.1. DC Cables

The Dc cable used in the PV systems can be divided into:

- PV module cables: These cables are normally pre-connected to the PV module. The string is formed by connecting several PV modules arranged in series.
- PV string cables: These kinds of cables are used to connect a string of modules to the Photovoltaic string combiner box.
- PV sub-array cables: this type of cable is used utilized to interconnect the PV array combiner box with the PV string combiner box, it is used in a large PV system.
- Inverter DC cables: These types of cable are connected the PV Array to the DC side of the inverter (used from the combiner box to the inverter dc side) [100].

3.5.2. AC Cables

The AC cables are utilized to connect the inverter (AC side) to the grid [26]. Cabling for AC systems should be constructed so that electricity from the inverters can be delivered to the transformers in a safe with a cost-effective method. Conductors should be scaled to account for operational currents and short-circuit currents (I_{SC}). The AC cables must meet the following specification [99, 100]:

- The cable needs to meet the highest estimated voltage rating.
- Conductors need to be the suitable size to prevent voltage drop outside of the permitted limits and to maintain equipment performance.
- Insulated, cable durability rating, and temperature in relation to the environment where it will be placed.
- Cables must conform to appropriate IEC standards.

Generally, when sizing the cables in the PV systems, there are three criteria must be followed [99]:

- The voltage rating of the cable.
- The current carrying capacity (CCC).
- The minimization of cable losses (CSA).

3.5.3. Managing Cables

Specialized cable trays or cable ties are utilized to route and tie over-ground cables, such as module and string cables, to the mounting structure. Cables need to be shielded from Direct sunlight, standing water, and sharping corners and edges of the support structure. It's best if they're as brief as possible [99]. Cable management can be reduced significantly the effect of lighting risk and electromagnetic fields. Figure 3.38. Shows cables lay methods [101].

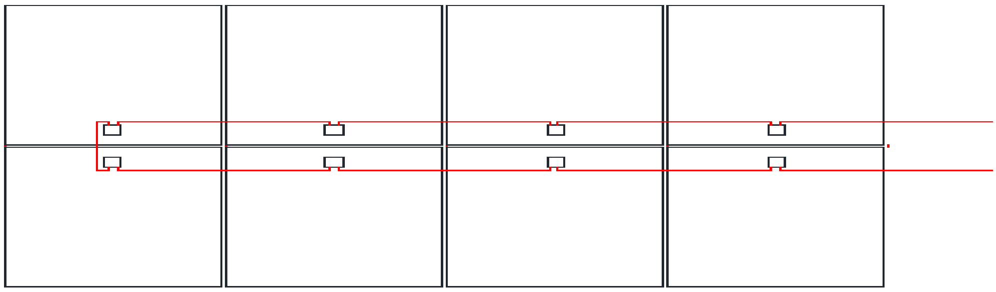

Figure 3.38. Cables lay methods (a) [101].

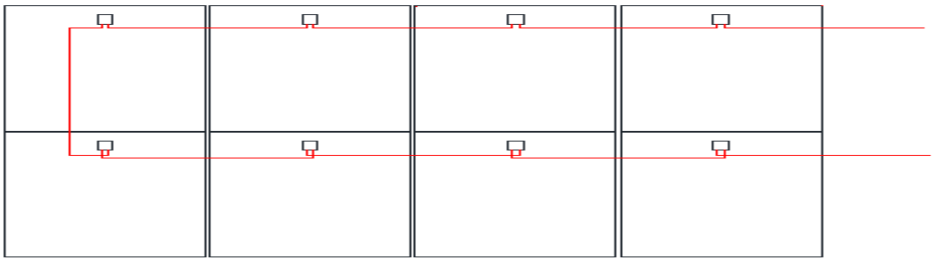

Figure 3.39. Cables lay methods (b) [101].

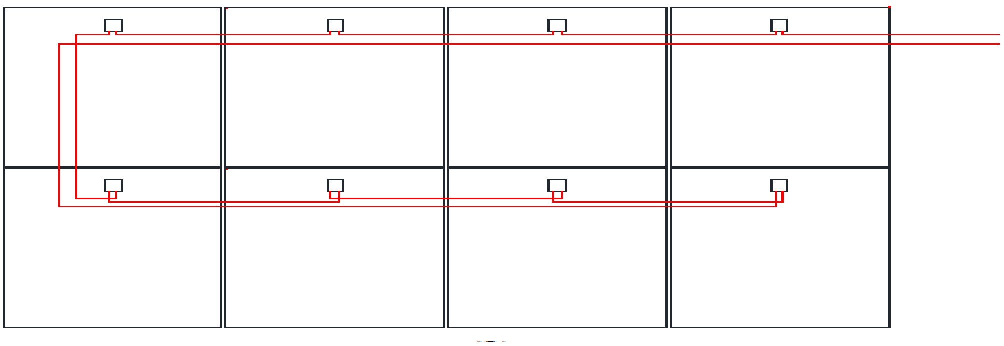

Figure 3.40. Cables lay methods (c) [101].

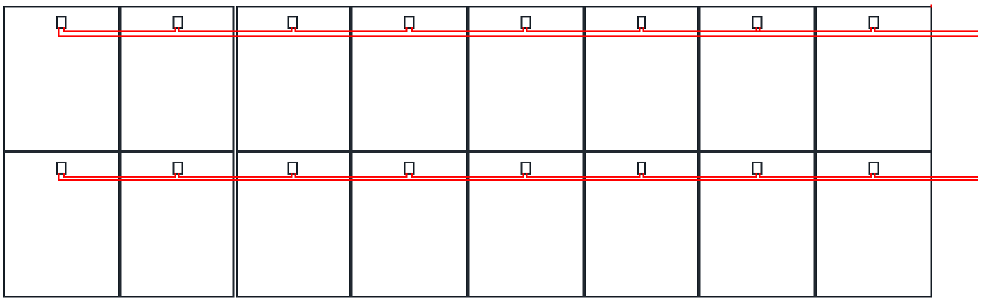

Figure 3.41. Cables lay methods (d) [101].

Table 3.6. Cable configuration and the effect of lighting ,electromagnetic field and cost [101].

Cable configuration	Risk of Lighting	Electromagnetic field	Cabling cost
a	High	stronger	low
b	low	strong	lowest
c	lower	weak	higher
d	lowest	weaker	high

3.6. TYPES OF PHOTOVOLTAIC SYSTEMS

Advances in the field of photovoltaic systems and use in various applications. Photovoltaic systems have been classified depending on component configurations, functional needs, and operational factors. [97]. PV systems can be classified into [83]:

- Grid-connected solar PV system.
- Stand-alone solar PV system.
- PV-Hybrid systems.

3.6.1. Grid –Connected System

In this system inverters converts DC energy generated by a PV array or module into AC electricity and connected them to the grid. These Types of systems don't required batteries since they are connected to the grid, which functions as a buffer, allowing an excess of PV electricity to be transfer to the grid, while the grid also provides electricity to the houses when PV power output is inadequate [83].

The safety merit in all grid-connected Photovoltaic systems and it guarantees that the photovoltaic system does not activate and feedback into the utility grid while the grid is offline (in the event of a grid failure, or maintenance situation) [97]. The inverter is linked to the Distribution board in small systems, such as those placed in residential houses, where the PV-generated power is delivered into the electrical grid or to AC devices in the house. In ($LSSPP_s$) all the PV electricity generated is delivered directly to the grid [83].

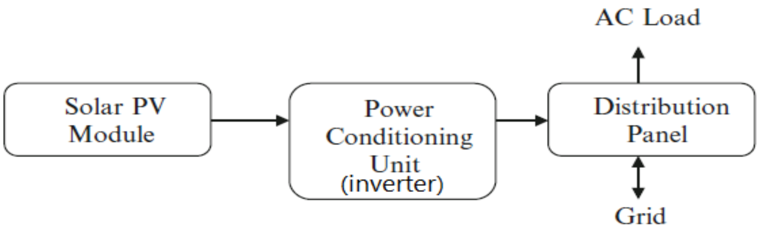

Figure 3.42. Grid –connected system block diagram [97].

Net metering is an important element of a grid-connected system. The fundamental distinction between stand-alone system and grid-connected systems are inverters. with a view to supplying excess energy to the grid. The inverter must be capable of line frequency synchronization. Net meters can record power generated or consumed in an exclusive summing manner [97]. Figure 3.43 shows a grid-connected Photovoltaic system. Utility firms that supply and install net meters are utility companies that offer grid-connection service systems .Net metered Photovoltaic power facilities are subsidized by state or municipal governments and are subject to certain contractual agreements [97].

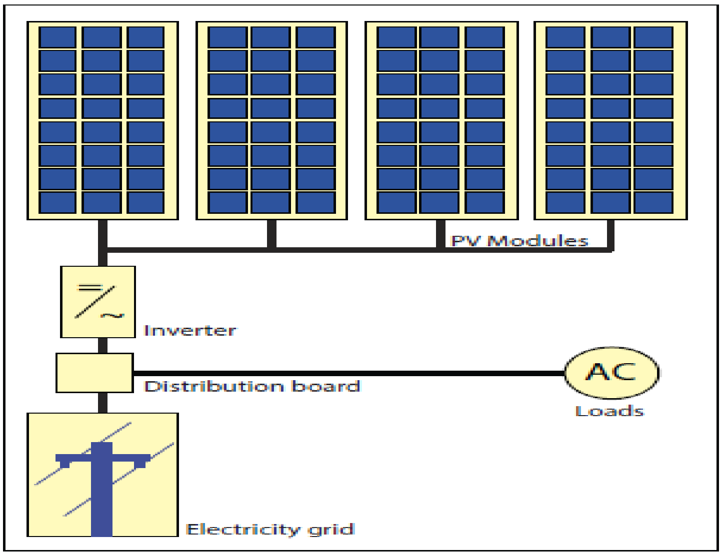

Figure 3.43. Shows grid-connected Photovoltaic system [83].

3.6.2. Stand-Alone System

Stand-alone systems depend on solar power. These systems can be represented as PV modules and a load (AC or DC load) or they might include energy storage batteries [83]. In the case of the DC of Photovoltaic array or modules are straightly linked to the DC load, in this state it is called a direct-coupled system as shown in Figure 3.44. And the load just runs during sunlight hours, in this case, there are no batteries (no electrical energy storage) this kind of stand–alone can be used in agriculture applications [97].

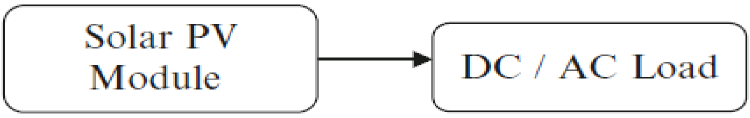

Figure 3.44. Block Diagram of direct coupled stand-alone system [97].

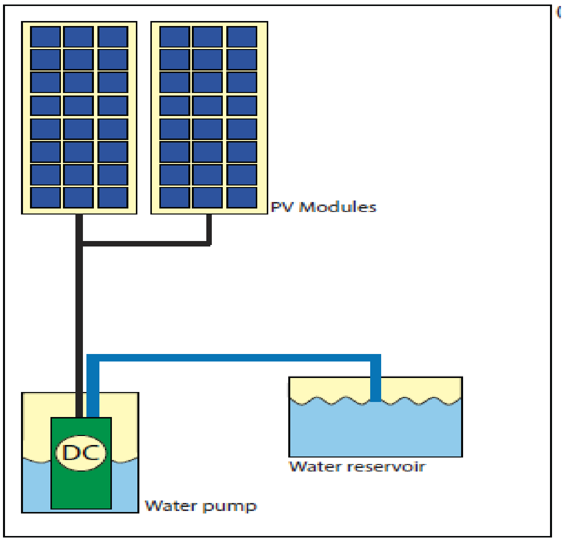

Figure 3.45. Stand-alone system in agriculture applications [83].

The stand-alone system with batteries is the same as the system without batteries, but in the case of the system containing batteries, we need to add some components such as a battery charger controller, which switches off the PV modules when batteries are full and may switch the load to protect the battery from discharge below a certain limit. Batteries must have sufficient capacity to remain the energy generated during the day so that they may use at night and during bad weather [83, 97]. Figure 3.45. Shows stand-alone system.

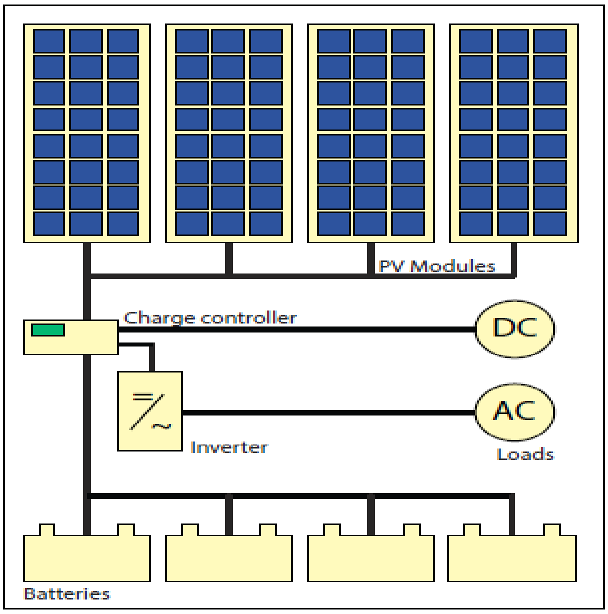

Figure 3.46. Stand-alone system [83].

A Battery bank is responsible for 20-30% of power losses because of the heat generated during operation (must be considered). Many factors can be affected in Stand-alone systems with a battery backup performance, such as a suitable location for batteries racks and room ventilation [83, 97].

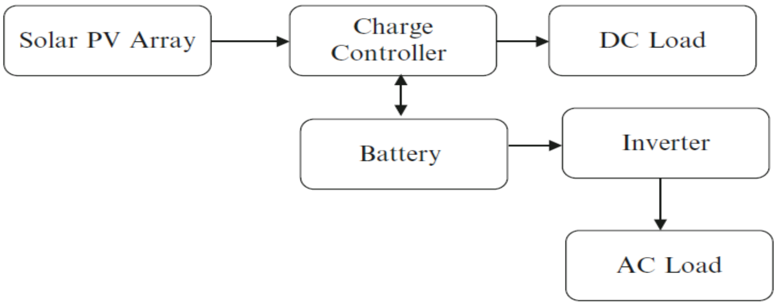

Figure 3.47. Stand-alone system with batteries backup Block Diagram [97].

3.6.3. Hybrid Systems

Hybrid systems combine PV modules with a backup source of power such as Diesel, Gas generators, Wind turbines, and Biomass (every other form of energy, whether renewable or not) [97]. Typically, the size of the PV generator would be selected to match the base load needs, and the backup resource would only be used when necessary. This system not only provides all the PV in terms of cheap maintenance and operation, but it also assures a reliable source [97]. To make the various techniques of power generating more efficiency [83].

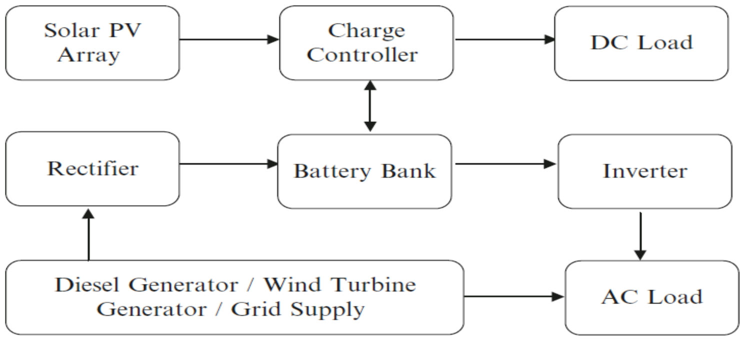

Figure 3.48. Hybrid system Block Diagram [97].

3.7. TYPES OF SOLAR TRACKER IN PV SYSTEMS

The location of the sun varies during the day, year, and season. To maximize the amount of energy produced by PV panels, they must be rotated accordingly. If PV panels are exposed to the sun for longer periods of time, more electricity is produced because more sunlight is received. It enhances the efficiency of the system while minimizing its size and total cost [102].

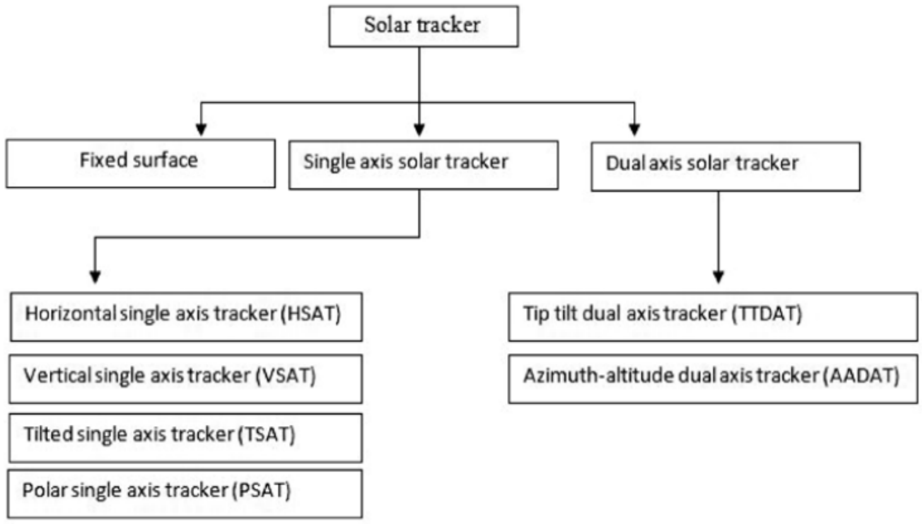

Figure 3.49. Block diagram of solar tracker types [102].

3.7.1. Fixed Mount Solar System

PV panels are faced south at a fixed tilt angle (local latitude). During the day(sunlight), PV panels are still unable to change position, to obtain the best result (output energy), their angular position might be changed during the year. (According to the season). Fixed surface solar systems are commonly used in domestic, small-scale commercial PV systems, and solar geysers [102, 103].

Figure 3.50. Fixed orientation [104].

3.7.2. Single Axis Tracking System

The sun is tracked in a single path by this system [102]. Which is often direction east to west. During the day, the sun rises in the east and sets in the west. In such techniques, the panel follows (moves in synch) the sun's path, attempting to maintain a perpendicular angle to the sun's rays. PV panels are faced south with an appropriate angle. In this system, it’s impossible to keep(panels) perpendicularly to the sun's rays all the time [103]. This type of solar tracker system can be implemented in various configurations [102]:

- Vertical single-axis tracker (VSAT).
- Horizontal single-axis tracker (HSAT).
- Polar aligned single-axis tracker (PSAT).
- Tilted single-axis tracker (TSAT).

Because this system moves in a single direction, it requires less operation and hence consumes less energy. Furthermore, because of its simplicity, it is durable, requiring little maintenance. On the other hand, because it is not properly aligned with the sun's rays, it harvests less energy and hence has low efficiency. Its toughness makes it ideal for PV power plants [102].

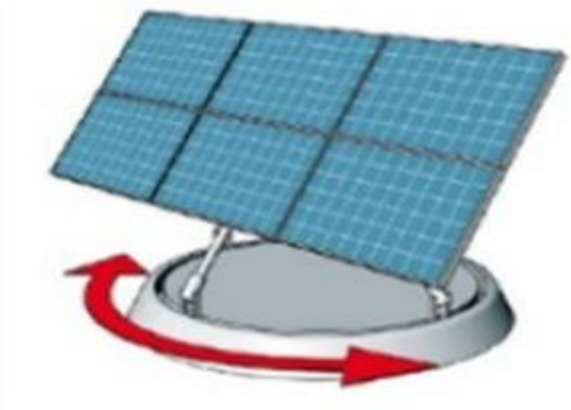

Figure 3.51. Vertical single axis tracker (VSAT) [104].

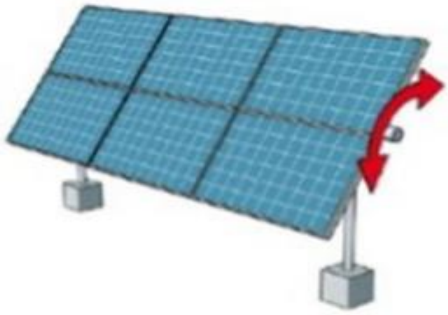

Figure 3.52. Horizontal single axis tracker system(HSAT) [104].

3.7.3. Dual Axis Solar Tracking System

The panels in this system can rotate in both left-right (east-west) directions, and up-down (north-south) directions, in this system the surfaces receive the greatest sunrays because they are always moving to stay perpendicular to the path of the sun's radiation. [103]. Such a system takes into consideration the sun's path's daily and seasonal fluctuations, exposing the PV panels to the maximum amount of solar radiation for maximum energy harvesting. This type of solar tracker system can be implemented in two configurations [102]:

- Tip-tilt dual-axis trackers (TTDAT).
- Azimuth-altitude dual-axis trackers (AADAT).

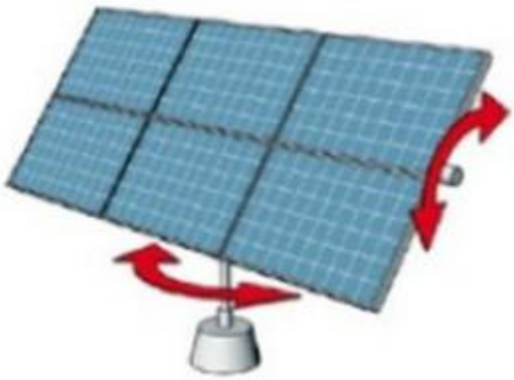

Figure 3.53. Dual-Axis Solar Tracker [104].

PART 4

DESIGNING 1MW PV POWER PLANT

4.1. INTRODUCTION

Designing an $LSPPP_S$ requires a high level of technical expertise and experience. The most significant design objective for most LSPPP is to reduce the levelized cost of energy (LCOE). Establishing a balance between equipment price and quality is essential. Engineering decisions need to be “informed” and "considered", else, a designed system chosen to save money now might result in higher future expenditures and revenue loss owing to high maintenance requirements and poor performance. Reduced system losses can improve the performance of a solar PV power plant. Reducing total loss enhances annual energy yield and hence income, while it may raise the plant's cost in some circumstances. Furthermore, Efforts to decrease one form of loss could clash with attempts to decrease another form of loss. The station designer's expertise is important to reach compromises that contribute to a plant that operates well at a low cost. Computer simulation software (such as pvsyst software) may be utilized to assist in the designing of the plant. Algorithms for describing the astronomical sun movement during the year at each point on the planet (Earth), These programs are included charting that shows the sun's height and azimuth angle. that, combined with module inter-row spacing information, could be utilized to compute shading and model yearly energy losses related to different tilt angles, orientation, and row spacing combinations.

4.2. SITE LOCATION OF PHOTOVOLTAIC POWER PLANT AND LOCATION COORDINATES

Choosing a suitable location is an important step in establishing a sustainable Photovoltaic plant. The absence of definition guidelines for choosing a location.

The constraints and effect of the location on the cost of power generated must be considered during the site selection process. there are some points that should take into account when selecting the site such as Local climate, Solar resources, Available area, Land use, Accessibility, Topography, land use policy or zoning/ Local regulations, Water availability, Grid connection, financial incentives, Geopolitical risks, and Geotechnical conditions. GIS mapping technologies can help in site selection by visually displaying restrictions, allowing various constraints to be considered for a single site, and determining the overall land area accessible for establishment [99].

Figure 4.1. PV power plant location By Google map.

The photovoltaic station project is in the northern of region Republic Iraq, the geographical coordinates 36º 20'N, 43º 10' E and sea level altitude 329 m. The site of the PV solar power plant is located northwest of Mosul city,45Km and the coordinate of the solar plant is 36° .62' North latitude and 42°. 78' East longitude. The annual average temperature is about of 20.6C° and the location receives 1825 kW per square meter of solar radiation on average per year. Table 4.1 shows the Meteo data for the site.

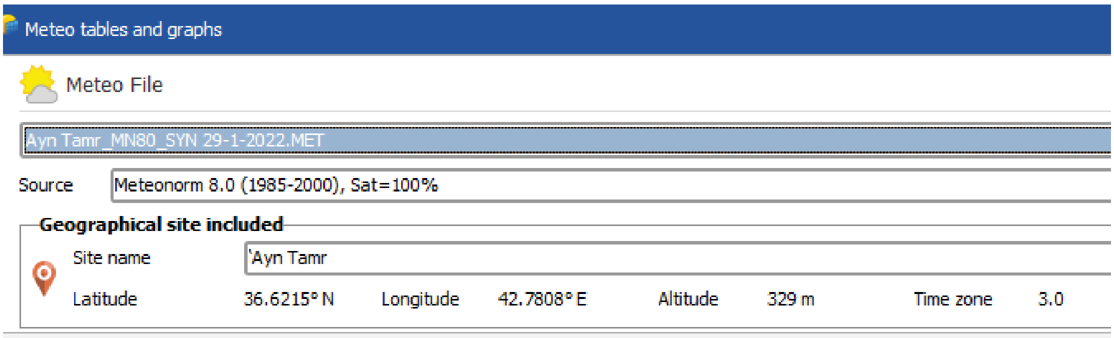

Figure 4.2. Meteonorm 8.0 weather database.

Table 4.1. Monthly values of Meteonorm8.0 (1985-2000), Sat=100% database.

Interval beginning	**GlobHor kWh per m^2per month**	**Diff Hor kWh per m^2per month**	**T-Amb C°**	**Wind Velocity meter per second**
January	78.8	33.8	6.8	3.6
February	92.0	40.7	8.7	3.6
March	138.3	63.9	13.3	3.7
April	170.5	76.1	17.6	3.5
May	196.4	87.9	24.5	3.5
June	233.3	73.4	31.0	4.0
July	232.2	74.3	35.0	3.6
August	212.1	67.3	34.2	3.3
September	177.2	45.7	29.0	3.3
October	128.6	48.0	23.1	3.1
November	99.60	32.4	14.1	3.1
December	75.0	28.3	8.9	3.5
Year	1825.0	671.7	20.6	3.5

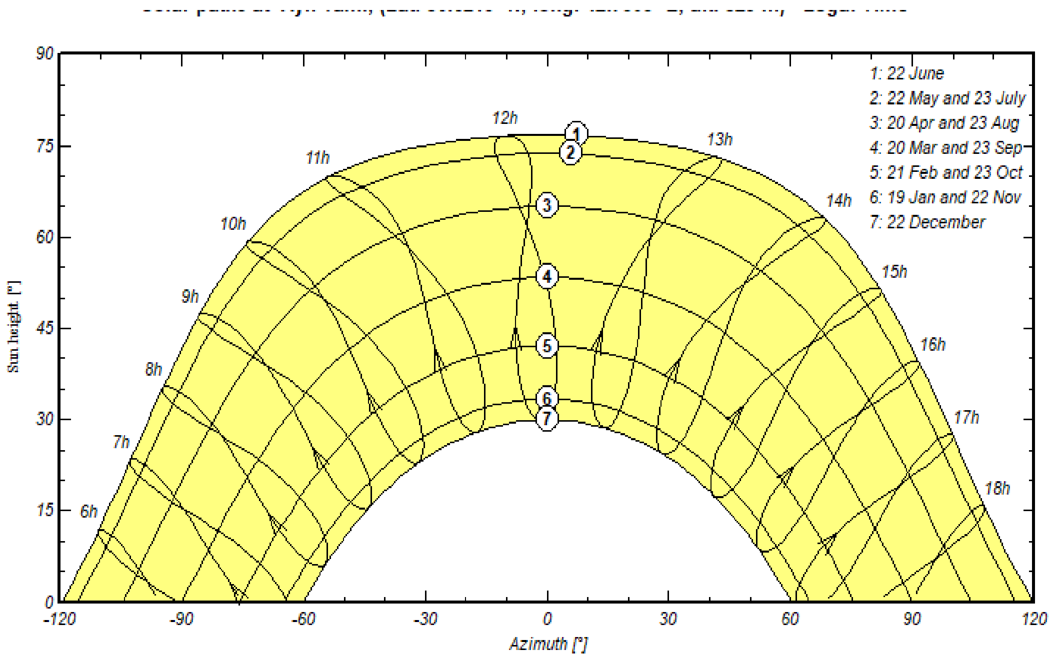

Figure 4.3. Solar Path at Site (latitude 36.62oN,longtude 42.78 Eo,altitude329m).

4.3. SOLAR POWER PLANT TILT ANGLE

For each site, there is a perfect tilt angle that increases the overall amount of irradiation received annually. The theoretical optimal tilt angle for fixed tilt grid-connected power plants may be calculated using the site's latitude. There are some factors that should be considered when we want to adjustment of the tilt angle calculation such as:

- Soiling: Soiling losses are reduced at higher tilt degrees. At higher tilt angles, Snow slides off more easily and panels are cleaned more effectively by the natural flow of rainwater.
- Shading: Modules with a higher angle of tilt provide more shade to modules behind them. And that leads to an increase in the yield energy, to reduce the effect of shading the inter-row distance between the PV modules should be calculated carefully and reduce the tilt angle.
- Distribution of seasonal irradiation: In the case of one season predominates in the yearly production of the solar resource, adjusting the tilt angle to cover the loss may be beneficial. The advantage of this approach may be analyzed using

simulation software. The tilt angle can be determined by using the equations explained in part Three (3.5), (3.8) (3.9).

$$\delta = 23.45 \sin\left[\frac{360}{365}\ (n_{day} - 81)\right] \quad (3.5)$$

$$\beta = 90^o - L + \delta \quad (3.6)$$

$$Tilt\ angle\ \alpha = 90^o - \beta \quad (3.7)$$

Where:

δ= Solar declination angle.

L=Is the latitude of the site=36.62 N^o.

β= Altitude angle.

α=Tilt angle.

n_{day}=The day number (during the year) , where day 1 is January 1st and day 365 is December 31st.

Table 4.2. Tilt angle , Solar declination angle, Altitude angle at each month's first day.

Month	n_{day} Day numbers for each month's first day	Solar declation angle (δ)	Altitude angle (β)	Tilt angle (α)
January	1	-21.1^o	32.2^o	57.8^o
firuary	32	-16.4^o	63.9^o	45.1^o
March	60	-7^o	64.3^o	43.7^o
April	91	3.98^o	57.2^o	32.8^o
May	121	14^o	67.3^o	22.7^o
June	152	21.8^o	75.1^o	14.8^o
July	182	22.9^o	76.2^o	13.8^o
Augest	213	16.4^o	69.7^o	20.3^o
Septemper	244	7^o	60.3^o	29.7^o
October	274	-3.5^o	49.8^o	40.2^o
Novemper	305	-8.4^o	44.9^o	45.1^o
December	335	-21.1^o	32.2^o	57.8^o

From Table (4.3) can evaluate the optimal tilt angle for PV plant depending on the mathematical calculations for tilt angle the value obtained in July month is the smallest angle for summer reason while the largest tilt angle we obtained it in the winter was in December by using pvsyst. The software can be determining the optimal Tilt angle with respect to the yearly irradiation yield, summer seasonal, and winter seasonal, respectively for different tilt angle values (15°, 20°, 25°, 30°,35°, 40°,45°, and 50°).

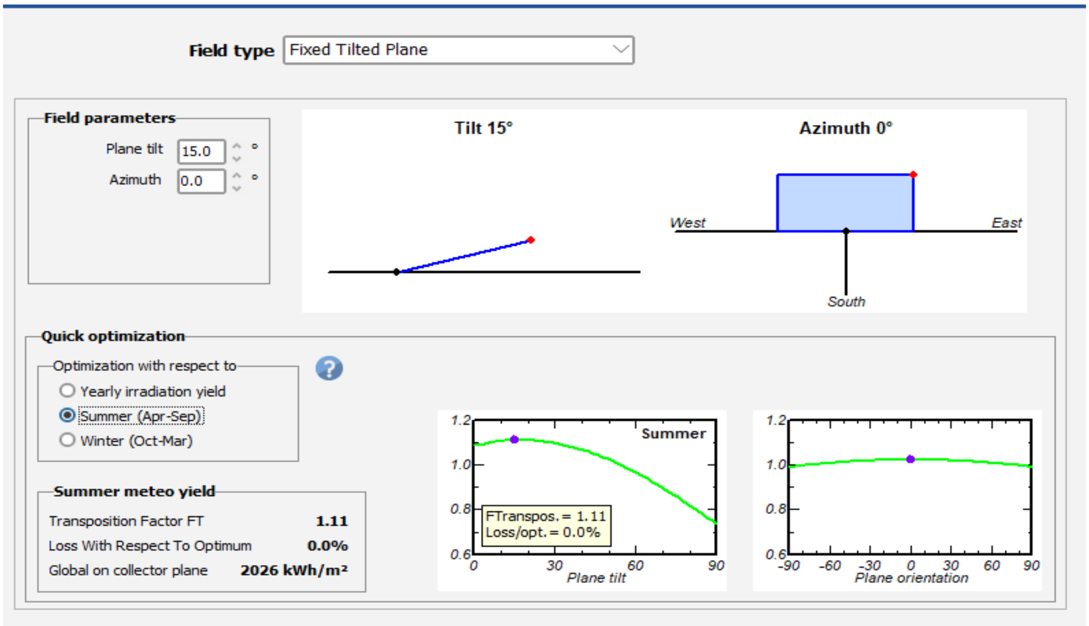

Figure 4.4. The optimal Tilt angle at value of 15o with respect to the summer season (April-September).

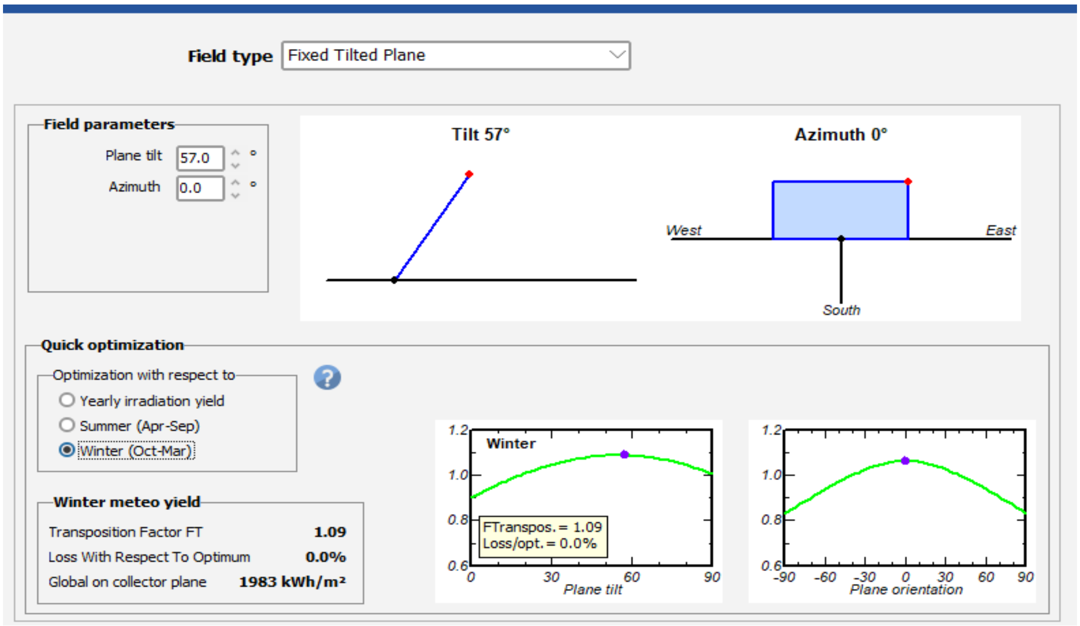

Figure 4.5. The optimal Tilt angle at value of 57o with respect to the winter season (October -March).

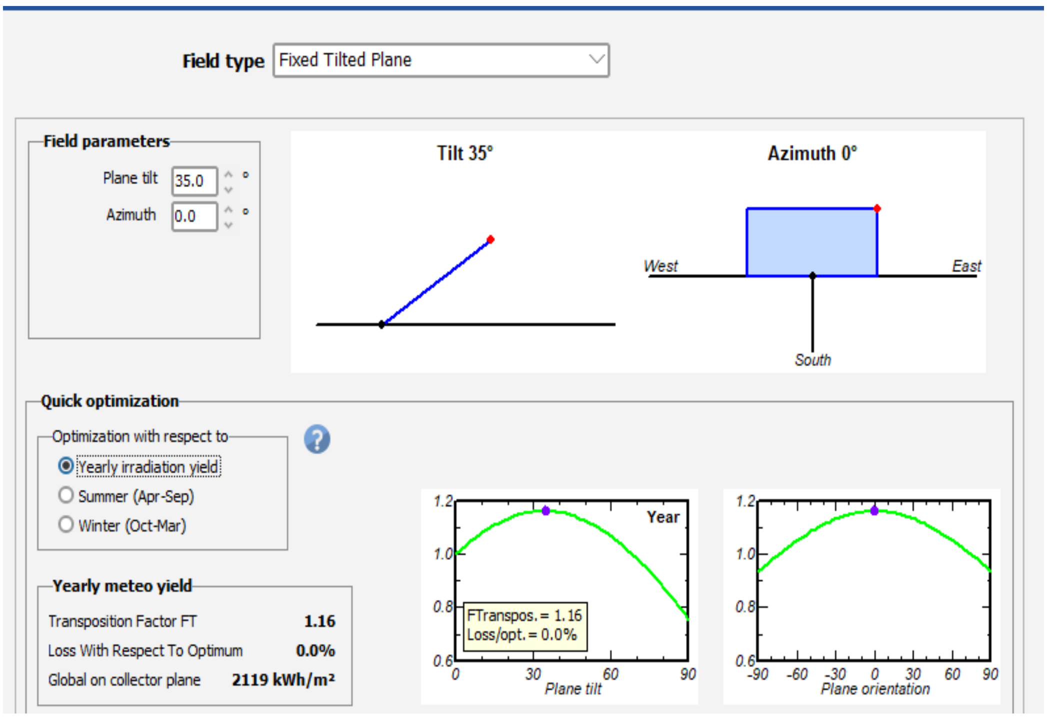

Figure 4.6. The optimal Tilt angle at value of 35o with respect to the yearly irradiation yield.

Table 4.3. Compression between different tilt angle values with respect of yearly irradiation yield, summer season, and winter season.

Tilt angle	Azimuth	Optimization with respect with	Transposition factor FT	Losses with respect to optimum %	Global energy on collector plane kWh/m^2	Energy injected into Grid MWh
15^o	0^o	Yearly	11.1	-4.4	2026	1713.7
15^o	0^o	Summer	11.1	0.0	2026	1040.3
15^o	0^o	Winter	11.1	-8.5	2026	673.4
20^o	0^o	Yearly	1.13	-2.4	2068	1747.8
20^o	0^o	Summer	1.13	0.0	2069	1039.2
20^o	0^o	Winter	1.13	-6.5	2068	708.6
25^o	0^o	Yearly	1.15	-1.0	2097	1771.7
25^o	0^o	Summer	1.15	-0.4	2098	1032.9
25^o	0^o	Winter	1.15	-4.8	2098	738.8
30^o	0^o	Yearly	1.16	-0.2	2114	1785.5
30^o	0^o	Summer	1.16	-1.2	2114	1021.1
30^o	0^o	Winter	1.16	-3.4	2114	764.4
35^o	0^o	Yearly	1.16	0.0	2119	1789
35^o	0^o	Summer	1.16	-2.2	2118	1004.2
35^o	0^o	Winter	1.16	-2.2	2118	784.8
40^o	0^o	Yearly	1.16	-0.4	2110	1782.1
40^o	0^o	Summer	1.16	-3.6	2110	981.7
40^o	0^o	Winter	1.16	-1.2	2110	800.4
45^o	0^o	Yearly	1.14	-1.5	2087	1765
45^o	0^o	Summer	1.14	-5.2	2088	954.1
45^o	0^o	Winter	1.14	-0.5	2088	810.9
50^o	0^o	Yearly	1.12	-3.1	2052	1737.8
50^o	0^o	Summer	1.13	-7.1	2053	921.3
50^o	0^o	Winter	1.13	-0.1	2053	816.5

From the Figures (4.4), (4.5), (4.6), And Table 4.2. Above can be estimated the optimal Tilt angle with respect to the yearly irradiation yield. since the PV system is fixed, the value of tilt angle is 35^o.

4.4. PV MODULES SUPPORT STRUCTURE SYSTEM DESIGN

The solar panel's support structures are designed according to the steel section structural standard. To ensure an effective anticorrosive coating on the structure, a coating with a hot-dip galvanization technique is used to treat the surface. A 45 m/s wind speed can the structure withstand it because of stainless steel(bolts) fasteners that secure it [106].

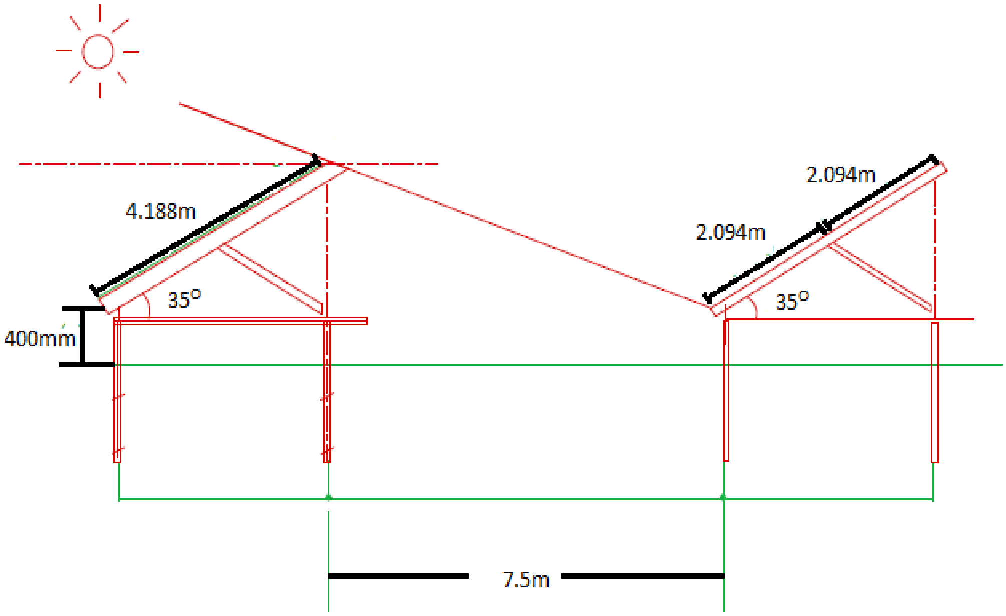

Figure 4.7. PV module support structure.

4.5. INTER-ROW SPACING

The shade is considered the biggest enemy of photovoltaic stations. The shade leads to the damage of photovoltaic panels (fixed shade) and reduces the energy produced from the photovoltaic system. It is not possible to reduce the shade between the panels. To zero, especially at the beginning and end of the day. Calculating the distance between the panels helps reduce the used cables, as well as reduce ohmic losses, and determine the area of the photovoltaic station. From the equation below the distance between inter-row spacing calculated [107].

$$\frac{d}{L_{mod}} = \cos\alpha + \frac{sin\alpha}{\tan\varepsilon} \tag{4.1}$$

$$\tan\varepsilon = 90^o - \partial - L \tag{4.2}$$

Where:

d= inter row distance.

L_{mod}= length of PV modules.

α = tilt angle.

∂ = ecliptic angle=23.5°.

L =geographical latitude.

Now from Equation (4.2).

$\tan \varepsilon = 90^o - 23.5^o - 36.6^o = 29.9^o\ Approximatelly\ 30^o$

From Equation (4.1).

$$\frac{d}{4.188} = \cos 35^o + \frac{sin35^o}{\tan 30^o}$$

d =7.5 m the inter row spacing.

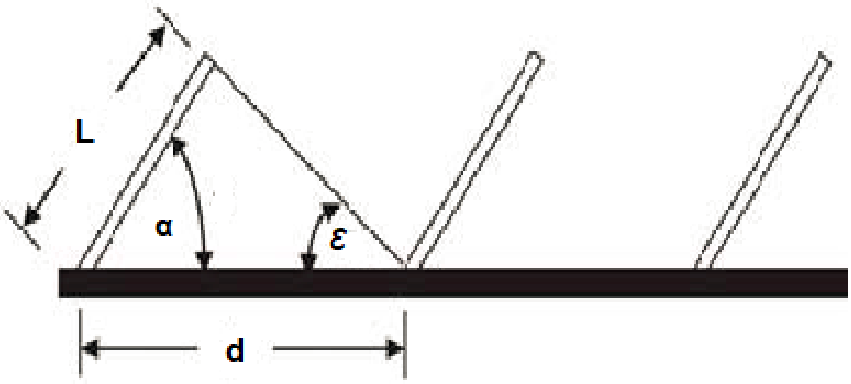

Figure 4.8. Inter-row modules distance of array [107].

4.6. ELECTRICAL DESIGNING

Electrical designing including all the electrical equipment for the electrical system. PV panels, inverters, combiner box cables Dc cables, Ac cables, and set up transformers.

4.6.1. PV Modules Sizing

PV modules are very important components in the PV system. The PV modules should be chosen under IEC standards. The life of good quality modules which have IEC certification is more than 25 years. In the field, the lifetime of crystalline modules has been proven between 25-30 years [99]. Table 4.3 shows and describes some of these standards.

Table 4.4. IEC standards Descriptions[99].

Test	Description	Comment
IEC 61215	Crystalline silicon (c-Si) terrestrial PV modules – Design qualification and type approval	Includes tests for thermal cycling, humidity and freezing، mechanical stress and twist and hail resistance. The standard certification uses a 2,400Pa pressure. Modules in heavy snow locations may be tested under more stringent 5,400Pa conditions.
IEC 61730	PV module safety qualification	Part 2 of the certification defines three different Application Classes: 1) Safety Class O - Restricted access applications. 2) Safety Class II - General applications. 3) Safety Class III - Low voltage (LV) applications.
IEC 60364-4-41	Protection against electric shock	Module safety assessed based on: 1) Durability. 2) High dielectric strength. 3) Mechanical stability. 4) Insulation thickness and distances.
IEC 61701	Resistance to salt mist and corrosion	Required for modules being installed near the coast or for maritime applications.

To increase the voltage, modules are connected in series and to increase the current, modules (strings) are connected in parallel (by using the combiner box) as a result of the connection of the PV modules in series and parallel together we will get a PV array configuration. Appling the following relationship, we can determine the total number of PV modules needed for the system. [108].

$$No. of\ PV\ modules\ needed\ in\ the\ system = \frac{The\ capacity\ of\ the\ PV\ plant\ in\ watt}{The\ capacity\ of\ single\ PV\ panale\ in\ watt} \quad (4.3)$$

$$No.\,of\ PV\ modules\ needed\ for\ project = \frac{1000000}{460} = 2173.9\ approximatelly\ 2174$$

While the No. of modules for project in pvsyst are equal to 2176 (We will depend on this value in our calculations) as Figure 4.9 illustrates.

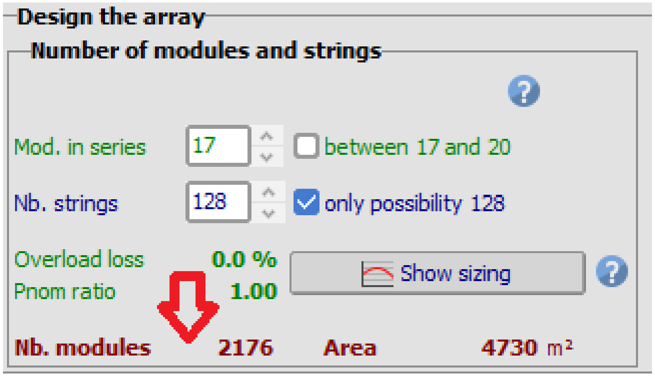

Figure 4.9. No.of PV modules for project(1 MW) by using pvsyst .

Table 4.5. PV Module characteristic Data Sheet.

Module	**LR4-72HPH-460M**
Manufacture	Longi Solar /2021
Electrical characteristic at STC :1.5 AM, 1000w/m^2,25^O C.	
Maximum Power ($P_{max/W}$)	460 w
Short circuit current (I_{SC})	11.73 A
Open circuit voltage (V_{OC})	49.7 V
Current at Maximum Power ($I_{mpp/A}$)	10.98 A
Voltage at Maximum Power ($V_{mpp/V}$)	41.9 V
Module Efficiency (%)	21.2
Dimension	2094 x1098x35 mm
Electrical characteristic at NOCT:1.5 AM ,800 w/m^2,20^O C.	
Maximum Power ($P_{max/W}$)	343.5 W
Sort circuit current ($I_{SC/A}$)	9.48 A
Open circuit voltage ($V_{OC/V}$)	46.6 V
Current at Maximum Power ($I_{mpp/A}$)	8.80 A
Voltage at Maximum Power ($V_{mpp/V}$)	39.0 V
Operation Parameters	
Operation Temperature	-40^O C ~+85^{O}C
Maximum System Voltage	DC 1500V
Maximum series Fuse Rating	20A

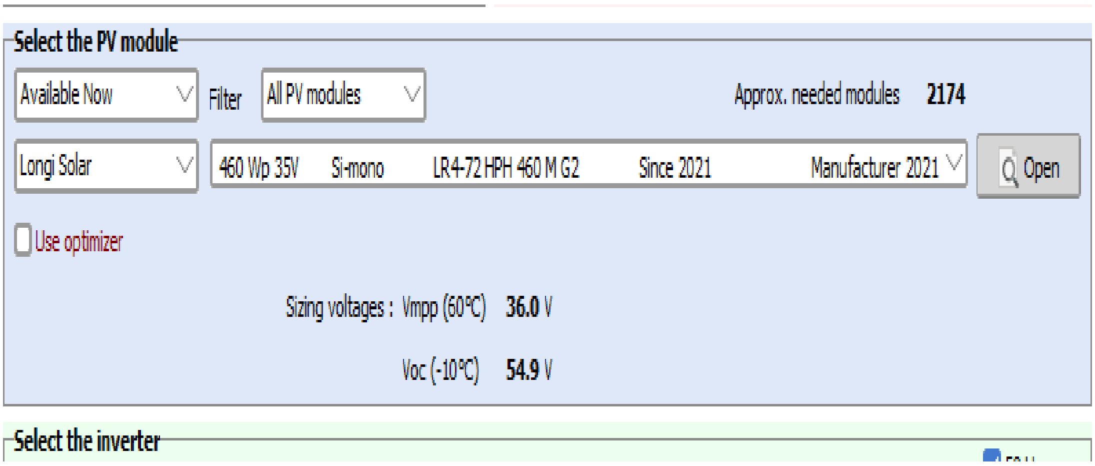

Figure 4.10. PV module select by pvsyst.

Now we will be finding the minimum and maximum PV string in the system theoretically and then finds it by using the pvsyst software.

- The Maximum No. Of The PV Modules in the series (string).

The total number of modules in a string is determined by $V_{(MAX,\ INV,\ DC)}$, which is the inverter's maximum DC input voltage to which the string will be connected. This voltage should not be exceeded under any circumstances. When the limit is exceeded, the inverter's operating lifetime is reduced, or the equipment is rendered unusable. The open-circuit voltage in the location's coldest daytime temps is the highest module voltage that can occur during operation [99]. From the following relations, we can find it [108].

$$V_{mod(max)} = V_{oc} * \left[1 + \left\{\left(T_{amb(\min)} - T_{STC}\right) * \frac{T_{PC}}{100}\right\}\right] \qquad (4.4)$$

$$\text{The max No. of the PV modules in the } = \frac{Max\ inverter\ input\left(V_{\text{inv,inp,max}}\right)}{V_{mod\ (\max)}} \qquad (4.5)$$

Where:

$V_{mod(max)}$ = Maximum module voltage predicted (at the site high temperature).

$T_{amb(min)}$ = Ambient low temperature of site.

T_{STC} = Temperature at standard test conditions.

$V_{inv,inp,max}$ =Maximum inverter input voltage.

T_{PC} = Temperature coefficient of maximum power (P_{max}).

From equation (4.4), (4.5).

$$V_{mod(max)} = 49.7 * \left[1 + \left\{(6.5 - 25) * \frac{-0.35}{100}\right\}\right] = 52.9 \text{ V}$$

$$\text{The max No. of the PV modules in the string } = \frac{1100}{52.9} = 20.7 \text{ } approximately \text{ } 20$$

So, the maximum No. of module /string are equal to 20 modules.

$$V_{OC(MODULE)} \text{at coldest module operating temperature} * N_{s,string,max} < V_{inv,inp,max.} \quad (4.6)$$

$N_{s,string,max}$ =Max No.of the PV modules in series string.

So, from equation (4.6)

52.9 * 20 < 1100.

1058 < 1100 it is acceptable value within limits.

- The Minimum Number of The PV Modules in The Series String. it is necessary to maintain system voltage within a range of the inverter's maximum power point (MPP), to dictate the minimum number of modules. The system will underperform, If the string voltage is lower than the minimum MPP inverter voltage. In the worst-case scenario, the inverter may shut down. in the circumstances when the module's maximum operating temperature, the lowest expected module voltage occurs [99].

$$V_{mod(min)} = V_{mpp} * \left[1 + \left\{\left(T_{amb(\max)} + T_{nom} - T_{STC}\right) * \frac{T_{PC}}{100}\right\}\right] \quad (4.7)$$

$$\text{The min No. of the PV modules in the } = \frac{Min \text{ } inverter \text{ } input\left(V_{\text{inv,inp,min}}\right)}{V_{mod(\min)}} \quad (4.8)$$

Where:

$V_{mod(min)}$= Mini module voltage predicted (at the site high temperature).

$T_{amb(max)}$ = Ambient high temperature of site.

T_{nom} = Nominal operation cell temperature.

$V_{inv,inp,min}$ =Minimum inverter input voltage.

From equation (4.7), (4.8).

$$V_{mod(max)} = 41.9 * \left[1 + \left\{(35 + 45 - 25) * \frac{-0.35}{100}\right\}\right] = 33.8\,V$$

$$\text{The min No. of the PV modules in the } = \frac{600}{33.8} = 17.7\ approximately\ 17$$

So, the minimum No. of module /strings in series are equal to 17 modules.

$$V_{MPP(MODULE)}\ \text{at highest module operating temperature} * N_{s,string\ min} > V_{inv,inp,min.} \qquad (4.9)$$

So, from equation (4.9)

52.9*17 > 600.

899.3 > 600 it is acceptable value within limits.

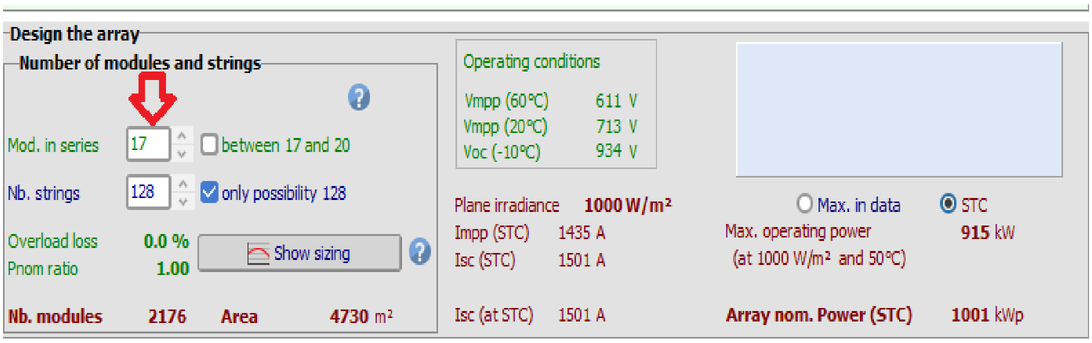

Figure 4.11. The Number of Maximum and Minimum modules (series) by pvsyst.

- The maximum PV array current and the maximum inverter current, determine the maximum number of parallel strings that can be utilized in a PV array. In general, this limit shouldn't be exceeded because it is lead to yield loss and accelerates inverter aging [99].

The No. of modules in the series connection equal to 17 modules. So,

$$The\ voltage\ in\ the\ series\ string = No\ of\ module\ in\ series * V_{oc\ of\ module} \quad (4.10)$$

$$V_{in\ sreies\ string} = 17 * 49.7 = 845\ v\ the\ value\ within\ inverter\ range\ inputs$$

The current of a series string is equal to 11.73(I_{SC} for a module). Now, we will find the number of parallel strings $N_{parallel\ strings.}$ The maximum Dc current for the inverter is equal to 1710 A in the datasheet. the $I_{string\ max}$ is the same value as I_{SC} which is equal to 11.73 A (series modules connection).

From the relation (4.11).

$$Number\ of\ parallel\ string(N_{parallel\ strings}) = \frac{I_{inv\ \max DC}}{I_{string\ max}} \quad (4.11)$$

$$N_{\text{parallel strings}} = \frac{1710}{11.73} = 145.7\ approximately\ 145\ parallel\ strings$$

By dividing this value on the No. of input of the selective inverter (8 inputs)

We will get the No. of parallel strings for each input of inverter.

$$\text{No. of parallel strings for each input of inverter} = \frac{145}{8} = 18.1 approximately\ 18$$

Now,

$$\text{No. of parallel strings for each input of inverter} * I_{SC} = 18 * 11.73 = 211.14\ A$$

By multiplying this current value by 8 (input of inverter) we will get a total input Dc current for inverter which equal to 1689.1 this value is very near the maximum Dc current for inverter 1710 A, (1689<1710).

$211.14 * 8 = 1689.1 A\ it\ within\ limits\ but\ it\ is\ high\ value$

The exact total No. of Parallel strings can be determined by dividing the total No. of PV module of the system (from equation 4.1), To the total No. of the Modules in a series string.as shown in the following relation.

$$\text{No. of Parallel strings}(N_{parallel\ strings}) = \frac{Total\ No.of\ PV\ modules\ for\ the\ system}{Total\ No.of\ modules\ in\ sreies\ string(N_{series\ string})} \quad (4.12)$$

$$\text{No. of Parallel strings}\left(N_{parallel\ strings}\right) = \frac{2176}{17} = 128\ parallel\ strings$$

Now we will find the No. parallel strings for each inverter input (8 inputs).

$$\text{No. parallel strings for each inverter} = \frac{128}{8} = 16\ Parallel\ strings\ per\ inverter\ input$$

The Maximum inverter DC current can be found by multiplying the No. of Parallel strings by the current (the current of series string) for each string then multiply the result by the number of inputs (8 inputs) of inverters shown below:

$$\text{Maximum inverter DC current } (I_{inv\max DC}) = 16 * 11.73 = 187.68\ A$$

$$\text{Maximum inverter DC current } (I_{inv\max DC}) = 187.68 * 8 = 1501.4\ A$$

1501.4 A It is an acceptable value and < 1710 A Maximum inverter DC current in the Datasheet. The Figure 4.16. Shows the Number of Parallel strings in the pvsyst software it is like our calculation.

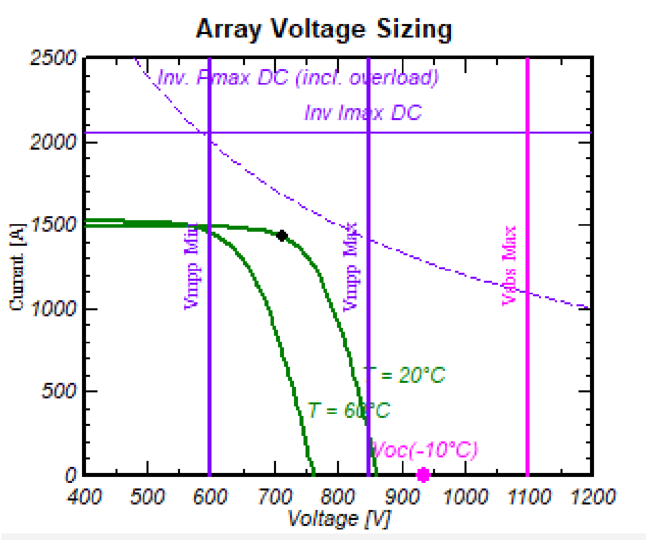

Figure 4.12. Array voltage sizing in case of the parallel strings is 128 string.

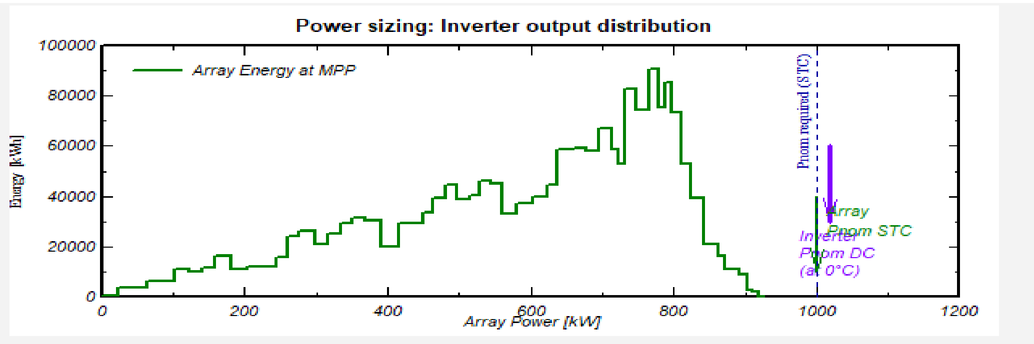

Figure 4.13. Power sizing inverter output distribution in case of the parallel strings is 128 string.

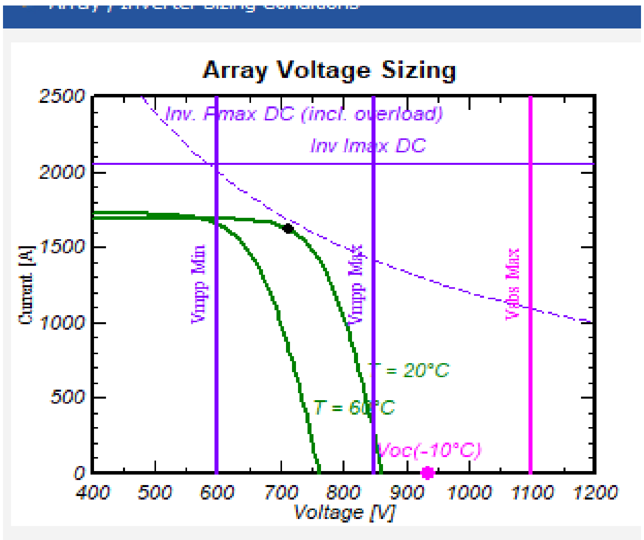

Figure 4.14. Array voltage sizing in case of the parallel strings is 145 string.

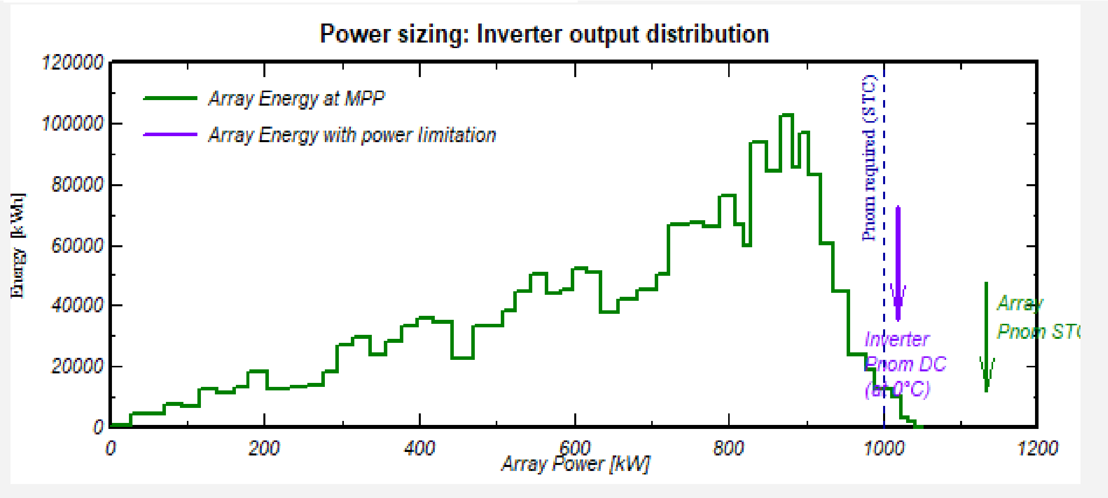

Figure 4.15. Power sizing inverter output distribution in case of the parallel strings is 145 string.

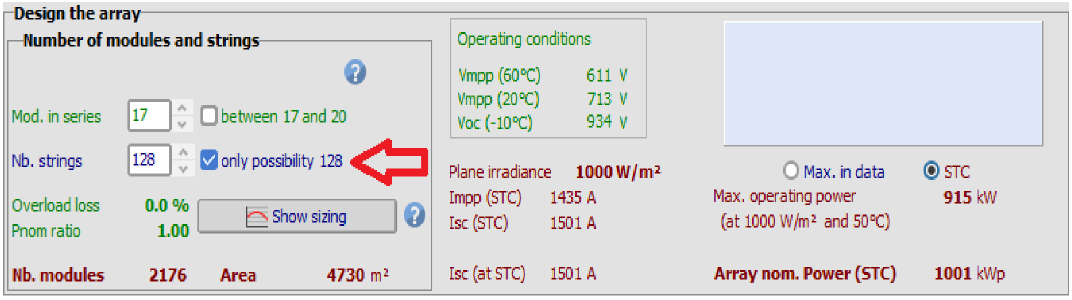

Figure 4.16. Shows the Number of Parallel strings in the pvsyst .

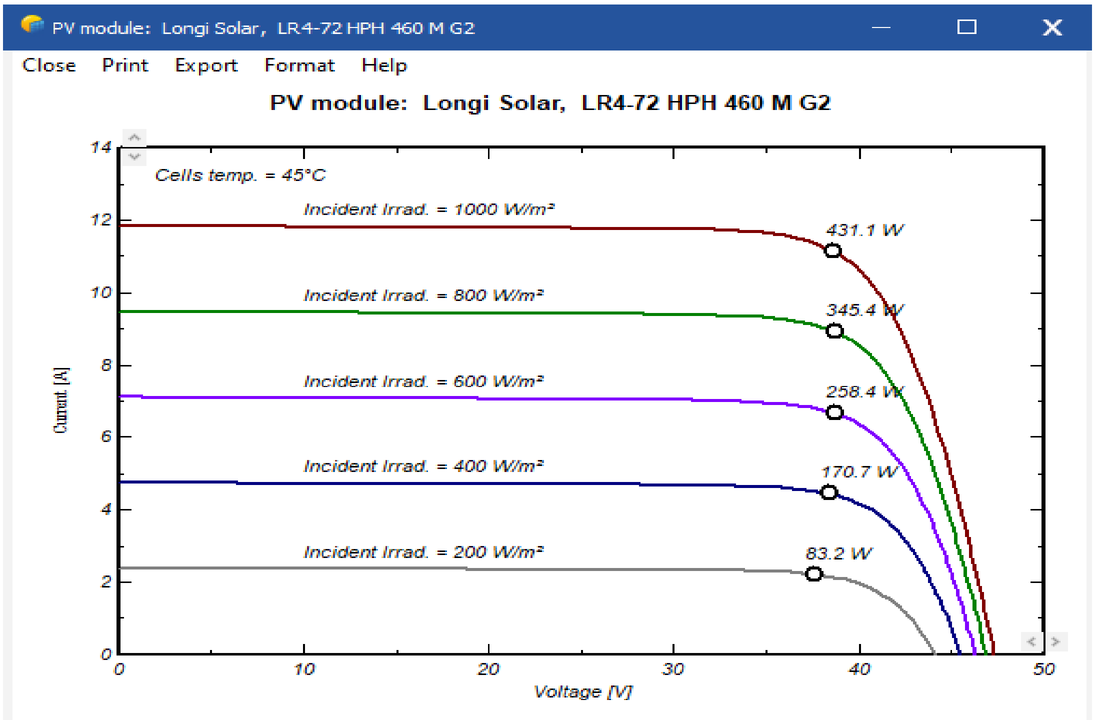

Figure 4.17. The current-voltage characteristics curve at different irradiation values for PV module by pvsyst.

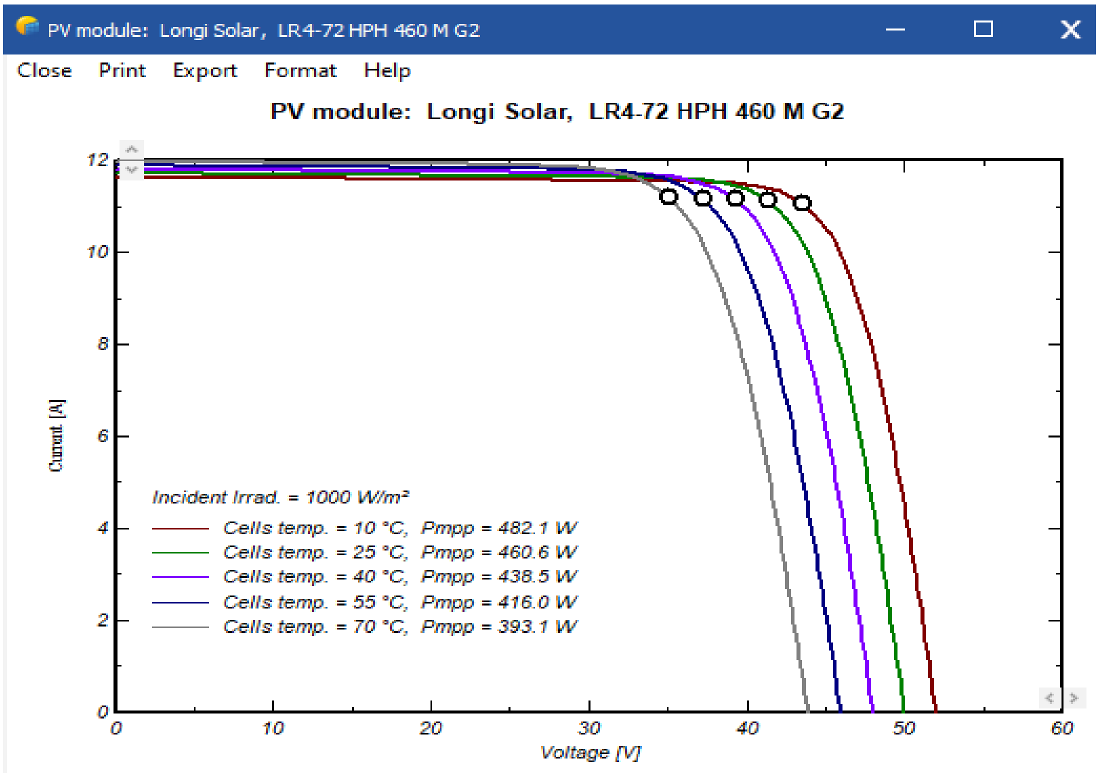

Figure 4.18. The current-voltage characteristics curve at incident Irradiation 1000W/m2 for PV module by pvsyst.

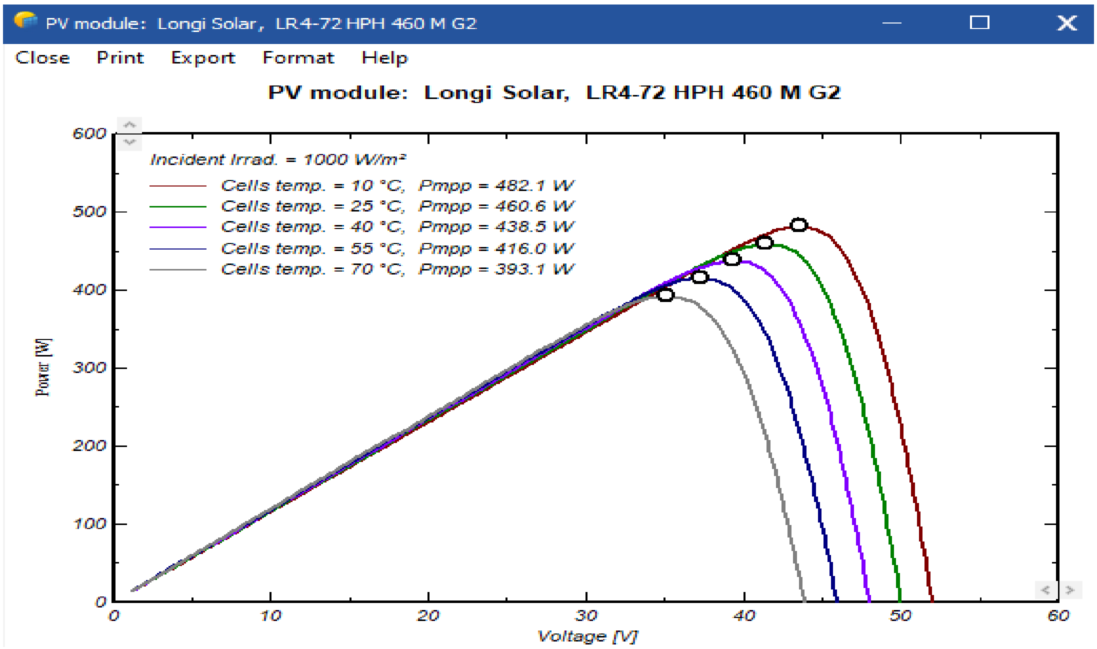

Figure 4.19. Power-Voltage characteristics curve at incident Irradiation.=1000W/m2 for PV module by pvsyst.

Table 4.6. Central inverter data sheet.

Module	ABB Central inverter
Type designation	PVS800-57-1000kW-C
Input Side (DC)	
Max DC Voltage ($U_{max\ (DC)}$)	1100 V
DC Voltage Range, mpp($U_{DC,mpp}$)	600-850 V
Number of Protected DC Inputs	8 - 20 (+/-)
Max Dc Current ($I_{max\ (DC)}$)	1710 A
Output Side (AC)	
Max Output Power	1200 W
Nominal Power ($P_{N(AC)}$)	1000 W
Nominal AC Current ($I_{N(AC)}$)	1445 A
Power at cosϕ	950 kW
Output Frequency	50/60 Hz
Nominal Output Voltage ($U_{N(AC)}$)	400 V
Efficiency	98.8 %
Dimension (Depth/Width/Height), mm(D,W,H)	708/3630/2130 mm

4.6.2. Inverter Sizing

It is difficult to come up with a generally applicable optimum inverter sizing When selecting an inverter. Solar resource and Module tilt angle are important to project parameters. The optimal sizing of the inverter is Depending on the characteristics of the plant design. The inverter sizing range for most plants will fall within the guidelines set by [99]:

$$1.2 > Power\ ratio > 0.8 \qquad (4.13)$$

The term "power ratio" is used to describe the relationship between the maximum DC input power of the inverter and the maximum power of the PV generator (array, string, or strings) being taken into consideration at STC.

$$Power\ ratio = \frac{P_{(\ Inverter\ DC\ rated)}}{P_{(PV\ peak)}} \qquad (4.14)$$

$$P_{(\ Inverter\ DC\ rated)} = \frac{P_{(\ Inverter\ AC\ rated)}}{\eta_{(100\%)}} \qquad (4.15)$$

Power inverter DC rated can be find from equation (4.15).

$$P_{(\ Inverter\ DC\ rated)} = \frac{1000\ kW}{98\%} = 1020.4\ kW$$

Power ratio can be found by using equation (4.14).

$$P_{(PV\ peak)} = 460 * 17 * 16 * 8 = 1000.96\ kW.$$

$$Power\ ratio = \frac{1020.4\ kW}{1000.96\ kW} = 1.09\ it\ is\ acceptable\ value\ within\ limits.$$

$From\ equation\ (4.13)\ \ The\ Power\ ratio\ is:$

$0.8 < 1.09 < 1.2$

From this acceptable result we choose the inverter for our system as shown in Table 4.5.

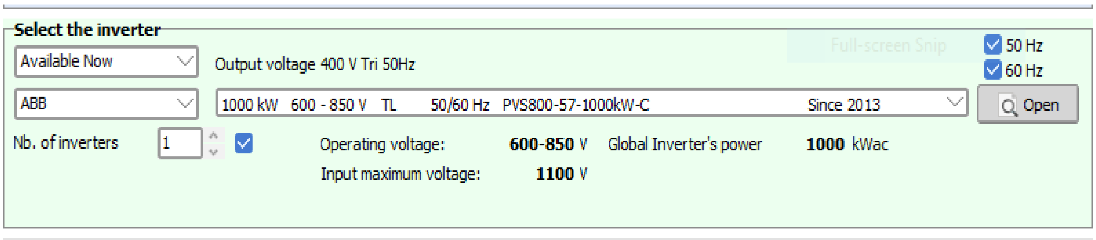

Figure 4.20. Shows the PV plant inverter in the pvsyst.

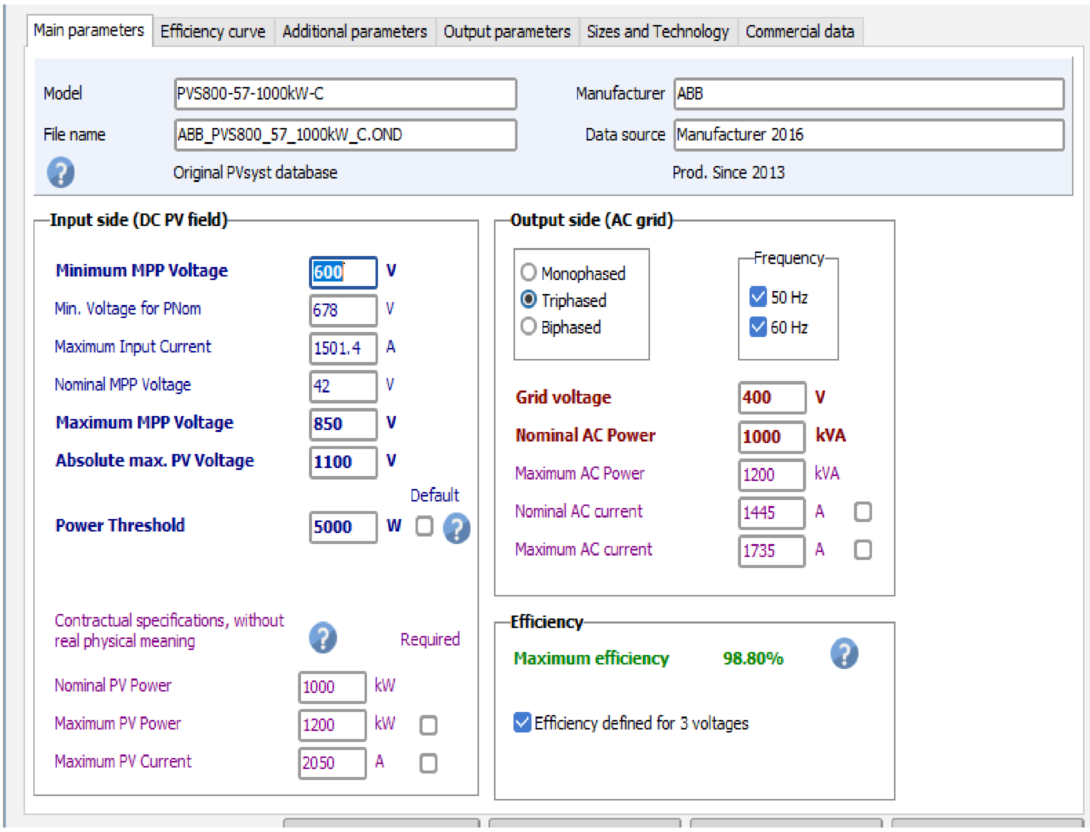

Figure 4.21. The main parameters of ABB PVS800-57-1000kWC in the pvsyst.

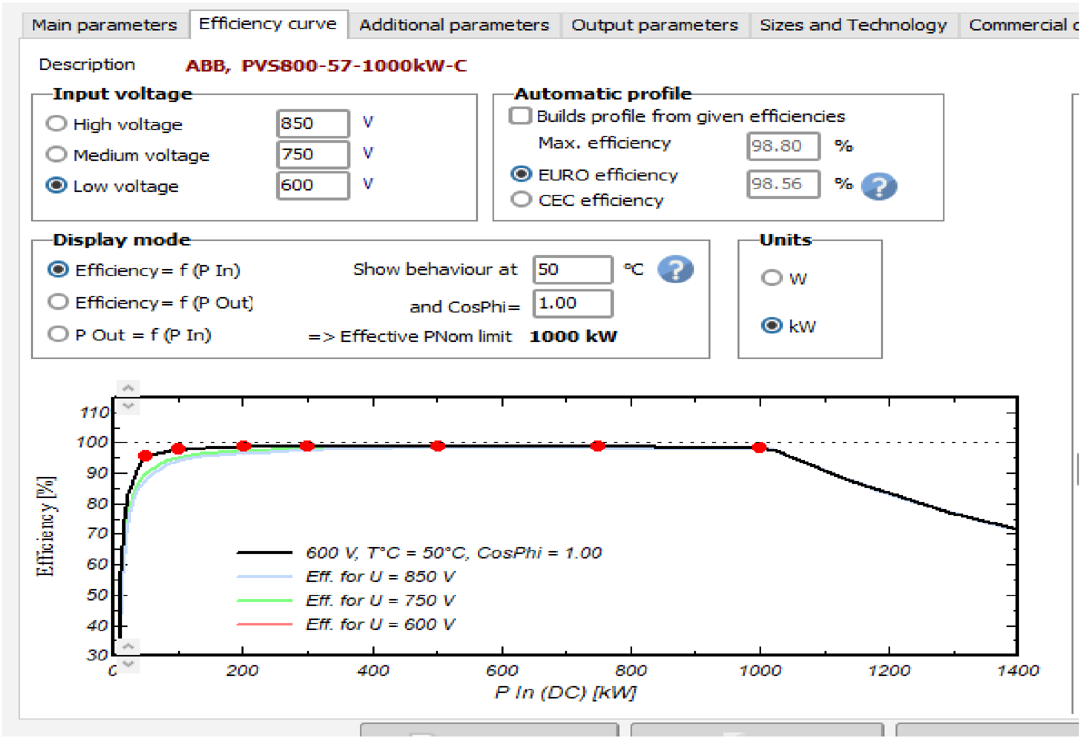

Figure 4.22. PVS800-57-1000kWC inverter efficiency curve in pvsyst.

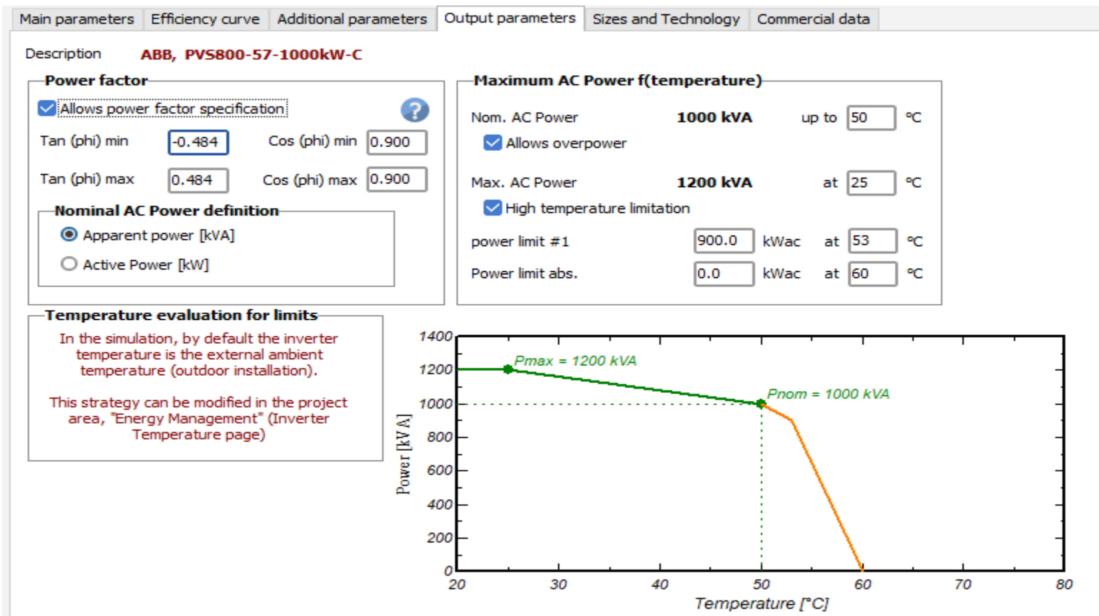

Figure 4.23. The out parameters and (Maximum AC power with Temperature curve) in pvsyst .

4.6.3. Combiner Box Sizing

Combiner boxes are required where an array's individual strings are organized and joined in parallel before being connected to the inverter through the main DC cables. Combiner boxes include isolation and protection devices such as load break switches (disconnects) and string fuses. A DC main switch device should be accordance with IEC 60364-7-712, and it must be capable of carrying 125 % of the PV array's short circuit current at STC. ($125\% * N_{Mod, parallel} * I_{Mod, Sc, STC}$) [94].

$$\text{current follow through the DC cable from the combiner box to the inverter input} = 125\% * \mathrm{N}_{\text{parallel strigs}} * I_{\text{Mod ,Sc ,STC}} \quad (4.16)$$

According to the parameters the value of the current follows through the DC cable from the combiner box to the inverter input is

$$1.25 * 16 * 11.73 = 234.6\ A\ it\ is\ within\ limits$$

$$\text{Rated total current} > \text{current follow through the DC cable from the combiner box to the inverter}$$

$$240A > 234.6A$$

IEC 60269 states that gR fuses linked in series in the string's negative and positive poles are to be utilized to safeguard the string cables from reverse currents which, due to the disadvantages of blocking diodes, have totally supplanted them as a method of preventing reverse currents. To calculate the fuse nominal current in compliance with IEC 60269 standards, the formula shown below is usually applied. [94].

$$\mathrm{I}_{\text{string SC STC}} \leq \mathrm{I}_{\text{nominal fuse}} \leq \mathrm{I}_{\text{string SC STC}} \quad (4.17)$$

It is also advised that the.

$$I_{nominal\ fuse} \geq 125\% \, I_{nominal\ string} \quad (4.18)$$

So, the I $_{nominal\ fuse}$ for each string can be determined:

$$I_{nominal\ fuse} = 1.25 * 11.73 = 14.6\ the\ suitable\ fuse\ used\ in\ the\ system\ is\ 15\ A$$

The string fuse must operate within the string fuse limits. Generally, string fuse rating is determined using the relation below [99].

$$String\ fuse\ voltage\ rating = V_{OC(STC)} * N_{s\ string} * 1.15 \qquad (4.19)$$

Where:

N = Number of Modules (in series string).

Now we will find the string fuse voltage rating.

$$String\ fuse\ voltage\ rating = 49.7 * 17 * 1.15 = 971.6\ V$$

Table 4.7. Combiner box specification.

Module	
Input	
Max No. of Input String	20
No. of Protection Fuse	40
Max Current per input (A)	12 A
Available Fuses	(15A/30A) Standards (32A,30A,25A,20A,16A,15A,12A,10A)
Type of Fuses	10x85mm, gPV fuses,30kA
Cable inlet	(n.4 cables entry diameter :6 - 10 mm for each gland) M40 cable glands
Max DC Voltage	1500 V dc
Inlet connections	Direct connection to fuse holders or distribution bar, wiring gauge 1.5 to 16 mm^2
Output	
Cable outlet	Up to 2 pairs of M50 cable glands (cable diameter :27 – 35 mm^2
Rated total Current (A)	240
Dc switch disconnected rating (A)	400
Outlet Connections	Direct connection on copper plates, wiring gauge up to 20 x 240 mm^2 per pole
General Information	
Operating Temperature Range	-20^{O} C - $+55^{O}$ C

Relative Humidity	0 to 95 %
Protection Rating	IP65
Max Altitude	2000 m.a.s.l
Size (mm)	320X1000x750 (DxWxH)
Electrical shock protection	Class II equipment
Grounding connection	M20cable gland (cable dimiter:7 to 13 mm, wiring gauge 2.5 – 35 mm^2)

4.6.4. Sizing and Designing Cables in PV System

After choosing the size of the inverter in the PV system. The single-line diagram and the PV plant scheme has drawn by AutoCAD software as shown in figures 4.23, 4.24,4.25. every 17 modules are first connected in series, then in parallel. through the junction box (combiner box) this series and parallel strings are connected to a combiner box with cables of different length and size.

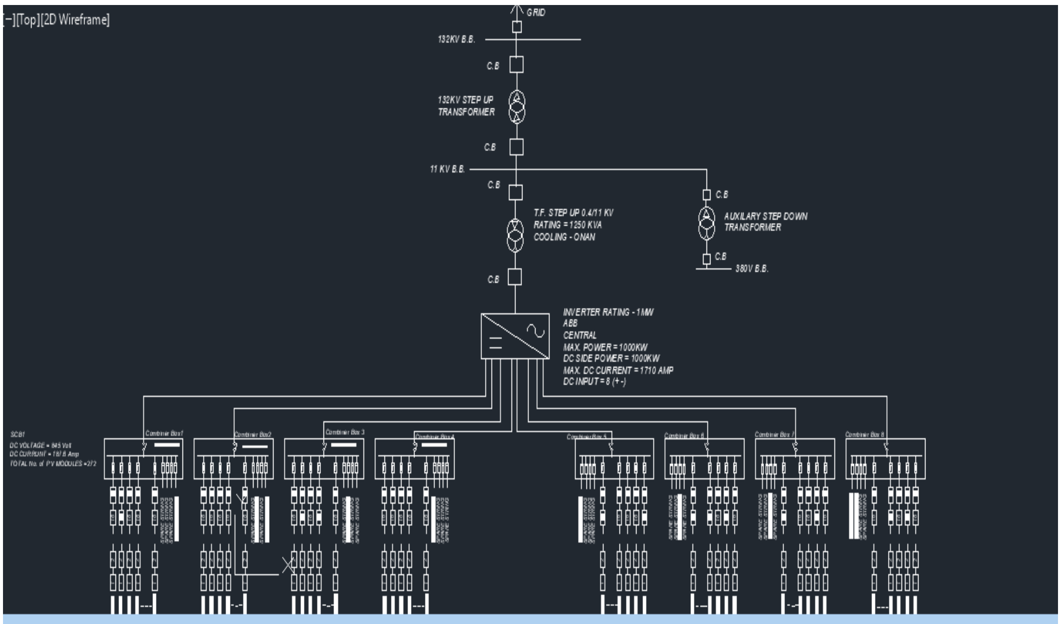

Figure 4.24. 1MW Photovoltaic station Single line Diagram by Autocad.

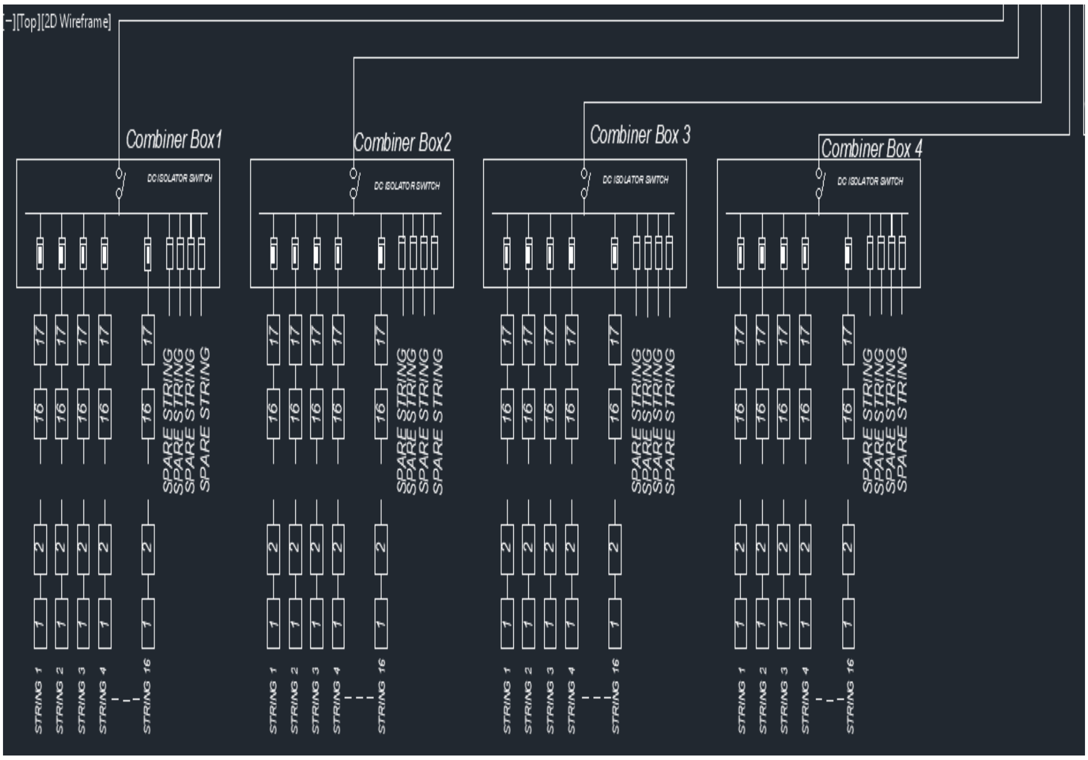

Figure 4.25. Series and parallel PV modules with combiner boxes from(1-4) Single line diagram.

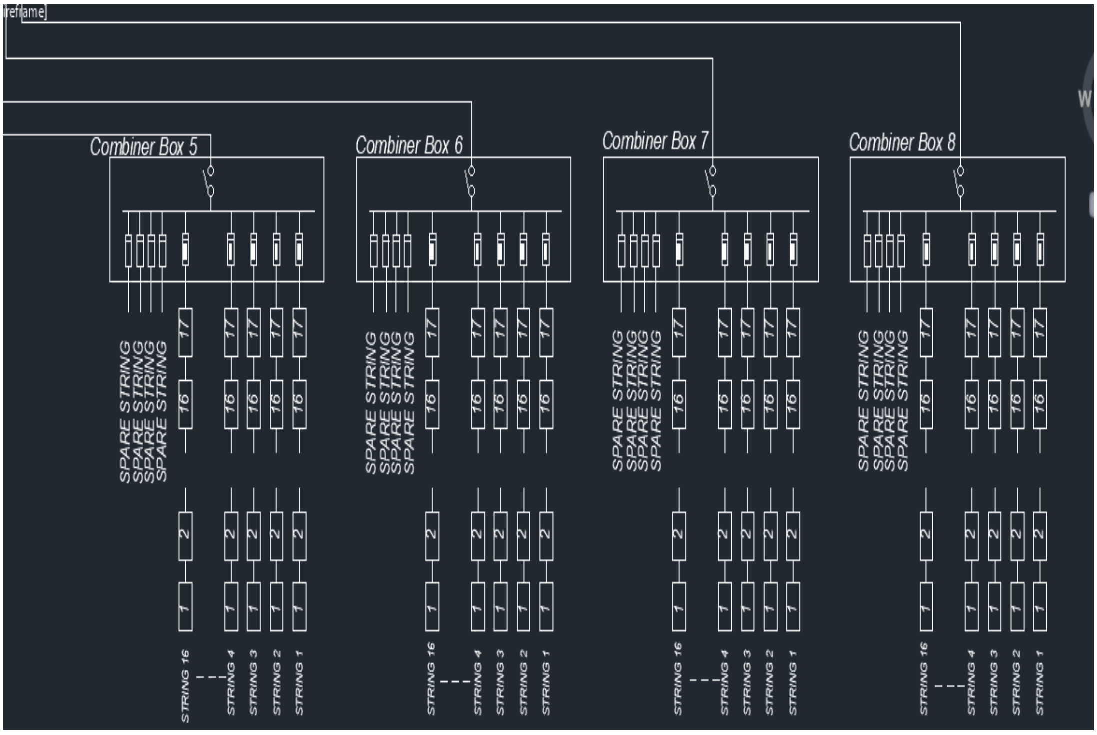

Figure 4.26. Series and parallel PV modules with combiner boxes from(5-8).

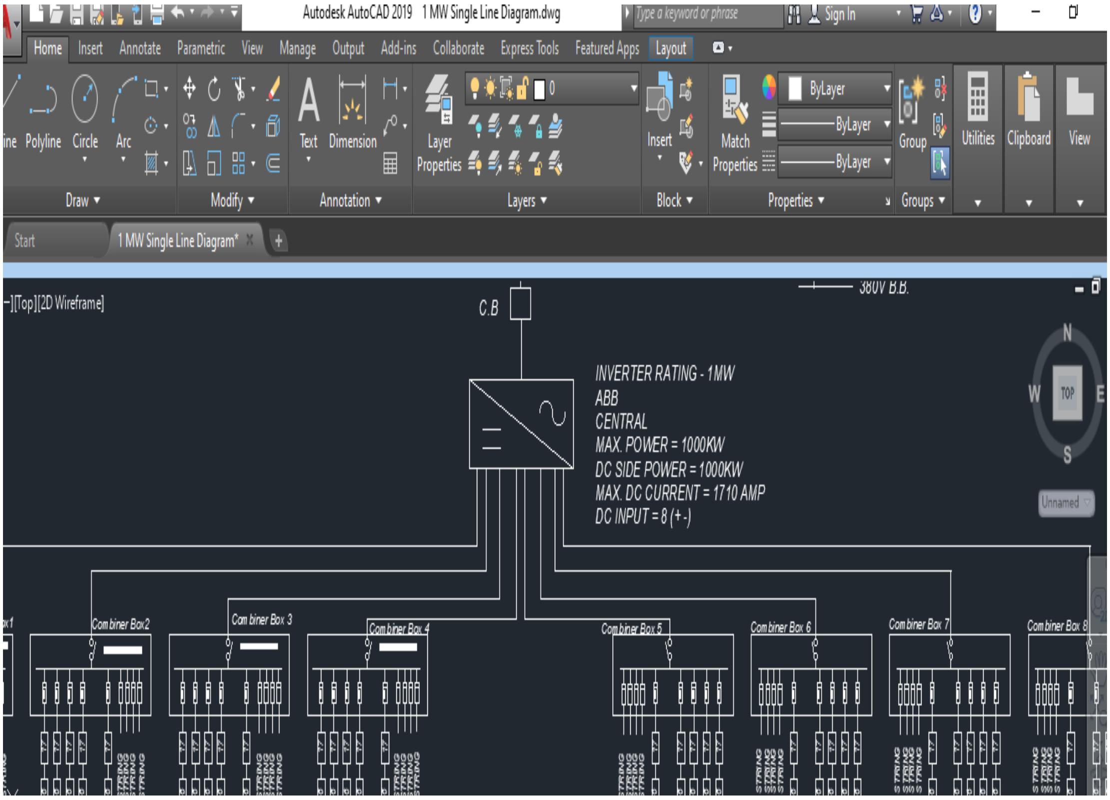

Figure 4.27. Combiner boxes with inverter in the Photovoltaic system.

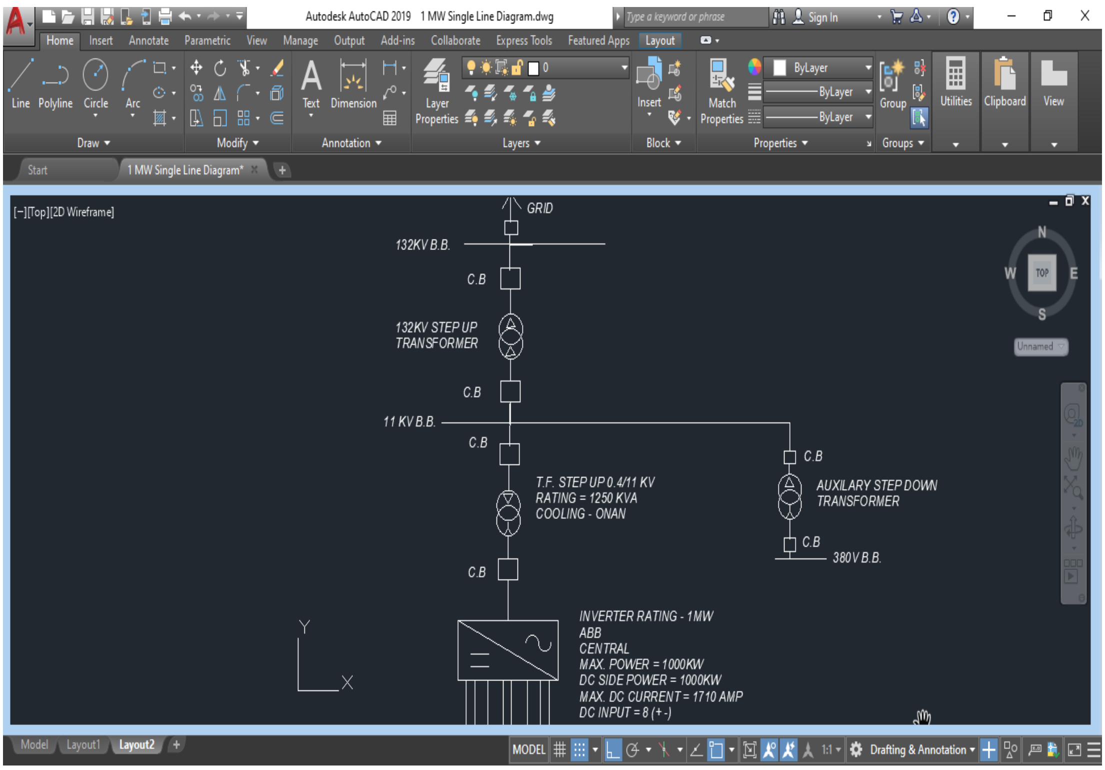

Figure 4.28. Inverter in the Photovoltaic system with the step-up transformers 11kv,132kv ,Single line diagram.

Generally, when sizing the cables in the PV systems, there are three criteria must be followed [99].

- The voltage rated of the cable.
- The current carrying capacity(ccc).
- The minimization of cable losses (CSA).

4.6.4.1. The Voltage Rated of the Cable

Designers of PV system plants take in the account that the voltage maximum rated. This voltage should not have excessed 1000V since the standard cable could only withstand a voltage of this value. The PV system nominal voltage should be between the range of 450 -1000 V, that mean there is no problems will be appear in this system. Since the several cables are installed outside in the large PV plants there are along strings, so that the voltage resistance of the cable should take in the account [94].

4.6.4.2. The Current Carrying Capacity

Each PV system's string cable should be capable of carrying all the possible current sources in the system. The over current protection limits are the value (amount) of the current capacity of passing safely through the various protection of the system. The CCC of a string should consider any over current in the system. In the case of the over-current protection will be installed, the CCC should be as following relation [100].

$$CCC \geq Rating\ of\ the\ string\ over\ current\ protection \tag{4.20}$$

In the case of the string overcurrent protection will not be installed the CCC can be represented by the following relation.

$$CCC \geq I_n + \left(1.25 * I_{MOD,SC}\right) * \left(N_{Parallel\ strings} - 1\right) \tag{4.21}$$

4.6.4.3. Minimization of the Cable Losses

Sizing the cables of a large PV plant should take into account the voltage drop in the cables of the system to reduce the cables losses as much as possible by choosing the suitable cross-section area of the cables. According to the standards the voltage drop through the cables should be less than 3%, for the system which contains string cables and array cables this proportion should be divided into the string and array cables, So the total voltage drop value should not exceed the value 3%, That means the voltage drop accepted value for each type of this cables should not exceed 1%.

4.6.5. Calculation the DC and AC Cable Size of the System

4.6.5.1. Sizing The DC Cables

In this section, the DC cable size for string and array will determine, according to the relations below [94].

$$\Delta V\% = \frac{2 * L_{DC\,Cable} * N_{Parallel\,strings} * I_{String,Mpp,STC}}{A_S * N_{Series,MOD} * V_{Mpp,MOD,STC} * \sigma_{cu}} \tag{4.22}$$

$$\Delta V\% = \frac{2 * L_{DC\,Cable} * I_{String,Mpp,STC}}{A_S * N_{Series,MOD} * V_{Mpp,MOD,STC} * \sigma_{cu}} \tag{4.23}$$

Where:

ΔV =Voltage drops value of DC cables for (string /array).

A_s= Cross section area of the cable.

$L_{DC\ Cable}$ = length of DC Cable (string/array).

$N_{Parallel\ string}$ =No.of parallel string in the PV system.

$I_{string,\ Mpp,\ Stc}$ = Max power point current of string at STC.

$N_{series,\ MOD}$ = No. of PV modules in series.

σ_{cu} = conductivity of copper which equal to 56 $m\Omega^{-1}.mm^{-2}$.

$V_{Mpp,\ MOD,\ stc}$ = Maximum power point voltage of PV module at STC.

Formula (4.22) used for Array cables and (4.23) equation used for string cables. We will have assumed the cross-section area value of the cable and then we will find the voltage drop and create a comparison between the results that we get, and the acceptable voltage drop value, which should be equal to or less than 3% (ΔV % $\leq$3%). We will use DC copper cables (with different lengths). From the Figure 4.28. And the Equation (4.23) we will calculate the Negative Dc cable and the Positive DC cables for a series string for sectors (A, B, ….to Q)

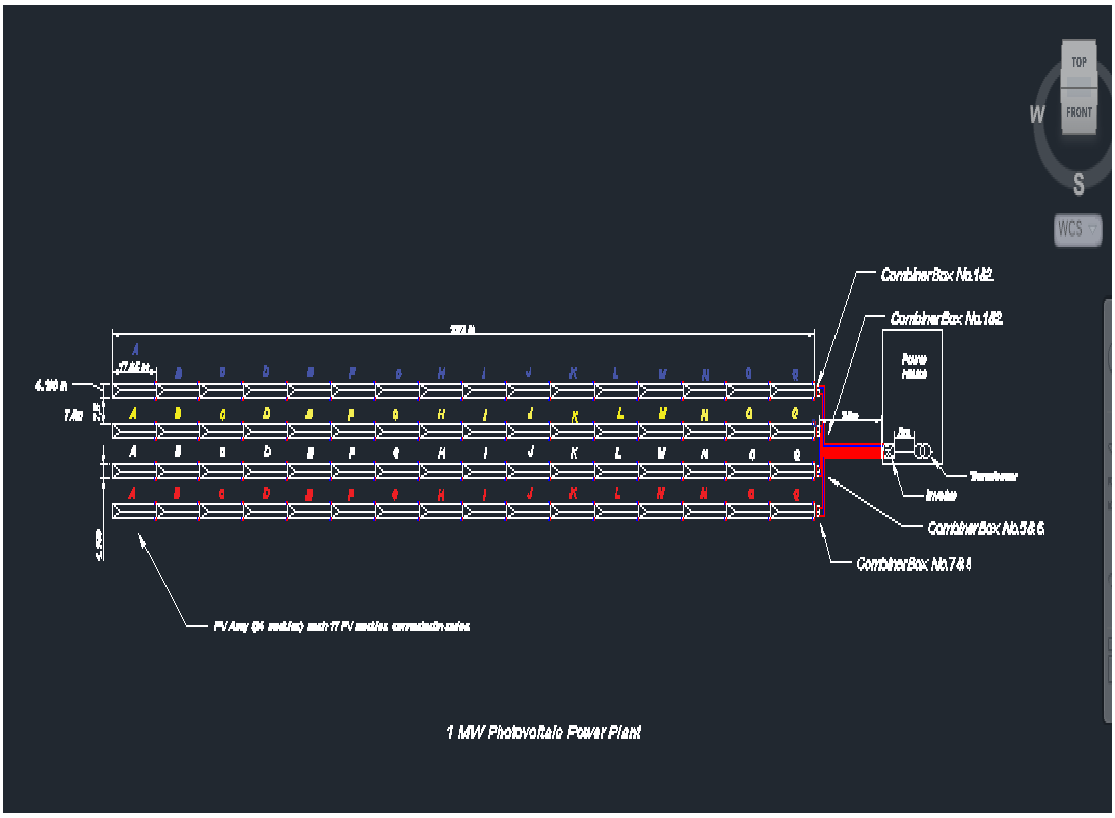

Figure 4.29. 1 MW Photovoltaic Power Plant Designing By AutoCAD.

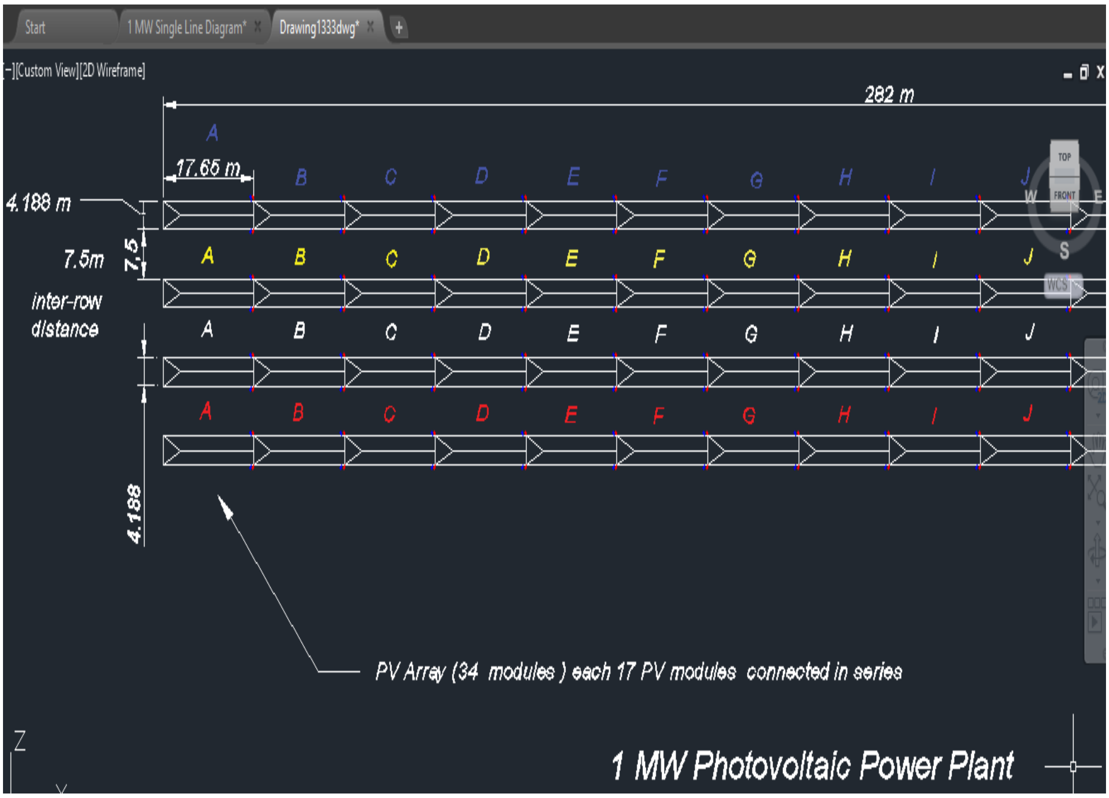

Figure 4.30. The PV arrays of 1MW Photovoltaic Power Plant by AutoCAD .

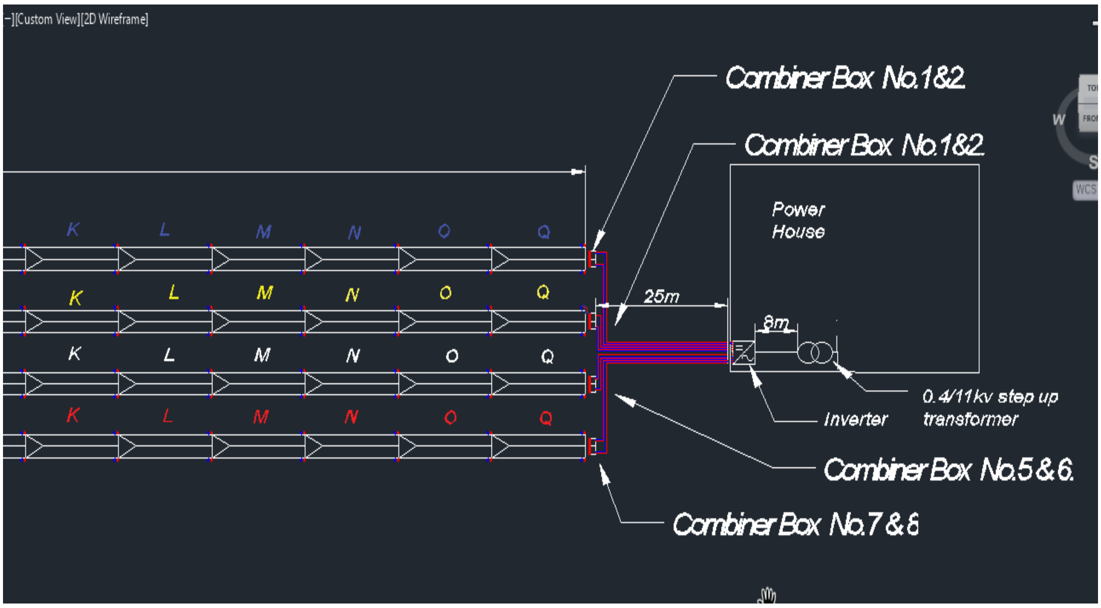

Figure 4.31. The PV parallel strings connections of 1MW Photovoltaic Power Plant by AutoCAD .

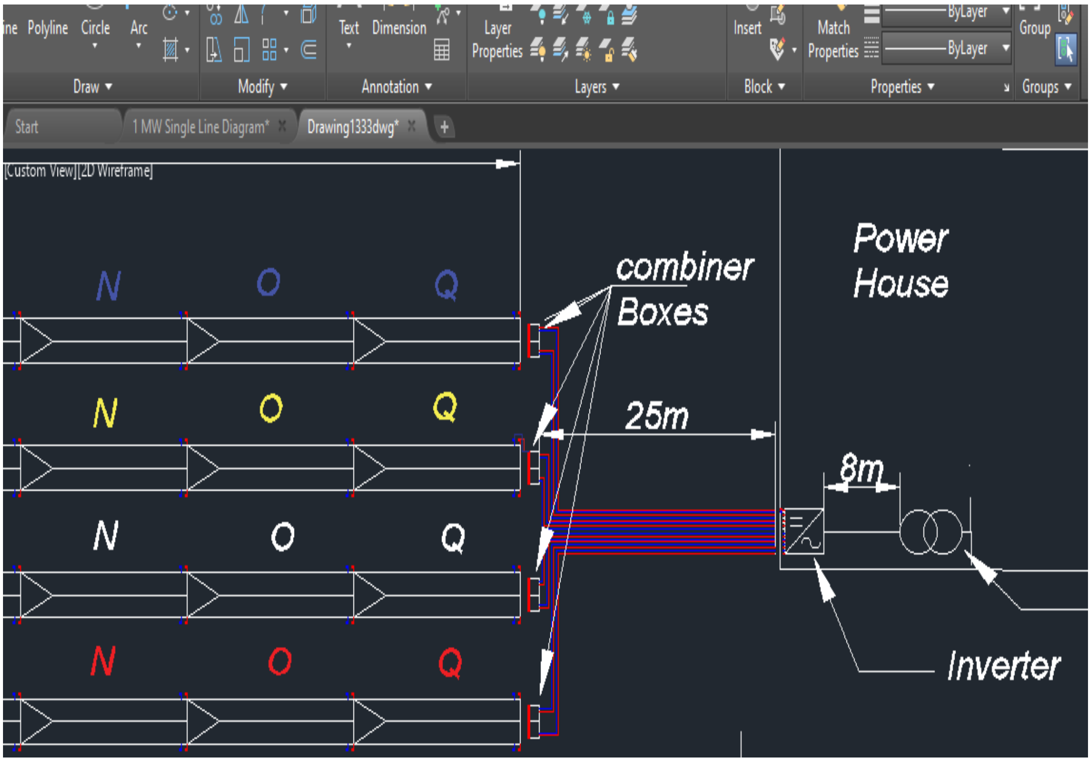

Figure 4.32. The PV parallel strings connections with the combiner Boxes with inverter of 1MW Photovoltaic Power Plant by AutoCAD .

- A^-

$$\Delta V = \frac{2 * L_{DC\ Cable} * I_{String,Mpp,STC}}{A_S * N_{Series\ ,MOD} * V_{Mpp,MOD,STC} * \sigma_{cu}}$$

$$\Delta V\% = \frac{2 * 282m * 10.98A}{10\ mm * 17 * 41.9V * 56m\Omega^{-1}.mm^{-2}} = 1.5\%$$

- A^+

$$\Delta V\% = \frac{2 * 264.4 * 10.98A}{10\ mm * 17 * 41.9V * 56m\Omega^{-1}.mm^{-2}} = 1.4\%$$

In the same way, we will calculate the other PV sector's voltage drop. We use a Cable cross-section area of 10mm^2.

- B^-

  ΔV= 1.4 %.

B^+

$\Delta V = 1.3\ \%$.

- C^-

  $\Delta V = 1.3\ \%$.

  C^+.

  $\Delta V = 1.2\ \%$.

- D^-.

  $\Delta V = 1.2\ \%$.

  D^+.

  $\Delta V = 1.1\ \%$.

- E^-.

  $\Delta V = 1.1\ \%$.

  E^+.

  $\Delta V = 1\ \%$.

- F^-.

  $\Delta V = 1\ \%$.

  F^+.

  $\Delta V = 0.97\ \%$.

In sector G of PV Modules, we change the Cable cross section area to $6mm^2$.

- G^-.

  $\Delta V = 1.6\ \%$.

  G^+.

  $\Delta V = 1.4\ \%$.

- H^-.

  $\Delta V = 1.4\ \%$.

  H^+.

  $\Delta V = 1.2\ \%$.

- I^-.

  $\Delta V = 1.2\ \%$.

  I^+.

  $\Delta V = 1.1\ \%$.

- J^-.

  $\Delta V = 1.1\ \%$.

  J^+.

ΔV= 0.7 %.

In sector K of PV Modules, we change the Cable cross section area to 4 $mm^{2.}$

- K^-.
  ΔV= 1.4 %.

  K^+.

  ΔV= 1.2 %.
- L^-.
  ΔV= 1.2 %.

  L^+.

  ΔV= 0.97 %.
- M^-.
  ΔV= 0.97 %.

  M^+.

  ΔV= 0.74 %.

  In sector N of PV Modules, we change the Cable cross section area to 2.5 mm^2.
- N^-.
  ΔV= 1.1 %.

  N^+.

  ΔV= 0.78 %.

  In sector O of PV Modules, we change the Cable cross section area to 1.5 mm^2.
- $O^{-.}$
  ΔV= 1.3 %.

  $O^{+.}$

  ΔV= 0.66 %.

  In sector Q of PV Modules, we change the Cable cross section area to 1.5 mm^2.
- $Q^{-.}$
  ΔV= 0.99 %.

  $Q^{+.}$

  ΔV= 0.02 %.

Now from equation (4.22) and Figure 4.31. we will find the Cable cross-section area for the Array cable (Array 1, 2,3, to… ,8).

$$\Delta V\% = \frac{2 * \ L_{DC\ Cable} \ * \ N_{Parallel\ strings} \ * \ I_{String,Mpp,STC}}{A_S \ * \ N_{Series\ ,MOD} \ * V_{Mpp,MOD,STC} \ * \sigma_{cu}}$$

For Array No.1&2.

$$\Delta V\% = \frac{2 * \ 45\ m * \ 16 \ * \ 10.98\ A}{25mm^2 \ * \ \ 17 * 41.9\ V * 56m\Omega^{-1}.mm^{-2}} = 1.5\ \%.$$

For Array No.3&4.

$$\Delta V\% = \frac{2 * \ 33m * \ 16 \ * \ 10.98\ A}{25mm^2 \ * \ \ 17 * 41.9\ V * 56m\Omega^{-1}.mm^{-2}} = 1.1\ \%.$$

For Array No.5&6.

$$\Delta V\% = \frac{2 * \ 29m * \ 16 \ * \ 10.98\ A}{16mm^2 \ * \ \ 17 * 41.9\ V * 56m\Omega^{-1}.mm^{-2}} = 1.5\ \%.$$

For Array No.7&8.

$$\Delta V\% = \frac{2 * \ 40m * \ 16 \ * \ 10.98\ A}{25mm^2 \ * \ \ 17 * 41.9\ V * 56m\Omega^{-1}.mm^{-2}} = 1.4\ \%.$$

DC cables must be chosen under standards of IEC and have the ability to work at high/low-temperature degree (-55to 125C^o) wide temperature range, having animal-resistant mechanical characteristics, stretching, bending, and compression, multi-core steel wire armoured cables suitable for main DC cables are, which are typically utilized in exposed or underground lines.

4.6.5.2. Sizing the AC Cables

In this section, the AC cables size will determine, according to the relations below [94].

$$\Delta V\% = \frac{\sqrt{3} * L_{AC\ Cable} * I_{Inverter\ AC} * Cos\varphi}{A_s\ * V_{Inverter\ AC} * \sigma_{cu}} \tag{4.24}$$

Where:

ΔV =Voltage drops value of AC cables.
$L_{AC\ Cable}$ = The AC cable's length
$I_{Inverter\ AC}$ = The Inverter AC current.
Cosφ = Inverter power factor.
A_S = Cross section area for AC Cable.
$V_{Inverter\ AC}$= AC voltage inverter.
σ_{cu} = conductivity of copper which equal to 56 $m\Omega^{-1} \cdot mm^{-2}$.

Like the DC sizing cables, We will assume the cross-section area value of the cable and then we will find the voltage drop, which should be equal to or less than 3% ($\Delta V\% \leq 3\%$).

From Figure 4.31. and equation (4.24). We will find the Voltage drop ΔV % for AC cable, we will estimate the cross-section area and find the voltage drop.

$$\Delta V\% = \frac{\sqrt{3} * 8\ m\ * 1445\ A * 0.95}{50mm^2 * 400\ V * 56m\Omega^{-1}.mm^{-2}} = 1.6\ \%\ It\ is\ acceptable\ value$$

So, the cross-section area of the AC Cable =50 mm^2.

When AC cables are chosen, we must consider. The conductor should be capable of passing both the operational and I_{SC} current safely, Cable needs to be rated for the maximum voltage allowed, Choosing the right No. of cores (single or multiple), and made sure the insulation is adequate for the installation environment [99].

4.6.6. DC Switching

To ensure protection and isolation, a solar PV system's DC sector contains switches. This section covers DC circuit breakers (CBs), disconnects, and DC switches [99].

4.6.6.1. DC Circuit Breakers (CB)

In the case of a fault, string fuses/MCBs cannot be depended upon to disconnect the power. This is because PV modules are current-limiting components with I_{SC} that are only slightly greater than the nominal current. (Because the fault current is smaller than the trigger current, the fuse will not blow or the MCB will not trip). As a result, most PV regulations and rules recommend placing main DC CBs between the PV array fields and the grid-connected inverters. DC CBs are included with some inverter model types. Installation of additional CBs may therefore be unnecessary [99].

4.6.6.2. DC Switches/Disconnects

Installing switching devices in PV array junction boxes is required by good design practice. DC switches enable complete PV arrays to be manually electrically isolated, which is necessary for maintenance and installation operations. The specifications for DC switches must be met conditions.

- Has the ability to break when fully loaded.
- Appropriate (Rated) for the system’s maximum current and voltage predicted.

PART 5

SIMULATION AND RESULTS

5.1. THE RESULTS OF DESIGNING A 1MW PV POWER PLANT

The results were obtained it from pvsyst. Software simulation for 1Mw Photovoltaic power plant which designed by this software, the plant contains from 2176 PV module (si-mono 460 w_p), The No. of photovoltaic modules linked in series are 17 Module (series strings) and the total number of parallel strings for the system is 128 strings (each string has 16 PV module connected in parallel) the parallel strings connected to a central inverter(1000kw) have 8 inputs to produce 1Mw.

The result obtained from pvsyst, shown in table (5.1) that the average annual ambient temperature for the site is 20.60 $C^{o,}$ and the average annual Horizontal global irradiation value is equal to 1825 kW/m^2 and this is a good value, also the Global incident irradiation in the plant is equal to 2099.5 kWh/m^2.

Table 5.1. The main result of 1MW PV power plant by pvsyst according weather parameters.

Month	$T._{Amb}$ C^o	Horizontal global Irradiation kW/m^2	Global incident in plant kWh/m^2	Horizontal Diffuse Irradiation kWh/m^2	Effective global, correspond for IAM and shading kWh/m^2
January	6.84	78.8	126.9	33.79	125.5
February	8.68	92.0	128.8	40.72	127.4
March	13.27	138.3	167.0	63.89	164.4
April	17.62	170.5	181.8	16.07	178.5
May	24.51	196.4	187.9	87.92	184.0

June	**30.99**	**233.3**	**211.8**	**73.42**	**207.2**
July	35.02	232.2	215.9	74.27	211.4
August	34.19	212.1	218.4	67.31	214.4
September	29.00	177.2	211.0	45.70	207.5
October	23.12	128.6	176.0	47.96	173.9
November	14.25	90.6	145.4	32.35	143.8
December	8.91	75.0	128.6	38.31	127.4
Year	20.60	1825.0	2099.5	671.71	2065.3

Where:

T_{Amb}: Ambient temperature.

Glob Inc: Global incident in plane.

DiffHor: Horizontal diffuse irradiation.

GlobEff: Effective Global, correspond for IAM and shadings.

GlobHor: Horizontal global irradiation.

Table 5.2. The main result of 1MW PV power plant by pv sys according Technical parameters.

	P.R ratio	**E_{Array} MWh**	**E_{Grid} MWh**
January	0.929	120	118
February	0.915	120	117.9
March	0.894	151	149.4
April	0.874	161.5	158.9
May	0.847	161.9	159.3
June	0.84	174.6	172.0
July	0.788	172.9	170.3
August	0.788	174.8	172.3
September	0.811	173.7	171.2
October	0.857	153.2	150.9
November	0.895	132.4	130.3
December	0.919	120.4	118.3
Year	0.851	1817	1789

Where:

E_{Array}: Effective energy at the array's output.

PR: Performance Ratio.

E_{Grid}: Energy exported to grid.

Table (5.2) shows other important parameters resulting from the simulation this parameter is the annual Performance ratio (P.R%), annual Effective energy at the array's output, and the annual Energy exported to the grid. (0.851, 1817 MWh, 1789 MWh) respectively.

The performance ratio can be defined as the ratio of the exporting AC yield to the theoretical production of the system, the theoretical yield that the system would generate if modules converted received irradiation into useful energy at their rated capacity [99].

$$P.R = \frac{AC\ Yield(kWh) * 1\ (kW/\ m^2)}{DC\ installed\ capacity(kWh) * (Plane\ of\ Array\ irradiation(kWh/\ m^2)}\ 100\% \quad (5.1)$$

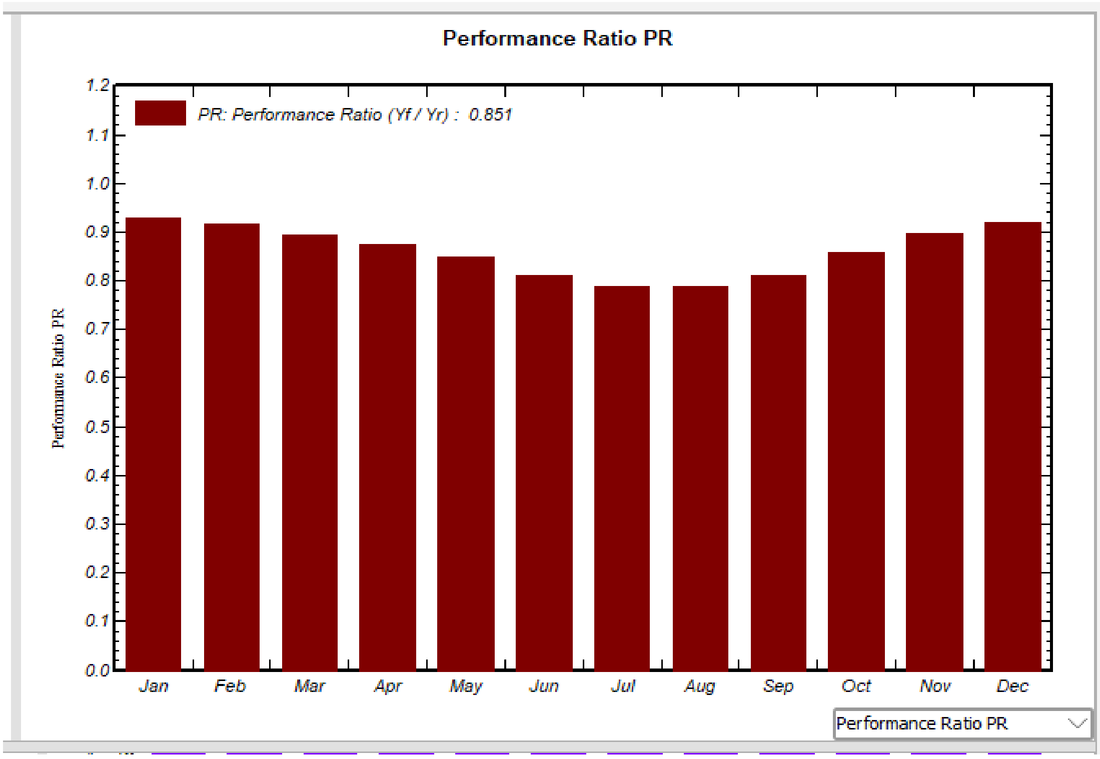

Figure 5.1. The Performance ratio of 1MW PV Power Plant by pvsyst.

Result of the simulation is shown in table 5.2. We can find the yield factor of the PV system (Y_f). which is referred to as the system's final yield of useful energy per day to the nominal power. unit is ($kWh/kW_p/day$) [105].

$$Y_f = \frac{E_{Array}}{P_{\text{nominal } at\ STC}} \tag{5.2}$$

Where:

Y_f = The yield factor.

$P_{\text{nominal array at STS}}$ = Nominal power array at Standard test condition (from pvsyst simulation as shown in Figure 5.2).

$$Y_f = \frac{1817\ MWh.year^{-1}}{1.001\ MW_P} = 1815\ {}^{MWh}/_{MW_P/year}$$

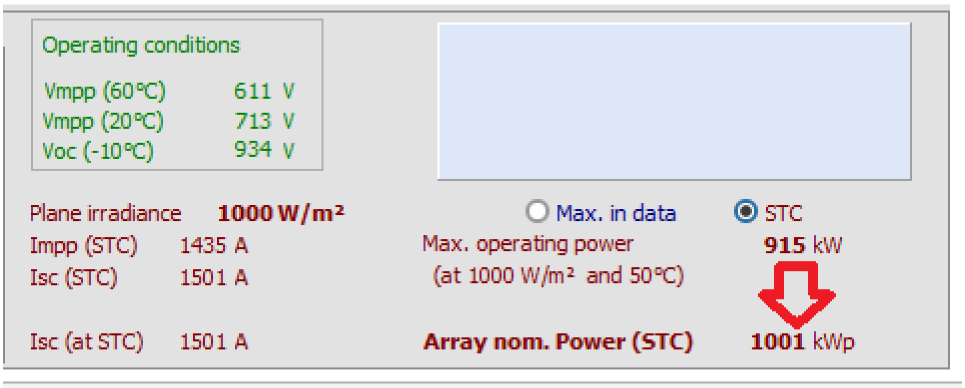

Figure 5.2. Nominal power array at Standard test condition.

From the (5.2) Table, we can find the capacity factor of a PV plant is a ratio of the energy generated by the station for a year to the installed capacity (Nominal Power) in case it had operate for the whole year [99]. In another word, it can be determined by dividing the yield factor by the day hours multiplied by the days of the year.

$$Capacity\ Ratio\ \% = \frac{Energy\ generated\ per\ annum\ (MWh)}{Installed\ Capacity\ (kWp) * 24 * 365} = \frac{Y_f}{8760} \tag{5.3}$$

$$Capacity\ Ratio\ \% = \frac{1815}{8760} = 20.7\ \%\ It\ is\ a\ good\ value$$

The value of the capacity factor ranges from 12-24 % (for PV plants of a fixed tilt). It is depending on the plant's performance ratio and solar resource.

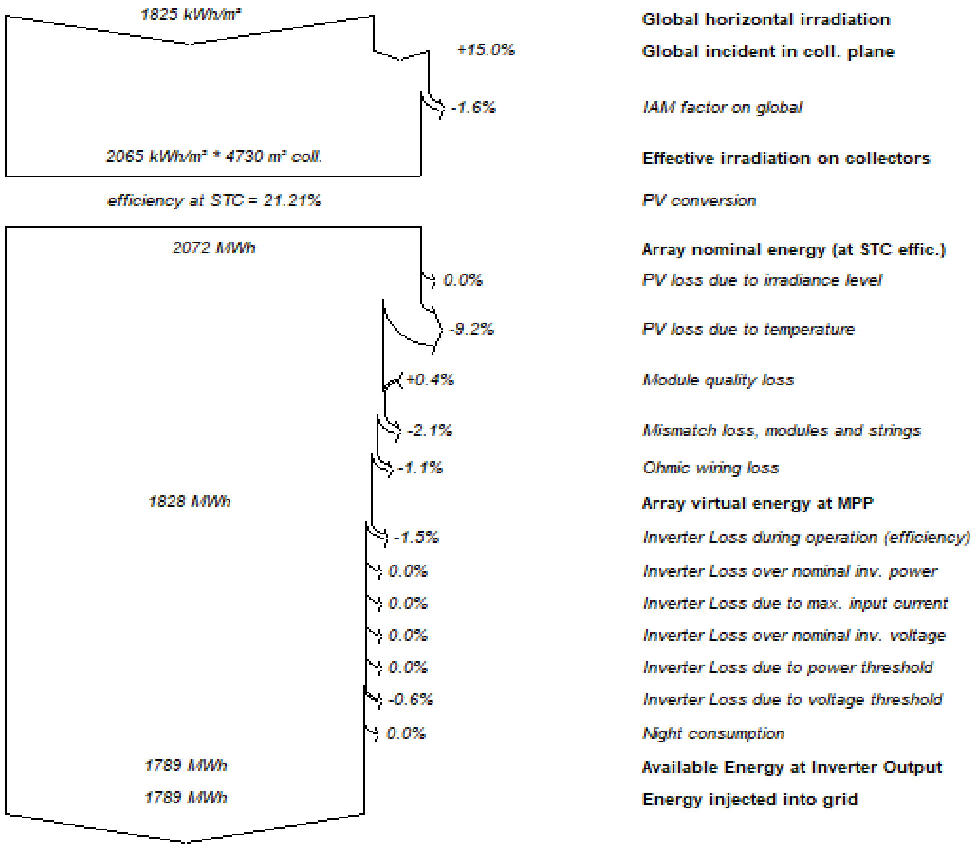

Figure 5.3. Losses diagram of 1 MW PV power plant by pvsyst.

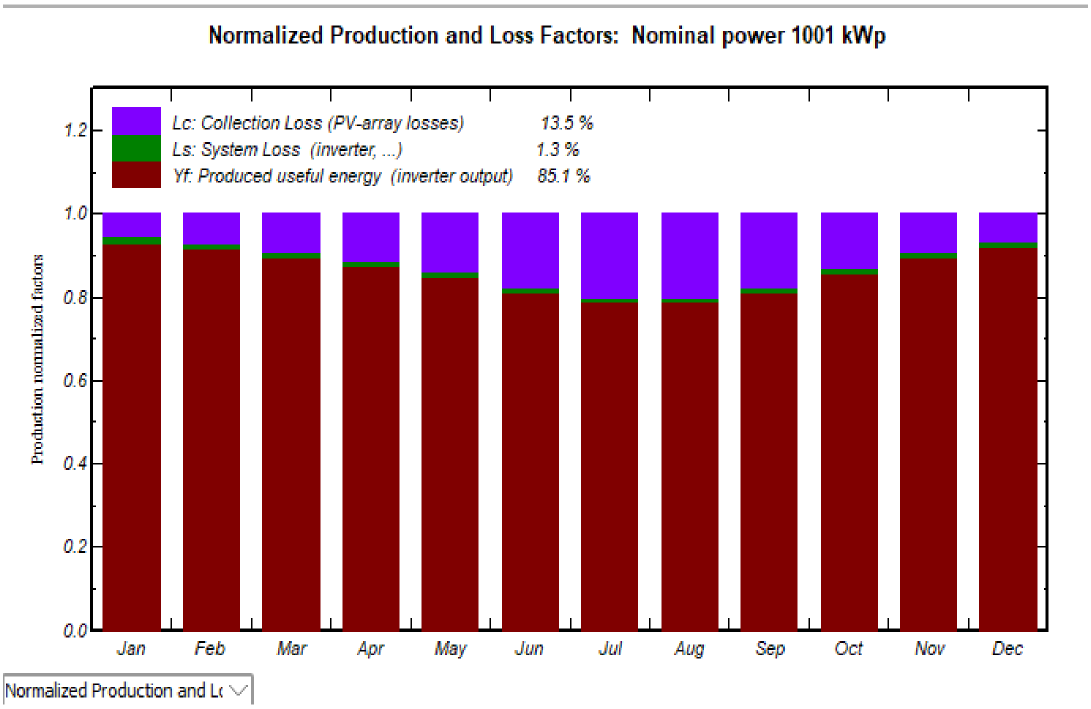

Figure 5.4. Nominal power for 1001kWp .

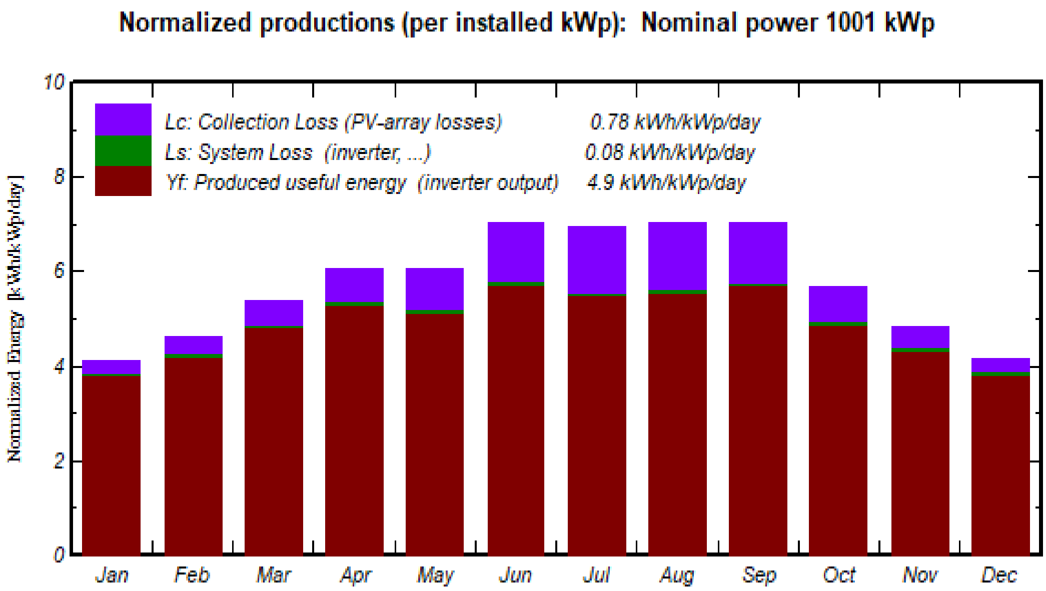

Figure 5.5. Nominal power for 1001kWp (per installed kWP).

5.2. THE RESULTS OF DESIGNING A100 MW PV POWER PLANT

The results were obtained from PVSYST Software simulation for 100Mw Photovoltaic power plant which designed by this software, the plant contains from 217600 PV module (si-mono 460 w_p), The No. of Photovoltaic modules linked in series 17 Module (series strings) and the system's total No. of parallel strings are 12800 strings (each string has 16 PV modules connected in parallel) the parallel strings are connected to a 100-unit of a central inverter (the capacity of each unit is 1000kW each unit has 8 inputs to produce 1MW).

The result obtained from pvsyst, shown in Table (5.3) that the average annual ambient temperature for the site is 20.60 C^{o,} and the average annual Horizontal global irradiation value is equal to 1825 kW/m^2/ year, and this is a good value.

Table 5.3. The main result of 100MW PV power plant by pvsyst according weather parameters.

Month	**Temp. Amb C^o**	**Horizontal global Irradiation kW/m^2**	**Global incident in plant kWh/m^2**	**Horizontal Diffuse Irradiation kWh/m^2**	**Effective global, correspond for IAM and shading kWh/m^2**
January	6.84	78.8	126.9	33.79	125.5
February	8.68	92.0	128.8	40.72	127.4
March	13.27	138.3	167.0	63.89	164.4
April	17.62	170.5	181.8	16.07	178.5
May	24.51	196.4	187.9	87.92	184.0
June	30.99	233.3	211.8	73.42	207.2
July	35.02	232.2	215.9	74.27	211.4
August	34.19	212.1	218.4	67.31	214.4
September	29.00	177.2	211.0	45.70	207.5
October	23.12	128.6	176.0	47.96	173.9
November	14.25	90.6	145.4	32.35	143.8
December	8.91	75.0	128.6	38.31	127.4
Year	20.60	1825.0	2099.5	671.71	2065.3

Table 5.4. The main result of 100MW PV power plant by pv sys according Technical parameters.

	P.R ratio	E Array MWh	E Grid MWh
January	0.927	11970	11774
February	0.913	11969	11764
March	0.892	15149	14907
April	0.872	16109	15858
May	0.845	16142	15888
June	0.809	17394	17140
July	0.785	17207	16955
August	0.784	17399	17151
September	0.808	17303	17058
October	0.854	15276	15052
November	0.893	13209	13001
December	0.917	12009	11806
Year	0.849	181136	178352

Table 5.4. shows other important parameters resulting from the simulation this parameter is the annual Performance ratio (P.R%), annual effective energy at the array's output, and the annual energy exported to the grid. (0.849, 181136 MWh, 1178352 MWh) respectively.

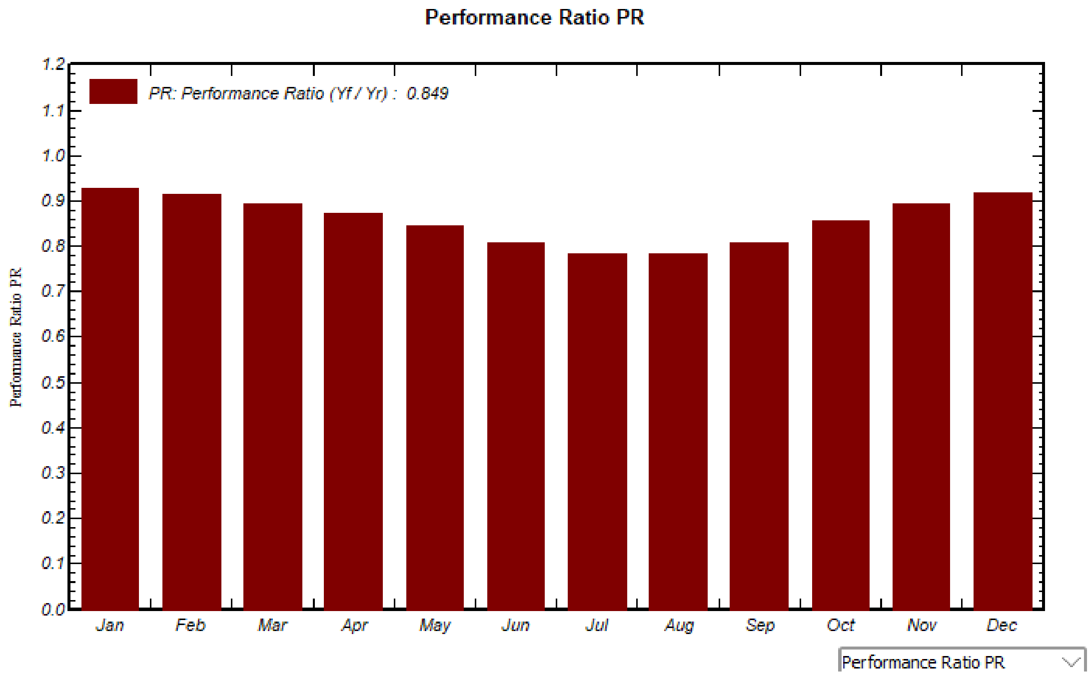

Figure 5.6. The Performance ratio of 100MW PV Power Plant by pvsyst.

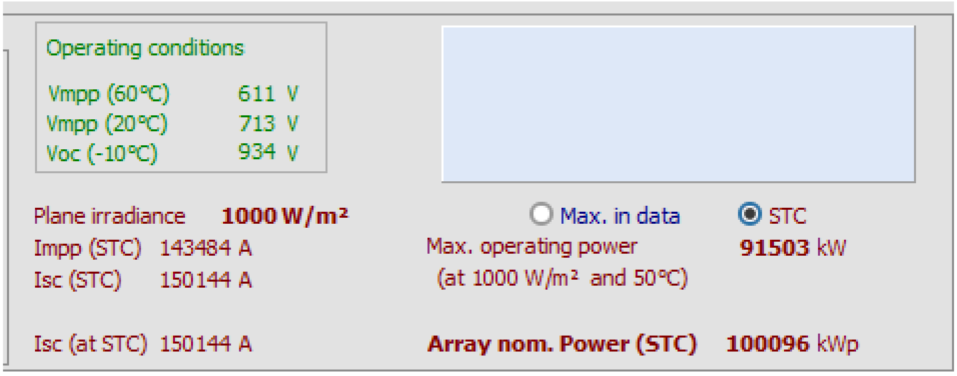

Figure 5.7. Nominal power array at Standard test condition (100 MW PV Plant).

The result of the simulation is shown in the table5.2. We can find the yield factor of the PV system (Y_f). which is referred to as the system's final yield of useful energy per day to the nominal power. unit is (kWh/kW_p/day).

$$Y_f = \frac{E_{Array}}{P_{\text{nominal } at\ STC}} \tag{5.2}$$

$P_{\text{nominal array at STS}}$ = Nominal power array at Standard test condition (from pv sys simulation as shown in Figure 5.7).

$$Y_f = \frac{181136\ MWh.year^{-1}}{100.096 MW_P} = 1809.6\ {}^{MWh}/_{MW_P/year}$$

From (5.4) Table We can find the capacity factor of a PV plant is a ratio of the energy generated by the station for a year to the installed capacity (Nominal Power) in case it had operate for a whole year [99]. in other words, it can be determined by dividing the yield factor by the day hours multiplied by the days of the year.

$$Capacity\ Ratio\ \% = \frac{Energy\ generated\ per\ annum\ (MWh)}{Installed\ Capacity\ (MWp) * \ 24 * 365} = \frac{Y_f}{8760} \tag{5.3}$$

$$Capacity\ Ratio\ \% = \frac{1809.6}{8760} = 20.6\ \%\ It\ is\ a\ good\ value$$

The value of the capacity factor ranges from 12-24 % (for PV plants of a fixed tilt). It is depending on the plant's performance ratio and solar resources.

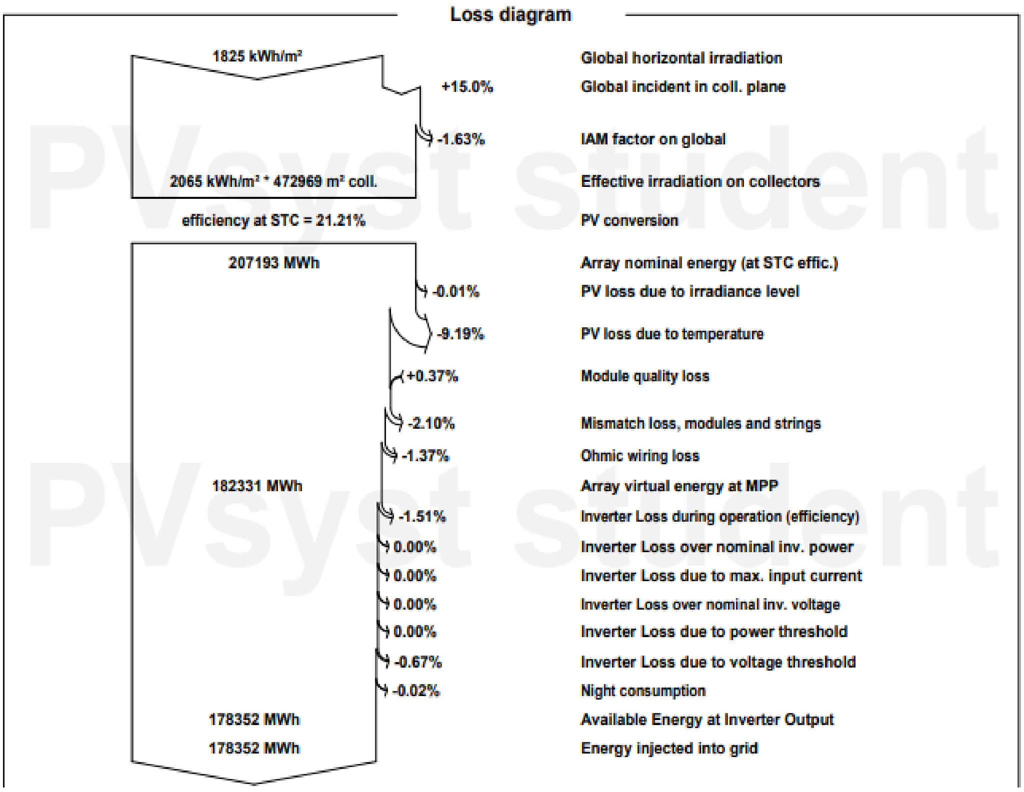

Figure 5.8. Losses diagram of 100 MW PV power plant by pvsyst.

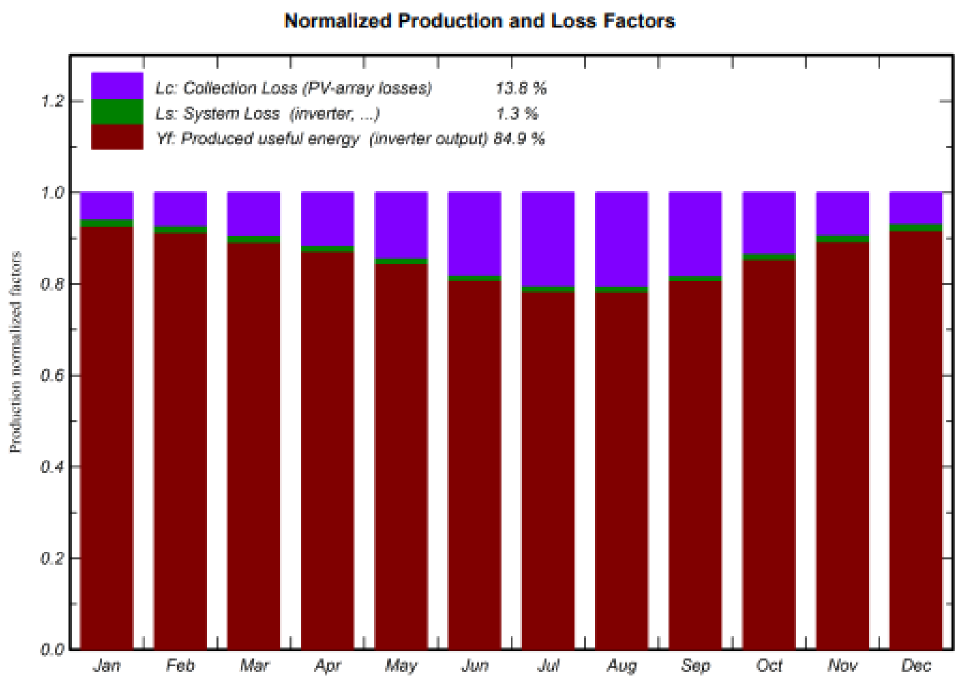

Figure 5.9. Nominal power for $1001MW_p$

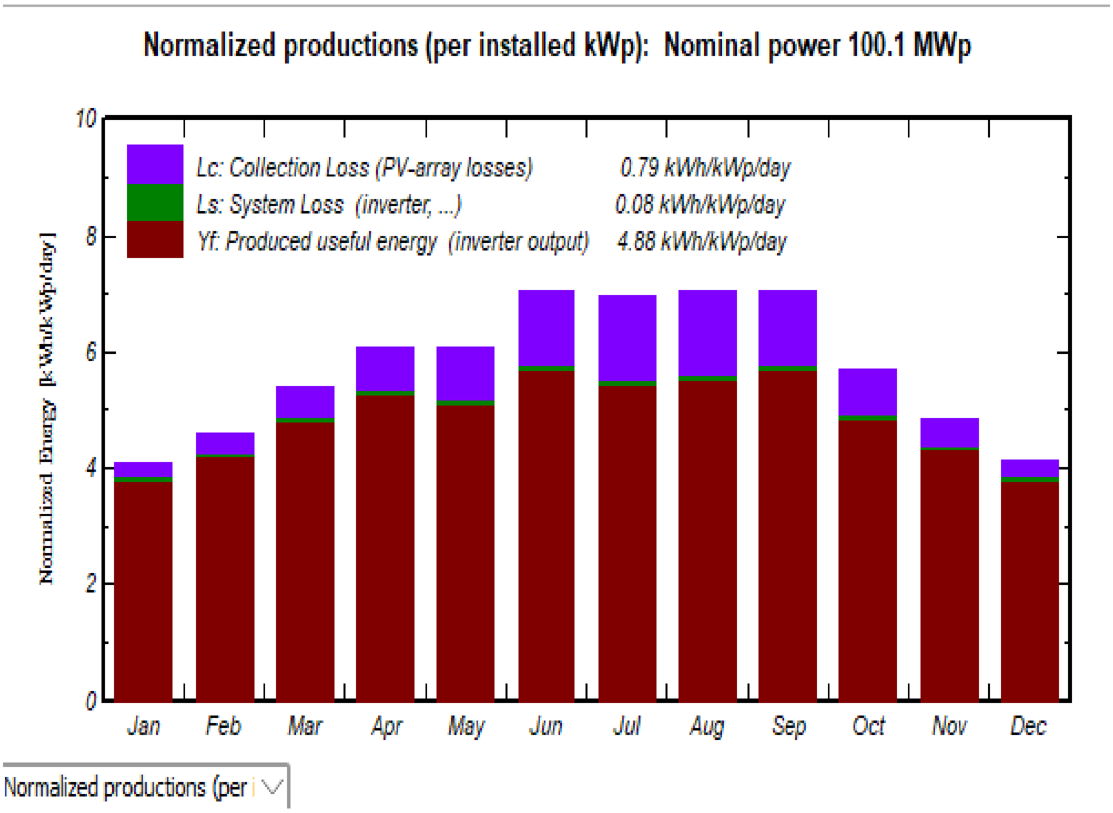

Figure 5.10. Nominal power for 1001MW$_P$. (Per installed kW$_P$).

PART 6

DISCUSSION

Results from research are presented in chapters (4,5) which are discussed in this chapter. The site of the Photovoltaic power plant (1MW) was selected taking into account that the site is far away from the demographic population (soiling pollution), and the water source is available (to clean the PV modules surface) and the national grid is available. The geographical data of the site is obtained by pvsyst simulation software (Meteonorm 8.0) it appears that the average annual horizontal irradiation is equal to 1825 kW/m^2 and the Global incident irradiation in the plant is equal to 2099.5 kWh/m^2 (it is a good value).

The tilt angle of the PV plant was selected by pvsyst simulation software. the optimum tilt angle for the summer season is 15^o and for the winter season is 50^o, since the PV plant is designed as a fixed tilt angle, the optimum fixed tilt angle for all seasons is 35^o (as appears in the pvsyst simulation software) and the azimuth is 0^o (Transformation factor is 1.16 and the losses are 0 % when the tilt angle is 35^o).

The distance between the PV module strings (inter-row spacing) is calculated depending on the equations (4.1) (4.2). The optimal distance is equal to 7.5m to avoid the inter-row shading.

The No. of photovoltaic modules needed in the system is calculated by using equation (4.3) the theoretical calculation. appears that the No. of Photovoltaic modules are 2174, But pvsyst simulation software appears the wholly No. of Photovoltaic is equal to 2176. The two values are acceptable (designing depending on the pvsyst values).

The maximum and the minimum PV modules in the series strings are calculated by the equations (4.4), (4.5), (4.6), (4.7), (4.8), (4.9). The theoretical result is identical to the pvsyst simulation software results.

The system parallel strings No. are calculated theoretically by using the equation (4.11). The results appear that the system parallel strings No. are 145 strings (each string has consisted of 18 Photovoltaic modules connected in parallel). it is within the limits range but it is a high value about inverter DC current (1689.1A) will be near the maximum inverter value (1710 A) by using the equation (4.12) in order to determine the suitable No. of parallel string in the system. results appear that the suitable number of parallel strings is 128 strings each string contain from 16 Photovoltaic modules linked in parallel. in this case value of inverter DC current is varying suitable value (1501.1A) Figure (4.15) shows the total number of the string in the system by using pvsyst simulation software.

The inverter power ratio determined to select the optimal size of inverter to installed in the system. by using the equations (4.13), (4.14), (4.15) to find the inverter power ratio (1.2>Power Ratio >0.8) the value of the inverter ratio for this system is equal to (1.09) it is within limits of choosing value. The figure (4.19) shows the selected inverter by pvsyst simulation software.

The combiner boxes used in the system are selected under IEC standards. The average total current flow through the combiner box is equal to 234.6 A it is within limits (234.6 A> 240 A) according to the relation (4.16).

The nominal current of the fuse that uses in the parallel string is determined by using the equation (4.17) also the rated voltage flow through string cables is determined it is equal to 971. V.

The cross-section area of the cables used in the design is determined by using equations (4.22), and (4.23). the cables calculations by assuming the cross-section area of the cable (array/ string) and determining the voltage drop (ΔV%) the total voltage drop of the string cables and the main cables should be less than 3%, if the voltage drop is more than 3% then the cross-section area of the cable must be changed by the high size of the cable . Also, in the same way the AC cable size is determined, but by using the relation (4.24).

The pvsyst simulation software results (Tables 5.1-5.2) appears that the annual horizontal irradiation is 1825 kW/m^2, performance ratio is 0.851, The annual output of array effective energy is equal to 1817 MW/h, the annual exported energy to grid is equal to 1789 MW/h, the PV losses due to the temperature is -9.2%., mismatch losses(modules and strings)is -2.1%, the ohmic wiring loss is -1.1 %, the inverter losses during operation (efficiency)-1.5 %, the yield factor (Y_f) of the system is determined by using the relation (5.2) Y_f is equal to 1815MWh/MW_p/year. the capacity ratio is determined by using the relation (5.3) the capacity ratio is equal to 20.7% which is a good value for PV plant of fixed tilt.

The pvsyst simulation software results (For 100MW PV Power Plant) appear that the annual horizontal irradiation is 1825 kW/m^2, performance ratio 0.849, the annual output of array effective energy is equal to 181136 MW/h, the annual exported energy to grid is equal to 178352 MW/h, the PV losses due to the temperature are -9.2%, mismatch losses (modules and strings) are -2.1%, the ohmic wiring loss is -1.1 %, the inverter losses during operation (efficiency)-1.5 %, and the yield factor (Y_f) of the system is determined by using the relation (5.2) Y_f is equal to 1815 MWh/MW_p/year. the capacity ratio is determined by using the relation (5.3) the capacity ratio is equal to 20.7% which is a good value for PV plant of fixed tilt.

PART 7

CONCLUSION

This thesis refers to the essential points that must consider when designing large-scale Photovoltaic plants. This point includes choosing the Photovoltaic plant site, choosing the optimal tilt angle (for PV modules), choosing the Photovoltaic plant elements like Photovoltaic modules (PV panels), Combiner Boxes, Inverters, DC with AC cables, also how collects this component to establish a PV system. All these points followed in this thesis. Also with help of pvsyst software simulation, the annual global irradiation of the site is determined, and the optimal tilt angle of Photovoltaic modules of the system in the site was achieved, No. of PV modules needed in the Photovoltaic station were determined, Also the number of inverters needed in the Photovoltaic station was calculated, the number of combiner boxes needed in the PV system was determined, the Length of DC and AC cables and the cross-section area of cables needed in the system was determined.

The annual energy generated from the PV arrays of the PV power plant was determined and the exported energy to the grid was calculated. The performance ratio, yield factor, and capacity factor of the system were determined in this research.

All the aims of the study were accomplished and thoroughly covered in chapters four and five, we may thus infer that the research work's aims and objectives have been met.

REFERENCES

1. Li, L., Lin, J., Wu, N., Xie, S., Meng, C., Zheng, Y., Wang, X., & Zhao, Y., "Review and outlook on the international renewable energy development", ***Energy and Built Environment,*** 3(2): 139–157 (2022).

2. Cabrera-Tobar, A., Bullich-Massagué, E., Aragüés-Peñalba, M., & Gomis-Bellmunt, O.," ***Topologies for large scale photovoltaic power plants. Renewable and Sustainable Energy Reviews,*** 5(9): 309–319 (2016).

3. Abed, F. M., Al-Douri, Y., & Al-Shahery, G. M. Y., "Review on the energy and renewable energy status in Iraq: The outlooks", ***Renewable and Sustainable Energy Reviews,*** 3(9): 816–827 (2014).

4. UNEP., "2020 Global status report for buildings and construction: Towards a zero-emission", ***Efficient and Resilient Buildings and Construction Sector,*** USA, 56-77 (2020).

5. Jassim, H. & Fakhri, A. H., "Environmental Impact of Electrical Power Generators in Iraq", ***International Journal of Engineering Technology, Management and Applied Sciences,*** 4(3): 122–134 (2016).

6. Shiva Kumar, B., & Sudhakar, K., "Performance evaluation of 10 MW grid connected solar photovoltaic power plant in India", ***Energy Reports***, 1(4): 184–192 (2015).

7. Kumar, N. M., Kumar, M. R., Rejoice, P. R., & Mathew, M., "Performance analysis of 100 kWp grid connected Si-poly photovoltaic system using PVsyst simulation tool", ***Energy Procedia,*** 11(7): 180–189 (2017).

8. Al-Najideen, M. I., & Alrwashdeh, S. S., "Design of a solar photovoltaic system to cover the electricity demand for the faculty of Engineering-Mu'tah University in Jordan", ***Resource-Efficient Technologies,*** 3(4): 440–445 (2017).

9. Rachit, S., & V.K., G., "Design of Grid Connected PV System using PVsyst", ***I-Manager's Journal on Electrical Engineering,*** 10(1): 14 (2016).

10. Siregar, Y., Hutahuruk, Y., & Suherman., "Optimization design and simulating solar PV system using PVSyst software. 2020 4th International Conference on Electrical, Telecommunication and Computer Engineering", ***ELTICOM 2020 - Proceedings***, Medan, Indonesia, 219–223 (2020).

11. Faiz, F. U. H., Shakoor, R., Raheem, A., Umer, F., Rasheed, N., & Farhan, M., "Modeling and Analysis of 3 MW Solar Photovoltaic Plant Using PVSyst at Islamia University of Bahawalpur, Pakistan", ***International Journal of Photo Energy,*** Pakistan, 20-21 (2021).

12. Kumarappa, S., & Naganagouda, H., "Design and Development of 5MW Solar PV Grid Connected Power Plant Using PVsyst", ***International Research Journal of Engineering and Technology (IRJET),*** 4(8): 778–785.

13. Snidvongs, S., "SEGA 07 Smart City and Urban Resiliency", ***SAGE Journal,*** 1(2): 45-79 (2020).

14. Lausch, D., Naumann, V., Breitenstein, O., Bauer, J., Graff, A., Bagdahn, J., & Hagendorf, C., "Potential-induced degradation (PID): Introduction of a novel test approach and explanation of increased depletion region recombination", ***IEEE Journal of Photovoltaics,*** 4(3): 834–840 (2014).

15. Wang, F., Wang, H., Yang, H., Chang, J., Zhao, P., Wang, A., & Song, D., "Effect of potential induced degradation on crystalline silicon solar modules in photovoltaic power plant", 2017 ***IEEE 44th Photovoltaic Specialist Conference,*** Portland, USA, 1025–1029 (2017).

16. Jörg Bagdahn, Matthias Ebert, Jens Fröbel, S. D., "Test Results of Potential Induced Degradation (Pid) of Solar Modules from Different Manufacturers", ***IECON 2013 - 39th Annual Conference of the IEEE Industrial Electronics Society,*** Vienna, Austria, 8090–8097 (2012).

17. Puranik, V. E., & Gupta, R., "Analysis and insight of electroluminescence imaging in the assessment of potential-induced degradation in crystalline silicon photovoltaic module", ***Engineering Failure Analysis,*** 13(4): 106-027 (2022).

18. Hylsky, J., Strachala, D., Hladisk, J., Cudek, P., Kazda, T., Vanek, J., Vyroubal, P., & Stary, J., "Design of P-Type Photovoltaic Cells Resistant to Potential-Induced Degradation", ***IEEE Journal of Photovoltaics,*** 8(5): 1215–1221 (2018).

19. Lu, S., Phung, B. T., & Zhang, D., "A comprehensive review on DC arc faults and their diagnosis methods in photovoltaic systems", ***Renewable and Sustainable Energy Reviews,*** 89(17): 88–98 (2018).

20. Klement, K., "DC Arc Flash Studies for Solar Photovoltaic Systems: Challenges and Recommendations", ***IEEE Transactions on Industry Applications,*** 51(5): 4239–4244 (2015).

21. Yuventi, J., "DC electric arc-flash hazard-risk evaluations for photovoltaic systems", ***IEEE Transactions on Power Delivery,*** 29(1): 161–167 (2014).

22. Strobl, C., & Meckler, P., "Arc faults in photovoltaic systems", ***Electrical Contacts, Proceedings of the Annual Holm Conference on Electrical Contacts,*** Austria, 216–222 (2010).

23. Barkhouse, D. A. R., Gunawan, O., Gokmen, T., Todorov, T. K., & Mitzi, D. B., "Yield predictions for photovoltaic power plants: empirical validation, recent advances and remaining uncertainties", ***Progress in Photovoltaics: Research and Applications,*** 20(1): 6–11 (2015).

24. Itako, K., & Alhabib, A., "A New Method of Detecting Hot Spots in PV Generation System Utilizing AI", ***IOP Conference Series: Earth and Environmental Science,*** 581(1): 56-88 (2020).

25. Moretón, R., Lorenzo, E., & Narvarte, L., "Experimental observations on hot-spots and derived acceptance/rejection criteria", ***Solar Energy,*** 11(8): 28–40 (2015).

26. Ghanbari, T., "Hot spot detection and prevention using a simple method in photovoltaic panels", ***IET Generation, Transmission and Distribution,*** 11(4): 883–890 (2017).

27. Al Mamun, M. A., Hasanuzzaman, M., & Selvaraj, J., "Experimental investigation of the effect of partial shading on photovoltaic performance", ***IET Renewable Power Generation,*** 11(7): 912–921 (2017).

28. Ramabadran, R., & Mathur, B., "Effect of Shading on Series and Parallel Connected Solar PV Modules", ***Modern Applied Science,*** 3(10): 56-88 (2009).

29. Hanitsch, R. E., Schulz, D., & Siegfried, U., "Shading Effects on Output Power of Grid Connected Photovoltaic Generator Systems", ***Renewable Energy,*** 5(6): 93–99 (2001).

30. Barkhouse, D. A. R., Gunawan, O., Gokmen, T., Todorov, T. K., & Mitzi, D. B., "Yield predictions for photovoltaic power plants: empirical validation, recent advances and remaining uncertainties", ***Progress in Photovoltaics: Research and Applications,*** 20(1): 6–11 (2015).

31. Vidyanandan, K. V., "An overview of factors affecting the performance of solar PV systems", ***Energy Scan***, 27(28): 216 (2017).

32. Bressan, M., El Basri, Y., Galeano, A. G., & Alonso, C., "A shadow fault detection method based on the standard error analysis of I-V curves", ***Renewable Energy,*** 9(9): 1181–1190 (2016).

33. Faiz, F. U. H., Shakoor, R., Raheem, A., Umer, F., Rasheed, N., & Farhan, M., "Modeling and Analysis of 3 MW Solar Photovoltaic Plant Using PVSyst", ***Islamic University of Bahawalpur International Journal of Photo Energy,*** 20-21 (2021).

34. Mujaahid, F., Nurhadi, P., Syahputra, R., Putra, K., & Widyasmoro., "Design of Solar Power Plant: Analyze Its Potential in Parangtritis Area Using PVsyst Simulator. Proceedings of the 4th International Conference on Sustainable Innovation 2020–Technology, Engineering and Agriculture (ICoSITEA 2020)", ***Atlantis Press,*** USA, 186–190 (2021).

35. Akram, I., Awais, M., Bashir, A., Khan, R. A. J., & Iqbal, J., "Design and analysis of 300MW solar configuration and its comparison with Quaid-e-Azam solar park", ***2018 International Conference on Engineering and Emerging Technologies,*** Lahore, Pakistan, 1–6 (2018).

36. Krunal, H., & Sweta. S. "Design of 50 MW Grid Connected Solar Power Plant", ***International Journal of Engineering Research,*** 9(4): 885–897 (2020).

37. Szabó, L., & Szaniszló, A., "Solar power plant station in fish land", ***International Review of Applied Sciences and Engineering***, 8(1): 37–43 (2017).

38. Hachicha, A. A., Al-Sawafta, I., & Said, Z., "Impact of dust on the performance of solar photovoltaic (PV) systems under United Arab Emirates weather conditions", ***Renewable Energy,*** 14(1): 287–297 (2019).

39. Adinoyi, M. J., & Said, S. A. M., "Effect of dust accumulation on the power outputs of solar photovoltaic modules", ***Renewable Energy,*** 6(10): 633–636 (2013).

40. Mallineni, J., Yedidi, K., Shrestha, S., Knisely, B., Tatapudi, S., Kuitche, J., & Tamizhmani, G., "Soiling losses of utility-scale PV systems in hot-dry desert climates: Results from four 4-16 years old power plants", ***2014 IEEE 40th Photovoltaic Specialist Conference,*** Denver, USA, 3197–3200 (2014).

41.

42. Elminir, H. K., Ghitas, A. E., Hamid, R. H., El-Hussainy, F., Beheary, M. M., & Abdel-Moneim, K. M., "Effect of dust on the transparent cover of solar collectors", ***Energy Conversion and Management,*** 47(19): 3192–3203 (2006).

43. Faifer, M., Lazzaroni, M., & Toscani, S., "Dust effects on the PV plant efficiency: A new monitoring strategy***", 20th IMEKO TC4 Symposium on Measurements of Electrical Quantities: Research on Electrical and Electronic Measurement for the Economic Upturn, together with 18th TC4 International Workshop on ADC and DCA Modeling and Testing,*** Italy, 580–585 (2014).

44. Dahlioui, D., Laarabi, B., Sebbar, M. A., Barhdadi, A., Dambrine, G., Menard, E., & Boardman, J., "Soiling effect on photovoltaic modules performance: New experimental results", ***Proceedings of 2016 International Renewable and Sustainable Energy Conference,*** Morocco, 111–114 (2017).

45. Chanchangi, Y. N., Ghosh, A., Sundaram, S., & Mallick, T. K., "An analytical indoor experimental study on the effect of soiling on PV, focusing on dust properties and PV surface material", ***Solar Energy,*** 20(3): 46–68 (2020).

46. Mehleri, E. D., Zervas, P. L., Sarimveis, H., Palyvos, J. A., & Markatos, N. C., "Determination of the optimal tilt angle and orientation for solar photovoltaic arrays", ***Renewable Energy,*** 35(11): 2468–2475 (2010).

47. Yunus Khan, T. M., Soudagar, M. E. M., Kanchan, M., Afzal, A., Banapurmath, N. R., Akram, N., Mane, S. D., & Shahapurkar, K., "Optimum location and influence of tilt angle on performance of solar PV panels", ***Journal of Thermal Analysis and Calorimetry***, 141(1): 511–532 (2020).

48. Kacira, M., Simsek, M., Babur, Y., & Demirkol, S., 'Determining optimum tilt angles and orientations of photovoltaic panels in Sanliurfa, Turkey", ***Renewable Energy,*** 29(8): 1265–1275 (2004).

49. Baumgartner, F. P., Büchel, A., & Bartholet, R., "Cable-based solar wings tracking system: two-axis system and progress of one-axis system", ***In Proceedings of the 25th European Photovoltaic Solar Energy Conference,*** Valencia, 56-78 (2010).

50. Bentaher, H., Kaich, H., Ayadi, N., Ben Hmouda, M., Maalej, A., & Lemmer, U., "A simple tracking system to monitor solar PV panels.", ***Energy Conversion and Management***, 7(8): 872–875 (2014).

51. Filik, T., & Başaran Filik, Ü., "Efficiency Analysis of the Solar Tracking Pv Systems in Eskisehir Region", ***Anadolu University Journal of Science and Technology, Applied Sciences and Engineering,*** 18(1): 209–209 (2017).

52. Bazyari, S., Keypour, R., Farhangi, S., Ghaedi, A., & Bazyari, K., "A Study on the Effects of Solar Tracking Systems on the Performance of Photovoltaic Power Plants", ***Journal of Power and Energy Engineering,*** 2(4): 718–728 (2014).

53. Barkhouse, D. A. R., Gunawan, O., Gokmen, T., Todorov, T. K., & Mitzi, D. B., "Yield predictions for photovoltaic power plants: empirical validation, recent advances and remaining uncertainties", ***Progress in Photovoltaics: Research and Applications,*** 20(1): 6–11 (2015).

54. Agyekum, E. B., Afornu, B. K., & Ansah, M. N. S., "Effect of Solar Tracking on the Economic Viability of a Large-Scale PV Power Plant", ***Environmental and Climate Technologies,*** 24(3): 55–65 (2020).

55. Amelia, A. R., Irwan, Y. M., Leow, W. Z., Irwanto, M., Safwati, I., & Zhafarina, M., "Investigation of the effect temperature on photovoltaic (PV) panel output performance", ***International Journal on Advanced Science, Engineering and Information Technology,*** 6(5): 682–688 (2016).

56. Vidyanandan, K. V., “An overview of factors affecting the performance of solar PV systems”, ***Energy Scan,*** 27(28): 216 (2017).

57. Fernández-Infantes, A., Contreras, J., & Bernal-Agustín, J. L., “Design of grid connected PV systems considering electrical, economic and environmental aspects: A practical case”, ***Renewable Energy***, 31(13): 2042–2062 (2006).

58. Yilmaz, S., & Dincer, F., “Impact of inverter capacity on the performance in large-scale photovoltaic power plants – A case study for Gainesville”, ***Renewable and Sustainable Energy Reviews,*** Florida, 15–23. (2017).

59. Alonso-Martínez, J., Eloy-García, J., & Arnaltes, S., “Direct power control of grid connected PV systems with three level NPC inverter”, ***Solar Energy,*** 84(7): 1175–1186 (2010).

60. Atasoy, B., & Tezcan, S. S., “Comparison of String and Central Inverter for 10MW PV Plant”, ***ISMSIT 2021 - 5th International Symposium on Multidisciplinary Studies and Innovative Technologies,*** 2(4): 182–186 (2021).

61. Kouro, S., Leon, J. I., Vinnikov, D., & Franquelo, L. G., “Grid-connected photovoltaic systems: An overview of recent research and emerging PV converter technology”, ***IEEE Industrial Electronics Magazine,*** 9(1): 47–61 (2015).

62. Kouro, S., Leon, J. I., Vinnikov, D., & Franquelo, L. G., “Grid-connected photovoltaic systems: An overview of recent research and emerging PV converter technology”, ***IEEE Industrial Electronics Magazine,*** 9(1): 47–61 (2015).

63. Ahmad, N. I., Ab-Kadir, M. Z. A., Izadi, M., Azis, N., Radzi, M. A. M., Zaini, N. H., & Nasir, M. S. M., “Lightning protection on photovoltaic systems: A review on current and recommended practices”, ***Renewable and Sustainable Energy Reviews,*** 8(2): 1611–1619 (2018).

64. Zhang, Y., Chen, H., & Du, Y., “Considerations of Photovoltaic System Structure Design for Effective Lightning Protection”, ***IEEE Transactions on Electromagnetic Compatibility***, 62(4): 1333–1341 (2020).

65. Karim, M. R., & Ahmed, M. R., “Lightning Effect on a Large-Scale Solar Power Plant with Protection System”, ***1st International Conference on Advances in Science, Engineering and Robotics Technology***, Bangladesh, 56-77 (2019).

66. Gan, C. K., Lee, Y. M., Pudjianto, D., & Strbac, G., “Role of losses in design of DC cable for solar PV applications”, ***2014 Australasian Universities Power Engineering Conference,*** Australia, 2–6 (2014).

67. Ekici, S., & Kopru, M. A., "Investigation of PV system cable losses", ***International Journal of Renewable Energy Research,*** 7(2): 807–815 (2017).

68. Desai, A., Pandya, V., Mukhopadhyay, I., & Ray, A., "Temperature Effects on DC Cable Voltage Drop in Utility Scale Rooftop Solar PV Plant Based on Empirical Model", ***Conference Record of the IEEE Photovoltaic Specialists Conference,*** Canada, 2397–2402 (2020).

69. Umar, N. H., Bora, B., Umar, N., Banerjee, C., & Panwar, B. S., "Study of different PV Technologies under Composite Climates using test beds at NISE View project PV module performance studies View project SEE PROFILE Comparison of different PV power simulation software: case study on performance analysis of 1 MW grid", ***PhD Thesis, Tripoli University,*** Libya, 11–24 (2018).

70. Gurupira, T., & Rix, A. J., "PV Simulation Software Comparisons: PVSyst, ***NREL SAM and PVLib.*** 3(4): 45-66 (2017).

71. Ramli, M. S., Wahid, S. S. A., & Hassan, K. K., "A comparison of renewable energy technologies using two simulation softwares: HOMER and RETScreen", ***AIP Publishing LLC,*** 7(5): 13-30 (2017).

72. Suh, J., Jang, Y., & Choi, Y., "Comparison of electric power output observed and estimated from floating photovoltaic systems: a case study on the Hapcheon Dam", ***Sustainability,*** 12(1): 276 (2019).

73. Ranjbaran, P., Yousefi, H., Gharehpetian, G. B., & Astaraei, F. R., "A review on floating photovoltaic (FPV)power generation units", ***Renewable and Sustainable Energy Reviews,*** 1(10): 332–347 (2019).

74. Sahu, A., Yadav, N., & Sudhakar, K., "Floating photovoltaic power plant: A review", ***Renewable and Sustainable Energy Reviews,*** 6(6): 815–824 (2016).

75. Syafiq, A., Pandey, A. K., Adzman, N. N., & Rahim, N. A., "Advances in approaches and methods for self-cleaning of solar photovoltaic panels", ***Solar Energy***, 162(17): 597–619 (2018).

76. Moharram, K. A., Abd-Elhady, M. S., Kandil, H. A., & El-Sherif, H., "Influence of cleaning using water and surfactants on the performance of photovoltaic panels", ***Energy Conversion and Management,*** 6(8): 266–272 (2013).

77. Khadka, N., Bista, A., Adhikari, B., Shrestha, A., & Bista, D., "Smart solar photovoltaic panel cleaning system", ***IOP Conference Series: Earth and Environmental Science,*** Thailand, 4-63 (2020).

78. Husain, A. A. F., Hasan, W. Z. W., Shafie, S., Hamidon, M. N., & Pandey, S. S., “A review of transparent solar photovoltaic technologies”, ***Renewable and Sustainable Energy Reviews,*** 94(7): 779–791 (2018).

79. Usman, Z., Tah, J., Abanda, H., & Nche, C., “A critical appraisal of pv-systems’ performance”, **Buildings,** 10 (11): 192 (2020).

80. Baharwani, V., Meena, N., Dubey, A., Brighu, U., & Mathur, J., “Life Cycle Analysis of Solar PV System: A Review”, ***International Journal of Environmental Research and Development,*** 4(2): 183–190 (2014).

81. Hernandez, R. R., Easter, S. B., Murphy-Mariscal, M. L., Maestre, F. T., Tavassoli, M., Allen, E. B., Barrows, C. W., Belnap, J., Ochoa-Hueso, R., Ravi, S., & Allen, M. F., “Environmental impacts of utility-scale solar energy”, ***Renewable and Sustainable Energy Reviews***, 2(9): 766–779 (2014).

82. Internet: NS ENERGY, “Sudair Solar Power Plant”, **https://www.nsenergybusiness.com/projects/sudair-solar-power-plant/** (2022).

83. Internet: Renewables, “Concentrated solar power project in Crete to boost capacity”, **https://balkangreenenergynews.com/concentrated-solar-power - project-in-crete-to-boost-capacity/**(2022).

84. Oliveti, G., Marletta, L., Arcuri, N., De Simone, M., Bruno, R., & Evola, G., “Solar energy”, ***Green Energy and Technology,*** 10(9): 159–214 (2014).

85. Internet: NASA, “The sun”, **https://www.nasa.gov/mission_pages/sunearth/science/Sunlayers.html/** (2022).

86. Roger, A. & Ventre, J., “Photovoltaic systems engineering”, ***CRC press,*** Germany, 23-55 (2003).

87. Kaltschmitt, M., Streicher, W. and Wiese, A. “Renewable Energy: Technology, Economics and Environment”, ***Springer,*** Switzerland, 12-19 (2007).

88. Lynn, P. A., “Electricity from sunlight: an introduction to photovoltaics”, ***John Wiley & Sons,*** USA, 45-66 (2011).

89. Olatunde, I., & Helmut, S., “Solar Photovoltaic Installation Supervision”, ***Springer,*** Germany, 56-77 (2017).

90. Kaltschmitt, M., Streicher, W., & Wiese, A., “*Renewable energy: technology, economics and environment*”, ***Springer Science & Business Media, Germany,*** 45-66 (2007).

91. Internet: Solar power, “A solar prominence”, **https://www.sciencelearn.org.nz /resources/1582-solar-power/(**2022).

92. Internet: Joseph, S., “A Plan To Replace Geographic Coordinates on Earth With Unique Strings of Three Words”, **https://www.smithsonianmag.com/science-nature/plan-replace-geographic-coordinates-earth-unique-strings -three-words-180949946/**(2022).

93. Masters, G. M., “Renewable and efficient electric power systems”, ***John Wiley & Sons,*** USA, 45-77 (2013).

94. Sace, A., “Technical application papers no. 10–photovoltaic plants”, ***A Division of ABB SpALV Breakers,*** 1(4): 41-43 (2010).

95. Deutsche, G. S., “Planning and installing photovoltaic systems: a guide for installers, architects and engineers”, ***Routledge,*** USA, 67-88 (2013).

96. Thanakodi, S., “Modeling and simulation of grid connected photovoltaic system using Matlab/Simulink", ***Ph.D. dissertation, University Technology Malaysia, Faculty of Electrical Engineering,*** Malaysia, 12-45 (2009).

97. Stalter, O., Kranzer, D., Rogalla, S., & Burger, B., “Advanced solar power electronics”, ***Proceedings of the International Symposium on Power Semiconductor Devices and ICs,*** Japan, 3–10 (2010).

98. Sumathi, S., Ashok Kumar, L., & Surekha, P., “Solar PV and Wind Energy Conversion Systems. In Green Energy and Technology”, ***Springer,*** Switzerland, 20-44 (2015).

99. Chen, S., Li, P., Brady, D., & Lehman, B., “Determining the optimum grid-connected photovoltaic inverter size”, ***Solar Energy,*** 87(1): 96–116 (2013).

100. Lumby, B., “Utility-scale solar photovoltaic power plants: a project developer’s guide”, ***The World Bank,*** USA, 1-216 (2015).

101. Cables, M., “Systems Design and Installation 8th Edition”, ***Springer,*** Switzerland, 30-37 (2020).

102. Tan, P. H., & Gan, C. K., “Methods of lightning protection for the PV power plant”, ***Proceeding - 2013 IEEE Student Conference on Research and Development,*** Malaysia, 221–226 (2013).

103. Khalil, F. A., Asif, M., Anwar, S., ul Haq, S., & Illahi, F., “Solar tracking techniques and implementation in photovoltaic power plants: A review”, ***Proceedings of the Pakistan Academy of Sciences: Part A,*** 54(3): 231–241 (2017).

104. Bazyari, S., Keypour, R., Farhangi, S., Ghaedi, A., & Bazyari, K., “A Study on the Effects of Solar Tracking Systems on the Performance of Photovoltaic Power Plants”, ***Journal of Power and Energy Engineering,*** 2(04): 718–728 (2014).

105. Alkaff, S. A., Shamdasania, N. H., Ii, G. Y., & Venkiteswaran, V. K., “A Study on Implementation of PV Tracking for Sites Proximate and Away from the Equator”, ***Process Integration and Optimization for Sustainability,*** 3(3): 375–382 (2019).

106. Internet: PVSYST, “PVsyst presents results in the form of a full report, specific graphs and tables, and data can be exported for use in other software”, **www.pvsyst.com**/(2022).

107. Jamil, I., Zhao, J., Zhang, L., Jamil, R., & Rafique, S. F., “Evaluation of Energy Production and Energy Yield Assessment Based on Feasibility, Design, and Execution of 3 × 50 MW Grid-Connected Solar PV Pilot Project in Nooriabad”, ***International Journal of Photo energy,*** 2(1): 243-347 (2017).

108. Aldali, Y., Henderson, D., & Muneer, T., “A 50 MW very large-scale photovoltaic power plant for Al-Kufra, Libya: Energetic, economic and environmental impact analysis”, ***International Journal of Low-Carbon Technologies,*** 6(4): 277–293 (2011).

109. Jadhav, S., & Thorat, A., “Technical and Financial Analysis of Commercial Solar Power Plant”, ***2021 International Conference on Nascent Technologies in Engineering,*** India, 1–6. (2021).

RESUME

Omer ALDABBAGH completed high school education in ALRESALA Secondary School, after that, he started the undergraduate program in Technical College/ Mosul (Northern Technical University) Department of Electrical Power Technology Engineering in 2004. Then in 2006, he started assignment as an engineer Assistant in the Ministry of Electricity / the General Company for the Production of Electricity in The Northern Region / Mosul Dam power stations and he is still working there now. To complete his M.Sc. education, he joined Karabük University,